TOWARDS IMPROVED ADAPTIVE CONTROL: HUMAN PILOT MODELS & MEMORY-AUGMENTED ARCHITECTURES

A THESIS SUBMITTED TO

THE GRADUATE SCHOOL OF ENGINEERING AND SCIENCE

OF BILKENT UNIVERSITY

IN PARTIAL FULFILLMENT OF THE REQUIREMENTS FOR

THE DEGREE OF

MASTER OF SCIENCE

IN

MECHANICAL ENGINEERING

By

Abdullah Habboush

July 2023

Towards Improved Adaptive Control: Human Pilot Models & Memory-Augmented Architectures
By Abdullah Habboush
July 2023

We certify that we have read this thesis and that in our opinion it is fully adequate, in scope and in quality, as a thesis for the degree of Master of Science.

Yıldıray Yıldız(Advisor)

Ömer Morgül

Ali Türker Kutay

Approved for the Graduate School of Engineering and Science:

Orhan Arıkan
Director of the Graduate School

ABSTRACT

TOWARDS IMPROVED ADAPTIVE CONTROL: HUMAN PILOT MODELS & MEMORY-AUGMENTED ARCHITECTURES

Abdullah Habboush
M.S. in Mechanical Engineering
Advisor: Yıldıray Yıldız
July 2023

To facilitate the implementation of adaptive control methods, this dissertation introduces novel solutions to key problems that hinder the employment of adaptive controllers in industrial applications. We present techniques that are inspired by humans' versatility in the control loop, where we focus on understanding how humans adapt in the face of anomalies, and how they use their memory to better recover from them. Towards that end, we propose adaptive human pilot models suited for the prediction of human behavior in the loop with an adaptive controller. These models serve as valuable tools to test the interactions between human pilots and adaptive control systems in the simulation environment in order to ensure safe operation in the presence of an anomaly. Furthermore, the development of the models is carried out based on rigorous Lyapunov stability analyses, which can provide analytical insights into how to better design adaptive controllers for manned applications. Apart from their unfavorable interactions with human pilots, another issue that accounts for the scarce employment of adaptive controllers in piloted applications lies in their transient characteristics. While numerous works are devoted to improving the transients of adaptive control systems, in this dissertation, we focus on taking advantage of it first by providing adaptive controllers with human-like memory capabilities. We propose a memory architecture that can make use of stored data about the transients of previously experienced anomalies to aid in obtaining a resilient system against uncertainties. Thus, the proposed memory architecture enables adaptive controllers to rely on memory rather than exploration to better recover from familiar anomalies. The effectiveness of the architecture is validated through numerical simulations, and a rigorous Lyapunov stability analysis is provided.

Keywords: Adaptive control, uncertain systems, human-in-the-loop control.

ÖZET

GELİŞMİŞ UYARLAMALI KONTROL'E DOĞRU: İNSAN PİLOT MODELLERİ & BELLEK İLE GELİŞTİRİLMİŞ YAPILAR

Abdullah Habboush
Makine Mühendisliği, Yüksek Lisans
Tez Danışmanı: Yıldıray Yıldız
Temmuz 2023

Bu tezde, endüstriyel uygulamalarda uyarlamalı kontrolcülerin kullanılmasını engelleyen temel sorunlara yeni çözümler sunuyoruz. İnsanların kontrol konusundaki uzmanlığından ilham alarak geliştirdiğimiz teknikleri bu tezde paylaşırken özellikle insanların anormallikler karşısında nasıl uyum sağladıklarını ve bunları daha iyi telafi etmek için hafızalarını nasıl kullandıklarını anlamaya odaklanıyoruz. Bu amaçla, uyarlamalı bir kontrolcü ile döngüdeki insan davranışını tahmin etmek için uyarlanabilir insan pilot modelleri öneriyoruz. Lyapunov kararlılık analizlerine dayalı olarak geliştirilen modeller, bir anormallik durumunda güvenli çalışmayı sağlamak için insan pilotlar ve uyarlamalı kontrol sistemleri arasındaki etkileşimleri simülasyon ortamında test etmeyi sağlayan değerli araçlardır. Bu, insanlı uygulamalar için uyarlamalı kontrolcülerin nasıl daha iyi tasarlanacağına ilişkin analitik yöntemler sağlayabilir. İnsan pilotlarla olumsuz etkileşimlerinin yanı sıra, uyarlamalı kontrolcülerin pilotlu uygulamalarda nadiren kullanılmasının bir başka nedeni de geçiş dönemindeki performanslarıdır. Uyarlamalı kontrol sistemlerinin geçiş dönemindeki performanslarını iyileştirmek için çok sayıda çalışma yapılmış olsa da, bu tezde, insan benzeri bellek yeteneklerine sahip uyarlamalı kontrolcüler geliştirerek önce geçiş döneminden yararlanmaya odaklanıyoruz. Belirsizliklere karşı esnek bir sistem elde etmeye yardımcı olmak için daha önce yaşanan anormalliklerin geçiş dönemleri hakkında depolanmış verileri kullanabilen bir bellek mimarisi öneriyoruz. Uyarlamalı kontrolcülerin, önceden deneyimlenmiş anormallikleri daha iyi telafi etmek için keşif yerine belleğe güvenmelerini sağlayan önerilen bellek mimarisinin etkinliği sayısal simülasyonlarla ve Lyapunov kararlılık analizi ile doğrulanmıştır.

Anahtar sözcükler: Uyarlamalı kontrol, belirsiz sistemler, döngüde-insan kontrol.

Acknowledgement

To begin with, I would like to express my deepest gratitude to my advisor Assoc. Prof. Yıldıray Yıldız for his invaluable support during my journey. His wise mentorship honed my research skills, helped me improve my scientific expertise, and has always boosted my passion to proceed with my academic career. I would also like to thank Prof. Ömer Morgül and Asst. Prof. Ali Türker Kutay for their valuable comments in my thesis defense. It is an honor to have them on my dissertation committee.

I wish to extend my gratitude to many friends who made this journey easier and more enjoyable. Starting with Emirhan İnanç, Özgür Can Gümüş, Batuhan Emre Kaynak, Aykut Bakan, and Yusuf Uzun. Lots of good memories exist thanks to them, and office nights would have been depressing without them. To the dear ones whose friendship has been a great support, Mohammed Alkhaled, Abdulrazak Masarani, Hashim Alhmood, Sayedus Salehin, Hammam Mohamed, Omair Mohamed, Burak Sarı, and Umar Rauf: I am grateful for getting to know you. Many thanks go to my colleagues in Systems Laboratory, our Paper-Club meetings were not only beneficial but also very amusing.

I wish to thank my parents Ibrahim and Majeda, my brothers Mohamed and Musaab, and my beloved sisters Zahra and Alaa for their everlasting encouragement and motivation. They are the reason I always thrive, and having them in my life is irreplaceable.

To my beloved wife, Şeymanur: Your boundless love and unwavering support have graced my life with countless blessings and delights. I am sincerely thankful for the privilege of having you always by my side. As we move on forward together on our shared journey, I look forward to the future that awaits us, brimming with joy and eager anticipation.

At last, I would like to thank the Scientific and Technological Research Council of Türkiye for their support of this work.

Contents

List of Figures

List of Tables

Chapter 1

Introduction

This thesis contributes to the field of adaptive control by introducing novel methodologies inspired by the intelligent capabilities of human operators. Particularly, we focus on two essential characteristics that a human operator brings to the control loop, namely their adaptability and use of memory.

In spite of the numerous efforts in the field of control theory, the human operator is still indispensable in the control loop of a variety of critical tasks, where uncertainty in the controlled elements and unanticipated external influences can lead to catastrophic events. Among the numerous control architectures developed to emulate human-like capabilities, are adaptive control methods, which are designed to cope with anomalies in the plant dynamics. While adaptive control theory is a well-established field, with multiple results providing rigorous stability and performance guarantees, several open-problems hinder their implementation in practical industrial applications [1].

One drawback of adaptive control systems is observed from their limited employment in applications where human operators exist in the loop. In fact, unfavorable interactions between human pilots and adaptive controllers have been reported in certain flight tests [2], owing to their highly nonlinear characteristics, which makes them hardly predictable. Consequently, to aid in the design

of adaptive controllers for piloted applications, a human-in-the loop analysis is deemed necessary. The validity of such analyses relies on how accurately the human control behavior is modeled.

Human pilot models play a crucial role in the evaluation of human-in-the-loop control systems as they allow the designer to test controllers through a simulation environment. Additionally, they provide analytical insights into how to better design controllers for manned applications. While several pilot models exist in the literature, usually providing a simple fixed representation of human pilots [3, 4], these models fail to capture how a pilot behaves adaptively in the face of unexpected anomalies in the system. To address this issue, a few adaptive human pilot models have been proposed in the literature for systems with uncertainties [5–7], which, unlike fixed models, can adapt to changes in the plant dynamics. However, just like fixed pilot models, the existing adaptive pilot models assume that the human operates on a simple time-invariant control system, making them unsuitable for the evaluation of adaptive control systems.

Therefore, to pave the way towards the implementation of adaptive controllers in piloted applications, the first contribution of this thesis is an adaptive human pilot model suited to be used in the loop with an adaptive controller. The model serves as a tool for testing adaptive controllers, which can help the designer manipulate the controller parameters in order to ensure smooth pilot-controller interactions. Furthermore, the development of the model is carried out based on a rigorous Lyapunov stability analysis, which can provide analytical insights into how to better design adaptive controllers.

Another drawback of adaptive controllers lies in their transient response characteristics. While having stability guarantees is commendable, it is not sufficient to guarantee a satisfactory performance as it relies heavily on the transients. For example, the design of an adaptive controller comprises the selection of several parameters, such as the learning rates, for which no rule of thumb is known [1]. On the one end, high learning rates give rise to undesirable oscillations or unfeasible control inputs, while low learning rates lead to ineffective coping with the uncertainty. This issue spurred efforts in the literature to enhance the transients

of adaptive controllers. In this thesis, however, unlike previous works that are only devoted to enhance the transients, we focus on taking advantage of it first.

One substantial feature that distinguishes humans' control from existing control architectures is their episodic memory, which enables them to remember self-experienced events to be used later if a similar event is encountered again [8, 9]. For example, when a human operator encounters a failure for the first time, they begin exploring the situation in an attempt to recover from it, which gives rise to unavoidable transients. While lethal, these transients are necessary to enable the operator to learn how to cope with the uncertainty. However, on a second encounter of a similar failure, the operator relies on his memory of the first encounter in order to compensate the failure with minimal exploration. Such a characteristic is missing in the adaptive control literature as adaptive controllers exhibits similar transients even for previously experienced failures.

Inspired by episodic memory in humans, the second contribution of this thesis is an analogous memory architecture that allows adaptive controllers to recall and use significant information about the past to aid in learning. This enables adaptive control architectures to take advantage of transients while they exist by storing valuable data, and use them to attain a better performance in the future.

This thesis is organized as follows. Chapter 2 introduces an adaptive human pilot model for adaptive control systems. Chapter 3 builds upon the model in Chapter 2 by proposing a more sophisticated pilot model that takes into account the time delay in the pilot's response while operating on an adaptive control system, which broadens the class of suitable applications. However, unlike Chapter 2, the pilot model in Chapter 3 is developed for a simpler uncertainty in the plant dynamics due to the major difficulty posed by the inclusion of time delay. In Chapter 4, we present a novel memory architecture that can make use of stored data about the transients of previously experienced anomalies to aid in obtaining a resilient adaptive control system. Finally, a conclusion is provided in Chapter 5. Throughout the thesis, the effectiveness of the proposed architectures are validated through numerical simulations, and rigorous Lyapunov stability analyses are provided.

Chapter 2

An Adaptive Human Pilot Model for Adaptive Control Systems

2.1 Introduction

Irrespective of the numerous advances in the field of control theory, the human operator is still irreplaceable in critical tasks where uncertainty in the controlled elements and unexpected external influences can lead to catastrophic events. And with a long way ahead before reaching highly intelligent controllers that can imitate the versatility and the adaptability of human operators in controlling complex systems, several mathematical human pilot models are developed aiming to enhance the aviation safety and handling quality measures by providing valuable guidance to the control system designer.

One of the most important pilot models is the crossover model proposed by McRuer [10], which is derived based on experimental observations that a human operator controls a system in such a way that results in a well-designed linear feedback system. The crossover model is followed by many extensions forming a large pool a designer can refer to for predicting the human behavior in the loop with a wide range of time-invariant controlled elements [3,4]. But, when it comes

to modeling systems that are prone to failures, damage, and sudden parametric changes, these fixed pilot models fail to resemble how a human is found to respond adaptively in such critical situations. This shortcoming led to the development of a few adaptive human pilot models.

A prominent adaptive human pilot model is the one proposed in [5] and [6], where the adaptation laws are based on expert knowledge, aiming to make the adaptive pilot model follow the dictates of the crossover model. Inspired by this idea, a promising experimentally-validated adaptive human pilot model is recently developed in [7] and [11], by resorting to model reference adaptive control (MRAC) techniques which allows a rigorous stability analysis using the Lyapunov-Krasovskii stability criteria. These studies are conducted assuming the adaptive human pilot is operating on a linear controller-plant combination. Although there exist studies such as [12, 13], where an adaptive controller is in the loop, the pilot model used is not adaptive.

Developing adaptive pilot models that are suitable for adaptively controlled systems is important because owing to their special nonlinear characteristics, unfavorable interactions of human pilots with the adaptive control systems are observed in certain flight tests [2].

In this chapter, we propose an adaptive human pilot model suited to be used in the loop with an adaptive controller, for the first time in the literature. The model serves as a tool for testing adaptive controllers, which can help the designer manipulate the controller parameters in order to ensure smooth pilot-controller interactions. The development of the model is carried out based on MRAC architecture, with a rigorous Lyapunov stability analysis. A preliminary version of this work was reported in our conference paper [14]. The results of this chapter have been published in [15].[§]

[§]

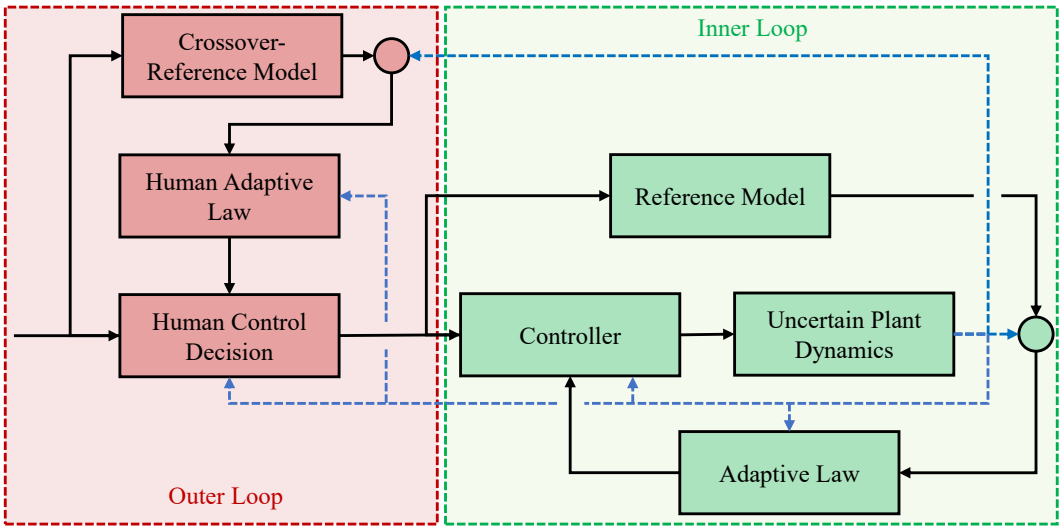

Figure 2.1: Block Diagram. © 2022 IEEE.

2.1.1 Notations

We use $\mathbb{R}^{p\times q}$ $[\mathbb{S}^{p\times q}]\{\mathbb{D}^{p\times q}\}$ to denote the set of real [symmetric real]{diagonal real} p by q matrices, and $\|.\|$ refers to the euclidean norm for vectors ($q = 1$), and the induced-2 norm for matrices. $\|.\|_F$ refers to the Frobenius norm for matrices, Tr{.} refers to the trace operator, and $(.)^T[(.)^{-1}]$ denotes the transpose [inverse] operator. Finally, we write $\lambda_{min}(A)$ for the minimum eigenvalue of the matrix A and we denote the set of positive definite real matrices by $\mathbb{R}_+^{p\times p}$.

2.2 Problem Statement

To model the human's adaptive control behavior with an adaptive controller in the loop, we start with a block diagram given in Fig. 2.1. In the figure, the block diagram is divided into inner and outer loops. The inner-loop consists of an adaptive controller controlling a plant with uncertain dynamics such that the plant states follow those of a reference model by adjusting the control parameters using an adaptive law.

The outer-loop consists of the human controlling the inner-loop such that the plant output follows a reference input. The human is assumed to be well trained, i.e., familiar with the nominal plant-controller dynamics. However, he/she is not aware of the uncertainties in the plant dynamics. This motivates modeling the human as an adaptive outer-loop controller, where an adaptive law is utilized to force the plant states to follow the states of the crossover-reference model.

2.3 Inner Loop

Consider the following uncertain plant dynamics

$$\begin{aligned} \dot{x}_p(t) =& A_p x_p(t) + B_p \Lambda u_p(t) + B_p W_p^T \sigma_p(x_p(t)), \\ y_1(t) =& C_1^T x_p(t), \\ y_2(t) =& C_2^T x_p(t), \end{aligned} \tag{2.1}$$

where $x_p(t) \in \mathbb{R}^{n_p}$ is the accessible state vector, $u_p(t) \in \mathbb{R}^m$ is the plant control input, $\sigma_p(x_p(t)) : \mathbb{R}^{n_p} \to \mathbb{R}^s$ is a known possibly non-linear basis function, $W_p \in \mathbb{R}^{s \times m}$ is an unknown weight matrix, $\Lambda \in \mathbb{R}_+^{m \times m} \cap \mathbb{D}^{m \times m}$ is an unknown control effectiveness matrix with the diagonal elements $\lambda_{i,i} \in (0, 1]$, $A_p \in \mathbb{R}^{n_p \times n_p}$ is an unknown system matrix, $B_p \in \mathbb{R}^{n_p \times m}$ is a known control input matrix, and $C_1 \in \mathbb{R}^{n_p \times m}$ and $C_2 \in \mathbb{R}^{n_p \times r}$ are both known output matrices. The outputs $y_1(t) \in \mathbb{R}^m$ and $y_2(t) \in \mathbb{R}^r$ are the outputs of interest for the inner and outer loops, respectively. Furthermore, it is assumed that the pair (A_p, B_p) is controllable.

Let the nominal plant dynamics be given as

$$\dot{x}_n(t) = A_n x_n(t) + B_p u_n(t), \tag{2.2}$$

where $u_n(t) \in \mathbb{R}^m$ is a nominal controller given as

$$u_n(t) = -L_x x_n(t) + L_r y_h(t), \tag{2.3}$$

where $y_h(t) \in \mathbb{R}^m$ is the human command, and $L_x \in \mathbb{R}^{m \times n_p}$ is such that $A_r \triangleq A_n - B_p L_x$ is Hurwitz. It is noted that the human input $y_h(t)$ is bounded due to physical manipulator limits. In the design of the outer loop, given in the next

section, human input saturation is considered in the stability analysis. Defining $B_r \triangleq B_p L_r$, the reference model is assigned as

$$\dot{x}_r(t) = A_r x_r(t) + B_r y_h(t). \tag{2.4}$$

For a constant y_h, at steady state, it is obtained using (2.4) that $\dot{x}_r(\infty) = 0 = A_r x_r(\infty) + B_r y_h$, and $x_r(\infty) = -A_r^{-1} B_p L_r y_h$. Hence, once $\lim_{t\to\infty} x_p(t) = x_r(t)$, the plant output $y_1(t)$, given in (2.1), takes the form $y_1(\infty) = -C_1^T A_r^{-1} B_p L_r y_h$. Selecting

$$L_r = -(C_1^T A_r^{-1} B_p)^{-1}, \tag{2.5}$$

results in $\lim_{t\to\infty} y_1(t) = y_h$.

Considering (2.1), which can be rewritten as

$$\dot{x}_p(t) = A_p x_p(t) + B_p \Lambda \left(u_p(t) + W^T \sigma_p(x_p(t))\right), \tag{2.6}$$

where $W^T \triangleq \Lambda^{-1} W_p^T \in \mathbb{R}^{m\times s}$ is an unknown parameter, we assume that there exist $K_x^* \in \mathbb{R}^{m\times n_p}$ and $K_r^* \in \mathbb{R}^{m\times m}$ such that the matching conditions

$$A_p - B_p \Lambda K_x^* = A_r, \tag{2.7a}$$

$$B_p \Lambda K_r^* = B_r \triangleq B_p L_r, \tag{2.7b}$$

are satisfied. The second matching condition implies that $K_r^* = \Lambda^{-1} L_r$. We define the plant control law as

$$u_p(t) = -\hat{K}_x(t) x_p(t) + \mathrm{diag}(\hat{\lambda}(t)) L_r y_h(t) - \hat{W}^T(t) \sigma_p(x_p(t)), \tag{2.8}$$

where $\hat{K}_x(t) \in \mathbb{R}^{m\times n_p}$, $\hat{\lambda}(t) \in \mathbb{R}^m$ and $\hat{W}(t) \in \mathbb{R}^{s\times m}$ are adjustable parameters serving as estimates for the ideal values K_x^*, λ^* and W, respectively. It is noted that $\mathrm{diag}\,(\lambda^*) = \Lambda^{-1}$ exists since Λ is diagonal positive definite.

Substituting (2.8) into (2.6), one can rewrite (2.6) as

$$\begin{aligned} \dot{x}_p(t) =& A_r x_p(t) + B_r y_h(t) + B_p \Lambda \mathrm{diag}(\tilde{\lambda}(t)) L_r y_h(t) \\ & - B_p \Lambda \left(\tilde{W}^T(t) \sigma_p(x_p(t)) + \tilde{K}_x(t) x_p(t)\right), \end{aligned} \tag{2.9}$$

where $\tilde{K}_x(t) \triangleq \hat{K}_x(t) - K_x^*$, $\tilde{\lambda}(t) \triangleq \hat{\lambda}(t) - \lambda^*$ and $\tilde{W}(t) \triangleq \hat{W}(t) - W$ are the adaptive parameters errors.

Defining $\Theta(t) \triangleq [\hat{W}^T(t),\ \hat{K}_x(t)]^T \in \mathbb{R}^{(s+n_p)\times m}$, with the ideal value $\Theta^* \triangleq [W^T,\ K_x^*]^T$, (2.9) can be rewritten as

$$\begin{aligned}\dot{x}_p(t) =& A_r x_p(t) + B_r y_h(t) + B_p \Lambda \text{diag}(\tilde{\lambda}(t)) L_r y_h(t) \\ & - B_p \Lambda \tilde{\Theta}^T(t) \sigma(x_p(t)),\end{aligned} \tag{2.10}$$

where $\tilde{\Theta}(t) \triangleq \Theta(t) - \Theta^*$ and $\sigma(x_p(t)) \triangleq [\sigma_p^T(x_p(t)),\ x_p^T(t)]^T \in \mathbb{R}^{s+n_p}$.

By subtracting (2.4) from (2.10), and exploiting the fact that $\Lambda \text{diag}(\tilde{\lambda}(t)) L_r y_h(t) = \text{diag}(L_r y_h(t)) \Lambda \tilde{\lambda}(t)$, we obtain that

$$\dot{e}_1(t) = A_r e_1(t) + B_p \text{diag}(L_r y_h(t)) \Lambda \tilde{\lambda}(t) - B_p \Lambda \tilde{\Theta}^T(t) \sigma(x_p(t)), \tag{2.11}$$

where $e_1(t) \triangleq x_p(t) - x_r(t)$ is the inner-loop tracking error. We define the inner-loop adaptive laws as

$$\dot{\tilde{\Theta}}(t) = \dot{\Theta}(t) = \gamma_\theta \sigma(x_p(t)) e_1(t)^T P_1 B_p, \tag{2.12a}$$

$$\dot{\tilde{\lambda}}(t) = \dot{\hat{\lambda}}(t) = \gamma_\lambda \text{Proj}\left(\hat{\lambda}(t),\ -\text{diag}(L_r y_h(t)) B_p^T P_1 e_1(t)\right), \tag{2.12b}$$

where Proj(.,.) is the projection operator [16, 17] used to bound the adaptive parameter $\hat{\lambda}(t)$ in a compact set with each element $\hat{\lambda}_i(t)$ having positive upper and lower bounds $\hat{\lambda}_{max_i}$ and $\hat{\lambda}_{min_i}$. Furthermore, $\gamma_\theta, \gamma_\lambda \in \mathbb{R}_+$ are learning rates, and $P_1 \in \mathbb{R}_+^{n_p \times n_p} \cap \mathbb{S}^{n_p \times n_p}$ is the solution of $A_r^T P_1 + P_1 A_r = -Q_1$, for some $Q_1 \in \mathbb{R}_+^{n_p \times n_p} \cap \mathbb{S}^{n_p \times n_p}$.

Lemma 2.1. Consider the uncertain dynamical system (2.1), the reference model (2.4), and the feedback control law given by (2.8) and (2.12). The solution $(e_1(t), \tilde{\Theta}(t), \tilde{\lambda}(t))$ is Lyapunov stable in the large. Furthermore, since the human command $y_h(t)$ is bounded, $\lim_{t\to\infty} e_1(t) = 0$ and $\dot{\tilde{\Theta}}(t)$ and $\dot{\tilde{\lambda}}(t)$ remain bounded along with all the signals in the inner-loop.

Proof. Consider the Lyapunov function candidate

$$V_1 = e_1^T P_1 e_1 + \gamma_\theta^{-1} \text{Tr}\{(\tilde{\Theta}\Lambda^{1/2})^T (\tilde{\Theta}\Lambda^{1/2})\} + \gamma_\lambda^{-1} \tilde{\lambda}^T \Lambda \tilde{\lambda}. \tag{2.13}$$

Differentiating along the trajectories (2.11) and (2.12) yields

$$\begin{aligned}\dot{V}_1 =&\dot{e}_1^T P_1 e_1 + e_1^T P_1 \dot{e}_1 + 2\gamma_\theta^{-1}\mathrm{Tr}\{\tilde{\Theta}^T\dot{\tilde{\Theta}}\Lambda\} + 2\gamma_\lambda^{-1}\tilde{\lambda}^T\Lambda\dot{\tilde{\lambda}}\\ =&-e_1^T Q_1 e_1 + 2\gamma_\theta^{-1}\mathrm{Tr}\{\tilde{\Theta}^T\dot{\tilde{\Theta}}\Lambda\} + 2\gamma_\lambda^{-1}\tilde{\lambda}^T\Lambda\dot{\tilde{\lambda}}\\ &-2\mathrm{Tr}\{\tilde{\Theta}^T\sigma(x_p)e_1^T P_1 B_p\Lambda\} + 2\tilde{\lambda}^T\Lambda\mathrm{diag}(L_r y_h)B_p^T P_1 e_1\\ =&-e_1^T Q_1 e_1 + 2\tilde{\lambda}^T\Lambda\Big(\mathrm{Proj}(\hat{\lambda}, -\mathrm{diag}(L_r y_h)B_p^T P_1 e_1)\\ &+\mathrm{diag}(L_r y_h)B_p^T P_1 e_1\Big).\end{aligned} \tag{2.14}$$

Using the property $(\theta_{i,j} - \theta^*_{i,j})(\mathrm{Proj}(\theta_{i,j}, Y_{i,j}) - Y_{i,j}) \leq 0$ and the fact that Λ is diagonal positive definite, it follows that

$$\dot{V}_1 \leq -e_1^T Q_1 e_1 \leq 0. \tag{2.15}$$

Hence, the solution $(e_1(t), \tilde{\Theta}(t), \tilde{\lambda}(t))$ is stable in the large.

Equation (2.4) indicates that the boundedness of $y_h(t)$ implies the boundedness of $x_r(t)$. The latter coupled with the fact that $e_1(t)$ is bounded imply the boundedness of $x_p(t)$, which in turn implies that $(\dot{e}_1(t), \dot{\tilde{\Theta}}(t), \dot{\tilde{\lambda}}(t))$ are bounded. It then follows from Barbalat's lemma that $\lim_{t\to\infty} e_1(t) = 0$. ■

2.4 Outer Loop

Using (2.7), and $\mathrm{diag}(\lambda^*) = \Lambda^{-1}$, (2.10) can be rewritten as

$$\dot{x}_p(t) = A_r x_p(t) + B_p\Lambda\mathrm{diag}(\hat{\lambda}(t))L_r y_h(t) - B_p\Lambda\tilde{\Theta}^T(t)\sigma(x_p(t)). \tag{2.16}$$

Since we assume that the human operator is familiar with the nominal dynamics (2.2) and (2.3), the only unknowns in (2.16) for the outer loop are the parameters Λ, $\hat{\lambda}(t)$ and $\tilde{\Theta}(t)$.

Consider the integral action

$$\dot{x}_c(t) = y_2(t) - r(t) + J(t)\Delta y(t), \tag{2.17}$$

where $x_c(t) \in \mathbb{R}^r$ is the integrator state, $r(t) \in \mathbb{R}^r$ is a bounded reference input, and $J(t) \in \mathbb{R}^{r\times m}$ is a control parameter defined below. The term $J(t)\Delta y(t)$,

which will be explained later, is included to avoid integrator windup, and it only takes action when the human input is saturated [18, 19]. Aggregating (2.16) and (2.17) results in the augmented dynamics

$$\begin{aligned}\dot{x}(t) =& Ax(t) + B_m r(t) - B_m J(t)\Delta y(t) \\ &+ BH^T(t)\sigma(x_p(t)) + B\Lambda_2(t)L_r y_h(t),\end{aligned} \tag{2.18}$$

where $x(t) \triangleq [x_p^T(t), x_c^T(t)]^T \in \mathbb{R}^n$ is the augmented state vector with $n = n_p + r$, $H^T(t) \triangleq -\Lambda\tilde{\Theta}^T(t)$ and $\Lambda_2(t) \triangleq \Lambda\text{diag}(\hat{\lambda}(t))$ are unknown time-varying parameters, and

$$A \triangleq \begin{bmatrix} A_r & 0_{n_p\times r} \\ C_2^T & 0_{r\times r}\end{bmatrix} \in \mathbb{R}^{n\times n}, \tag{2.19a}$$

$$B \triangleq \begin{bmatrix} B_p^T & 0_{m\times r}\end{bmatrix}^T \in \mathbb{R}^{n\times m}, \tag{2.19b}$$

$$B_m \triangleq \begin{bmatrix} 0_{r\times n_p} & -I_{r\times r}\end{bmatrix}^T \in \mathbb{R}^{n\times r}. \tag{2.19c}$$

The goal of the human is to control the system such that the plant states follow that of a unity feedback reference model with an open-loop crossover model transfer function. We refer to the latter as the *crossover-reference model* (Fig. 2.1). Let the crossover-reference model be given as

$$\dot{x}_m(t) = A_m x_m(t) + B_m r(t), \tag{2.20}$$

where $x_m(t) \in \mathbb{R}^n$ is the crossover-reference model state vector, and $A_m \in \mathbb{R}^{n\times n}$ is Hurwitz.

In an ideal case where the human input is not saturated, and both $H(t)$ and $\Lambda_2(t)$ are known, the following control law achieves the crossover-reference model dynamics

$$\mathcal{G}^*(t) = -\theta_x x(t) - L_r^{-1}H^T(t)\sigma(x_p(t)), \tag{2.21a}$$

$$y_h^*(t) = L_r^{-1}\Lambda_2^{-1}(t)L_r\mathcal{G}^*(t), \tag{2.21b}$$

where we assume that there exists $\theta_x \in \mathbb{R}^{m\times n}$ such that $A_m = A - BL_r\theta_x$. We define the human control input by augmenting the baseline PI-control term

$-\theta_x x(t)$ with adaptive components as

$$\mathcal{G}(t) = -\theta_x x(t) - L_r^{-1}\hat{H}^T(t)\sigma(x_p(t)), \tag{2.22a}$$

$$v(t) = L_r^{-1}\text{diag}(\hat{\lambda}_2(t))L_r\mathcal{G}(t), \tag{2.22b}$$

$$y_{h_i}(t) = \begin{cases} v_i(t), & \text{if } |v_i(t)| \leq y_{o_i}, \\ y_{o_i}\text{sgn}(v_i(t)), & \text{if } |v_i(t)| > y_{o_i}, \end{cases} \tag{2.22c}$$

where $\hat{H}(t)$ and $\hat{\lambda}_2(t)$ are adjustable parameters serving as estimates for the ideal values $H(t)$ and $\lambda_2^*(t)$, respectively. It is noted that $\text{diag}\,(\lambda_2^*(t)) = \Lambda_2^{-1}(t)$ exists for all $t \geq 0$ since $\Lambda_2(t)$ is diagonal positive definite at all time instants. Finally, (2.22c) is an element-wise saturation function where $y_{o_i} \in \mathbb{R}_+$ is the saturation limit of $y_{h_i}(t)$ (the i^{th} element of $y_h(t)$).

Remark 2.1. Such a θ_x exists only if A_m is selected such that

$$A_m \triangleq \begin{bmatrix} A_r - B_r\phi & -B_r\psi \\ C_2^T & 0_{r\times r} \end{bmatrix} \in \mathbb{R}^{n\times n}, \tag{2.23}$$

for some $\phi \in \mathbb{R}^{m\times n_p}$ and $\psi \in \mathbb{R}^{m\times r}$. Then, θ_x can be assigned as

$$\theta_x \triangleq \begin{bmatrix} \phi & \psi \end{bmatrix} \in \mathbb{R}^{m\times n}. \tag{2.24}$$

Assumption 2.1. It is assumed that there exists a matrix $M \in \mathbb{R}^{r\times m}$ such that $M\psi \in \mathbb{R}^{r\times r}$ is Hurwitz. This assumption is used in Theorem 2.1. below.

Substituting (2.22) into (2.18), we obtain that

$$\begin{aligned} \dot{x}(t) =& A_m x(t) + B_m r(t) - B_m J(t)\Delta y(t) + B\Lambda_2(t)L_r\Delta y(t) \\ & - B\tilde{H}^T(t)\sigma(x_p(t)) + B\Lambda_2(t)\text{diag}(\tilde{\lambda}_2(t))L_r\mathcal{G}(t), \end{aligned} \tag{2.25}$$

where $\tilde{H}(t) \triangleq \hat{H}(t) - H(t)$ and $\tilde{\lambda}_2(t) \triangleq \hat{\lambda}_2(t) - \lambda_2^*(t)$ are outer-loop adaptive parameters errors, and $\Delta y(t) \triangleq y_h(t) - v(t)$ is the control deficiency due to human input saturation.

Subtracting (2.20) from (2.25), and exploiting the fact that $\Lambda_2(t)\text{diag}(\tilde{\lambda}_2(t))L_r\mathcal{G}(t) =$

$\text{diag}(L_r\mathcal{G}(t))\Lambda_2(t)\tilde{\lambda}_2(t)$ results in the outer-loop error dynamics

$$\begin{aligned}\dot{e}_2(t) =& A_m e_2(t) - B_m J(t)\Delta y(t) + B\Lambda_2(t)L_r\Delta y(t) \\ & - B\tilde{H}^T(t)\sigma(x_p(t)) + B\text{diag}(L_r\mathcal{G}(t))\Lambda_2(t)\tilde{\lambda}_2(t),\end{aligned} \tag{2.26}$$

where $e_2(t) \triangleq x(t) - x_m(t)$ is the outer-loop tracking error.

We generate an auxiliary signal $e_\Delta(t)$ as in [20, 21]

$$\begin{aligned}&\dot{e}_\Delta(t) = A_m e_\Delta(t) - B_m J(t)\Delta y(t) + B\text{diag}(\hat{\lambda}_3(t))L_r\Delta y(t), \\ &e_\Delta(t_0) = 0,\end{aligned} \tag{2.27}$$

where $\hat{\lambda}_3(t)$ is an adjustable parameter serving as an estimate for the ideal value $\lambda_3^*(t)$, and $\text{diag}(\lambda_3^*(t)) = \Lambda_2(t)$. Defining an augmented error signal $e_y(t) \triangleq e_2(t) - e_\Delta(t)$, and using the fact that $\text{diag}(\tilde{\lambda}_3(t))L_r\Delta y(t) = \text{diag}(L_r\Delta y(t))\tilde{\lambda}_3(t)$ yields

$$\begin{aligned}\dot{e}_y(t) =& A_m e_y(t) - B\text{diag}(L_r\Delta y(t))\tilde{\lambda}_3(t) \\ & - B\tilde{H}^T(t)\sigma(x_p(t)) + B\text{diag}(L_r\mathcal{G}(t))\Lambda_2(t)\tilde{\lambda}_2(t),\end{aligned} \tag{2.28}$$

where $\tilde{\lambda}_3(t) \triangleq \hat{\lambda}_3(t) - \lambda_3^*(t)$. Equation (2.28) is in a standard error model form. We propose the adaptive laws

$$\dot{\hat{H}}(t) = \gamma_H \text{Proj}\left(\hat{H}(t),\ \sigma(x_p(t))e_y^T(t)P_2B\right), \tag{2.29a}$$

$$\dot{\hat{\lambda}}_2(t) = \gamma_2 \text{Proj}\left(\hat{\lambda}_2(t),\ -\text{diag}(L_r\mathcal{G}(t))B^TP_2e_y(t)\right), \tag{2.29b}$$

$$\dot{\hat{\lambda}}_3(t) = \gamma_3 \text{Proj}\left(\hat{\lambda}_3(t),\ \text{diag}(L_r\Delta y(t))B^TP_2e_y(t)\right), \tag{2.29c}$$

where $\gamma_H, \gamma_2, \gamma_3 \in \mathbb{R}_+$ are learning rates, and $P_2 \in \mathbb{R}_+^{n\times n} \cap \mathbb{S}^{n\times n}$ is the solution of $A_m^TP_2 + P_2A_m = -Q_2$, for some $Q_2 \in \mathbb{R}_+^{n\times n} \cap \mathbb{S}^{n\times n}$. In addition, we impose bounds on the elements of $\hat{\lambda}_2(t)$ with each element $\hat{\lambda}_{2_i}(t)$ having positive upper and lower bounds $\hat{\lambda}_{2max_i}$ and $\hat{\lambda}_{2min_i}$. This ensures that $\text{diag}(\hat{\lambda}_2(t))$ is always invertible.

Finally, regarding the anti-windup term used in (2.17), and with Assumption 2.1 satisfied, we define $J(t)$ as

$$J(t) = ML_r^{-1}\text{diag}(\hat{\lambda}_2(t))^{-1}L_r, \tag{2.30}$$

which is bounded since $\hat{\lambda}_{2min_i} > 0$, $i = 1, ..., m$.

Remark 2.2. It follows from Lemma 2.1 that $\tilde{\Theta}(t)$, $\hat{\lambda}(t)$, $\dot{\tilde{\Theta}}(t)$ and $\dot{\hat{\lambda}}(t)$ are bounded, which implies the boundedness of $H(t)$, $\Lambda_2(t)$, $\dot{H}(t)$ and $\dot{\Lambda}_2(t)$. Therefore, there exist $h \in \mathbb{R}_+$, $\dot{h} \in \mathbb{R}_+$, $\beta_3 \in \mathbb{R}_+$ and $\dot{\beta}_3 \in \mathbb{R}_+$ such that $\|H(t)\| \leq h$, $\|\dot{H}(t)\| \leq \dot{h}$, $\|\Lambda_2(t)\|_F \leq \beta_3$ and $\|\dot{\Lambda}_2(t)\|_F \leq \dot{\beta}_3$ for all $t \geq 0$. The latter implies that $\|\lambda_3^*(t)\| \leq \beta_3$ and $\|\dot{\lambda}_3^*(t)\| \leq \dot{\beta}_3$. Moreover, as $\hat{\lambda}_{min_i} > 0$ for $i = 1, ..., m$, there exists $\beta_2 \in \mathbb{R}_+$ such that $\|\Lambda_2^{-1}(t)\|_F \leq \beta_2$. And since $\frac{\mathrm{d}\Lambda_2^{-1}}{\mathrm{d}t} = -\Lambda_2^{-1}\dot{\Lambda}_2\Lambda_2^{-1}$, then there exists $\dot{\beta}_2 \in \mathbb{R}_+$ such that $\|\frac{\mathrm{d}\Lambda_2^{-1}}{\mathrm{d}t}\|_F \leq \dot{\beta}_2$. This implies that $\|\lambda_2^*(t)\| \leq \beta_2$ and $\|\dot{\lambda}_2^*(t)\| \leq \dot{\beta}_2$ for all $t \geq 0$.

Theorem 2.1. Consider the uncertain dynamical system (2.1), the adaptive controller given by (2.4), (2.8) and (2.12), and the adaptive pilot model given by (2.17), (2.20), (2.22) and (2.29). Then, the solution $(e_y(t), \tilde{H}(t), \tilde{\lambda}_2(t), \tilde{\lambda}_3(t))$ remains bounded for all $t \geq 0$ and converges to the compact set

$$E \triangleq \left\{ \left(e_y(t), \tilde{H}(t), \tilde{\lambda}_2(t), \tilde{\lambda}_3(t)\right) : \|e_y(t)\|^2 \leq \eta, \|\tilde{H}(t)\| \leq \tilde{h}, \|\tilde{\lambda}_2(t)\| \leq \tilde{\alpha}_2 \text{ and } \|\tilde{\lambda}_3(t)\| \leq \tilde{\alpha}_3 \right\}, \tag{2.31}$$

where

$$\eta \triangleq \frac{2\gamma_H^{-1}\tilde{h}\dot{h} + 2\gamma_2^{-1}\tilde{\alpha}_2\beta_3\dot{\beta}_2 + \gamma_2^{-1}\tilde{\alpha}_2\dot{\beta}_3\tilde{\alpha}_2 + 2\gamma_3^{-1}\tilde{\alpha}_3\dot{\beta}_3}{\lambda_{min}(Q_2)}, \tag{2.32}$$

$\tilde{h} \triangleq \|\hat{H}_{max}\| + h$, $\tilde{\alpha}_2 \triangleq \|\hat{\lambda}_{2max}\| + \beta_2$, $\tilde{\alpha}_3 \triangleq \|\hat{\lambda}_{3max}\| + \beta_3$, and h, $\dot{h}$, β_2, $\dot{\beta}_2$, β_3 and $\dot{\beta}_3$ are defined in Remark 2.2. Furthermore, all system signals are bounded.

Proof. Consider the Lyapunov function candidate

$$V_2(e_y, \tilde{H}, \tilde{\lambda}_2, \tilde{\lambda}_3) = e_y^T P_2 e_y + \gamma_H^{-1}\mathrm{Tr}\{\tilde{H}^T\tilde{H}\} + \gamma_2^{-1}\tilde{\lambda}_2^T\Lambda_2\tilde{\lambda}_2 + \gamma_3^{-1}\tilde{\lambda}_3^T\tilde{\lambda}_3. \tag{2.33}$$

Differentiating along the trajectories (2.28) and (2.29) yields

$$\begin{aligned}
\dot{V}_2 =& \dot{e}_y^T P_2 e_y + e_y^T P_2 \dot{e}_y + 2\gamma_H^{-1}\mathrm{Tr}\{\tilde{H}^T\dot{\tilde{H}}\} \\
&+ 2\gamma_2^{-1}\tilde{\lambda}_2^T\Lambda_2\dot{\tilde{\lambda}}_2 + \gamma_2^{-1}\tilde{\lambda}_2^T\dot{\Lambda}_2\tilde{\lambda}_2 + 2\gamma_3^{-1}\tilde{\lambda}_3^T\dot{\tilde{\lambda}}_3 \\
=& - e_y^T Q_2 e_y - 2\mathrm{Tr}\{\tilde{H}^T\sigma(x_p)e_y^T P_2 B\} \\
&+ 2\tilde{\lambda}_2^T\Lambda_2\mathrm{diag}(L_r\mathcal{G})B^T P_2 e_y - 2\tilde{\lambda}_3^T\mathrm{diag}(L_r\Delta y)B^T P_2 e_y \\
&+ 2\gamma_H^{-1}\mathrm{Tr}\{\tilde{H}^T\dot{\hat{H}}\} - 2\gamma_H^{-1}\mathrm{Tr}\{\tilde{H}^T\dot{H}\} \\
&+ 2\gamma_2^{-1}\tilde{\lambda}_2^T\Lambda_2\dot{\tilde{\lambda}}_2 - 2\gamma_2^{-1}\tilde{\lambda}_2^T\Lambda_2\dot{\lambda}_2^* + \gamma_2^{-1}\tilde{\lambda}_2^T\dot{\Lambda}_2\tilde{\lambda}_2 \\
&+ 2\gamma_3^{-1}\tilde{\lambda}_3^T\dot{\tilde{\lambda}}_3 - 2\gamma_3^{-1}\tilde{\lambda}_3^T\dot{\lambda}_3^* \\
=& - e_y^T Q_2 e_y + \gamma_2^{-1}\tilde{\lambda}_2^T\dot{\Lambda}_2\tilde{\lambda}_2 \\
&- 2\gamma_H^{-1}\mathrm{Tr}\{\tilde{H}^T\dot{H}\} - 2\gamma_2^{-1}\tilde{\lambda}_2^T\Lambda_2\dot{\lambda}_2^* - 2\gamma_3^{-1}\tilde{\lambda}_3^T\dot{\lambda}_3^* \\
&+ 2\mathrm{Tr}\left\{\tilde{H}^T\left(\mathrm{Proj}(\hat{H}, Y_H) - Y_H\right)\right\} \\
&+ 2\tilde{\lambda}_2^T\Lambda_2\left(\mathrm{Proj}(\hat{\lambda}_2, Y_2) - Y_2\right) \\
&+ 2\tilde{\lambda}_3^T\left(\mathrm{Proj}(\hat{\lambda}_3, Y_3) - Y_3\right),
\end{aligned} \tag{2.34}$$

where $Y_H \triangleq \sigma(x_p)e_y^T P_2 B$, $Y_2 \triangleq -\mathrm{diag}(L_r\mathcal{G})B^T P_2 e_y$ and $Y_3 \triangleq \mathrm{diag}(L_r\Delta y(t))B^T P_2 e_y$. Using the projection property $(\theta_{i,j} - \theta_{i,j}^*)(\mathrm{Proj}(\theta_{i,j}, Y_{i,j}) - Y_{i,j}) \leq 0$, Remark 2.2, and the fact that $\Lambda_2(t)$ is diagonal positive definite, we obtain

$$\begin{aligned}
\dot{V}_2 \leq& - e_y^T Q_2 e_y + \gamma_2^{-1}\tilde{\lambda}_2^T\dot{\Lambda}_2\tilde{\lambda}_2 \\
&- 2\gamma_H^{-1}\mathrm{Tr}\{\tilde{H}^T\dot{H}\} - 2\gamma_2^{-1}\tilde{\lambda}_2^T\Lambda_2\dot{\lambda}_2^* - 2\gamma_3^{-1}\tilde{\lambda}_3^T\dot{\lambda}_3^* \\
\leq& - \lambda_{min}(Q_2)\|e_y\|^2 + \lambda_{min}(Q_2)\eta.
\end{aligned} \tag{2.35}$$

Hence, $\dot{V}_2 < 0$ outside the compact set (2.31), which proves the boundedness of $(e_y(t), \hat{H}(t), \hat{\lambda}_2(t), \hat{\lambda}_3(t))$. The boundedness of all the signals in the inner-loop, including $x_p(t)$, follows from Lemma 2.1. According to (2.20), since $r(t)$ is bounded, $x_m(t)$ is also bounded, which leaves us only to prove that $x_c(t)$ is bounded to complete the proof.

We prove the boundedness of $x_c(t)$ (and hence $x(t)$) by considering the cases where a) $\Delta y(t) = 0$ and b) $\Delta y(t) \neq 0$.

Case a) $\Delta y(t) = 0$: It follows from (2.27) that $e_\Delta(t)$ is bounded which by the fact that $e_y(t)$ is bounded, shows the boundedness of $e_2(t)$ and $x(t)$.

Case b) $\Delta y(t) \neq 0$: Using $\Delta y(t) = y_h(t) - v(t)$, (2.17) can be rewritten as

$$\dot{x}_c(t) = C_2^T x_p(t) - r(t) + J(t)y_h(t) - J(t)v(t). \tag{2.36}$$

Substituting (2.22b) and (2.22a), one can rewrite (2.36) as

$$\begin{aligned}\dot{x}_c(t) =& C_2^T x_p(t) - r(t) + J(t)y_h(t) \\ &+ J(t)L_r^{-1}\text{diag}(\hat{\lambda}_2(t))L_r\theta_x x(t) \\ &+ J(t)L_r^{-1}\text{diag}(\hat{\lambda}_2(t))\hat{H}^T(t)\sigma(x_p(t)).\end{aligned} \tag{2.37}$$

Using (2.24), it is obtained by substituting $\theta_x x(t) = \phi x_p(t) + \psi x_c(t)$ and (2.30) into (2.37) that

$$\begin{aligned}\dot{x}_c(t) =& J(t)L_r^{-1}\text{diag}(\hat{\lambda}_2(t))L_r\psi x_c(t) + w(t), \\ =& M\psi x_c(t) + w(t), \\ w(t) \triangleq& (C_2^T + M\phi)x_p(t) - r(t) + J(t)y_h(t) + ML_r^{-1}\hat{H}^T(t)\sigma(x_p(t)).\end{aligned} \tag{2.38}$$

As $r(t), \hat{H}(t), y_h(t), J(t)$ and $x_p(t)$ are bounded, then so is $w(t)$. Therefore, it follows from Assumption 2.1 and (2.38) that $x_c(t)$ is bounded which implies the boundedness of $x(t)$.

The boundedness of $e_2(t)$ follows from the boundedness of $x(t)$ as $x_m(t)$ is bounded. Since $e_y(t) = e_2(t) - e_\Delta(t)$ is bounded, then $e_\Delta(t)$ is also bounded, which implies by (2.27) that $\Delta y(t)$ is bounded and completes the proof. ■

2.5 Special Case: Systems with Free Integrators

The assignment of L_r given in (2.5) is invalid when $C_1^T A_r^{-1} B_p$ is singular. This may happen, for example, when the pilot commands attitude rates to the inner-loop controller aiming to achieve desired attitude angles. In such a case, (2.1) can be modified by separating the states as

$$\begin{aligned}\begin{bmatrix}\dot{x}_s \\ \dot{x}_\theta\end{bmatrix} =& \begin{bmatrix}A_s & 0 \\ C_{1s}^T & 0\end{bmatrix}\begin{bmatrix}x_s \\ x_\theta\end{bmatrix} + \begin{bmatrix}B_s \\ 0\end{bmatrix}\Lambda(u_p(t) + W^T\sigma_p(x_s(t))), \\ y_1(t) =& \dot{x}_\theta(t) = C_{1s}^T x_s(t), \\ y_2(t) =& x_\theta(t) = C_2^T x_p(t),\end{aligned} \tag{2.39}$$

where $x_s(t) \in \mathbb{R}^{n_s}$, $x_\theta(t) \in \mathbb{R}^m$, and $x_p(t) \triangleq [x_s^T,\ x_\theta^T]^T \in \mathbb{R}^{n_p}$. To ensure the existence of L_r, the adaptive controller is made responsible only for the control of $x_s(t)$ dynamics while making sure that the human input $y_h(t)$ is being tracked by the plant. This yields inner-loop dynamics similar to (2.10) as

$$\begin{aligned}\dot{x}_s(t) =& A_{rs}x_s(t) + B_{rs}y_h(t) + B_s\Lambda \mathrm{diag}(\tilde{\lambda}(t))L_r y_h(t) \\ &- B_s\Lambda\tilde{\Theta}^T(t)\sigma(x_s(t)),\end{aligned} \tag{2.40}$$

where the pair (A_{rs}, B_{rs}) describe the modified reference model dynamics with the nominal dynamics of $x_s(t)$ represented by (A_{ns}, B_s). Augmenting (2.40) with $x_\theta(t)$ dynamics results in a closed loop system similar to (2.16) which directly extends the previous results of this chapter to the case in hand.

2.6 Simulations

Consider a large transport aircraft model [22] linearized at Mach 0.3 and altitude 1000m in the form of (2.39), where

$$x_s(t) = \begin{bmatrix}\alpha & q & \beta & p & r\end{bmatrix}^T, \quad \dot{x}_\theta(t) = \begin{bmatrix}p & q & r\end{bmatrix}^T, \tag{2.41}$$

α (rad) is the angle of attack, β (rad) is the side-slip angle, and p, q and r (rad/s) are the roll, pitch and yaw rates, respectively. The input vector is defined as

$$u_p(t) = \begin{bmatrix}\delta_e & \delta_a & \delta_r\end{bmatrix}^T, \tag{2.42}$$

consisting of the deflections (in rad) of 2 ganged elevators δ_e, 2 ganged ailerons δ_a and 2 ganged rudders δ_r. The numerical data used in the simulations are given in Table 2.1.

The matched system uncertainty $W_p^T\sigma_p(x_s(t))$ is given by $\sigma_p(x_s(t)) \triangleq [1, q, p, r]^T$. A pilot is controlling the aircraft to achieve desired attitude angles by feeding attitude rate commands to the inner-loop controller using a side-stick.

To design the crossover-reference model (2.20), the LQR method is used with $Q_{LQR} = \mathrm{diag}([0_{1\times 8}, 5, 5, 5])$ and $R_{LQR} = 5I_{3\times 3}$ which yields θ_x in (2.24) with the

Table 2.1: Numerical data used in the simulations. © 2022 IEEE.

A_{ns}	[-0.6582 0.9705 0 0 0; -3.3105 -1.4741 0 0 0; 0 0 -0.1706 -0.0075 -1; 0 0 -2.4792 1.3585 0.5897; 0 0 0.8050 0.0559 -0.5584]
A_s	[-0.8489 1.1494 -0.0356 -0.0014 -0.0087; -12.8627 7.4865 -1.7827 -0.0688 -0.4341;-0.1071 -0.0004 -0.6684 -0.0140 -1.6727; -0.0807 -0.0474 -0.6318 3.0151 -0.3975;1.0380 0.0093 5.3771 -0.0697 6.0156]
A_{rs}	[-0.6582 0.9705 0 0 0; -3.3105 -1.4741 0 0 0; 0 0 -0.1161 0.0321 -0.9471; 0 0 0 -1.5 0; 0 0 0 0 -1]
B_s	[-0.0734 0 0;-3.6764 0 0;0 0 0.0256; 0 1.0924 0.1240;0 -0.1240 -0.2600]
W_p	[0.5 0.5 0.5;0.2 0.2 0.2;0.1 0.1 0.1;0.5 0.5 0.5]

sub-matrix $\psi = I_{3\times3}$. As all eigen values of ψ have positive real parts, we assume $M = -100I_{3\times3}$ which ensures that $M\psi$ is Hurwitz. In addition, the Lyapunov matrices are taken as $Q_1 = I_{5\times5}$ and $Q_2 = 2I_{11\times11}$, and the human pilot's learning rates are assumed to be $\gamma_H = \gamma_2 = \gamma_3 = 20$. The human's command is saturated as in (2.22c) with $y_{o_i} = 20$ deg/s for $i = 1, \ldots, 3$, $\Lambda = I_{3\times3}$ for $t < 40$ sec, and we introduce a failure into the system by making $\Lambda = 0.3I_{3\times3}$ for $t \geq 40$ sec.

Figs 2.2 and 2.3 show the aircraft attitude angles and the evolution of the pilot commands, respectively for different inner-loop learning rates. Good tracking performance is observed for the cases where $\gamma_\theta = \gamma_\lambda = 100$ and $\gamma_\theta = \gamma_\lambda = 50$ while the pilot commands show an oscillatory behavior when an uncertainty is introduced to the system. However, for the cases where $\gamma_\theta = \gamma_\lambda = 40$ and $\gamma_\theta = \gamma_\lambda = 10$, despite the boundedness of all the signals, the tracking performance significantly deteriorates resulting in consistent high amplitude oscillations. Furthermore, pilot commands saturate in the pitch direction since the pilot spends more effort to maintain a satisfactory performance due to a slower adaptive controller.

The simulations in Figs 2.2 and 2.3 are not aimed towards providing high-performance controller implementation examples, but rather to demonstrate a use case for the presented modeling approach where the effect of the adaptive controller learning rate on the behavior of the pilot is investigated.

2.7 Summary

In this chapter, we propose an adaptive human pilot model that describes the human behavior in the loop with an adaptive controller. The pilot is modeled as a model-reference adaptive control architecture where, when faced with an anomaly, the pilot adapts in such a way that results in following the dictates of the crossover model. Furthermore, a numerical simulation of a transport aircraft is provided, where we demonstrate a use case for the presented model.

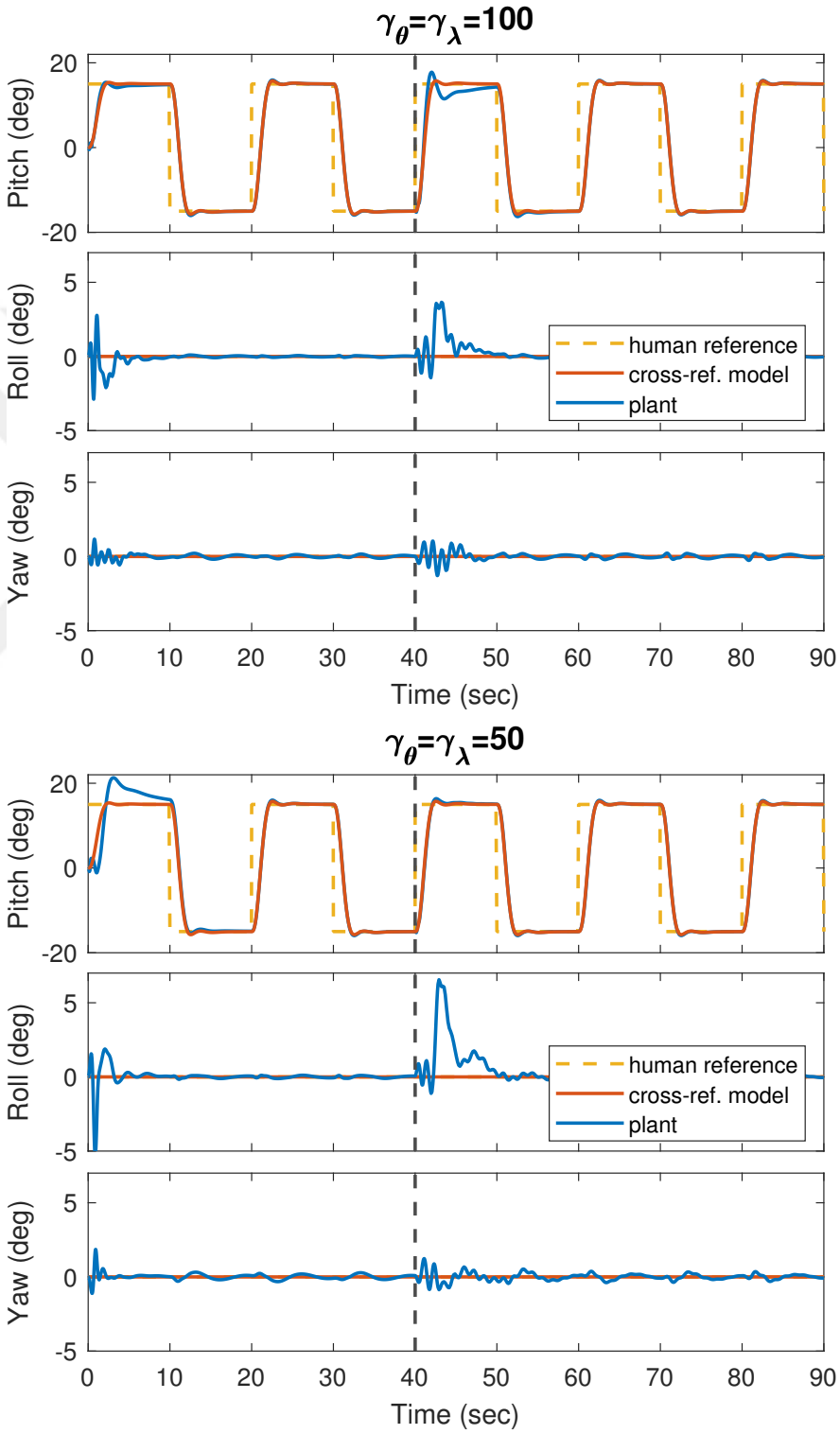

Figure 2.2: Attitude angles for different inner-loop learning rates.

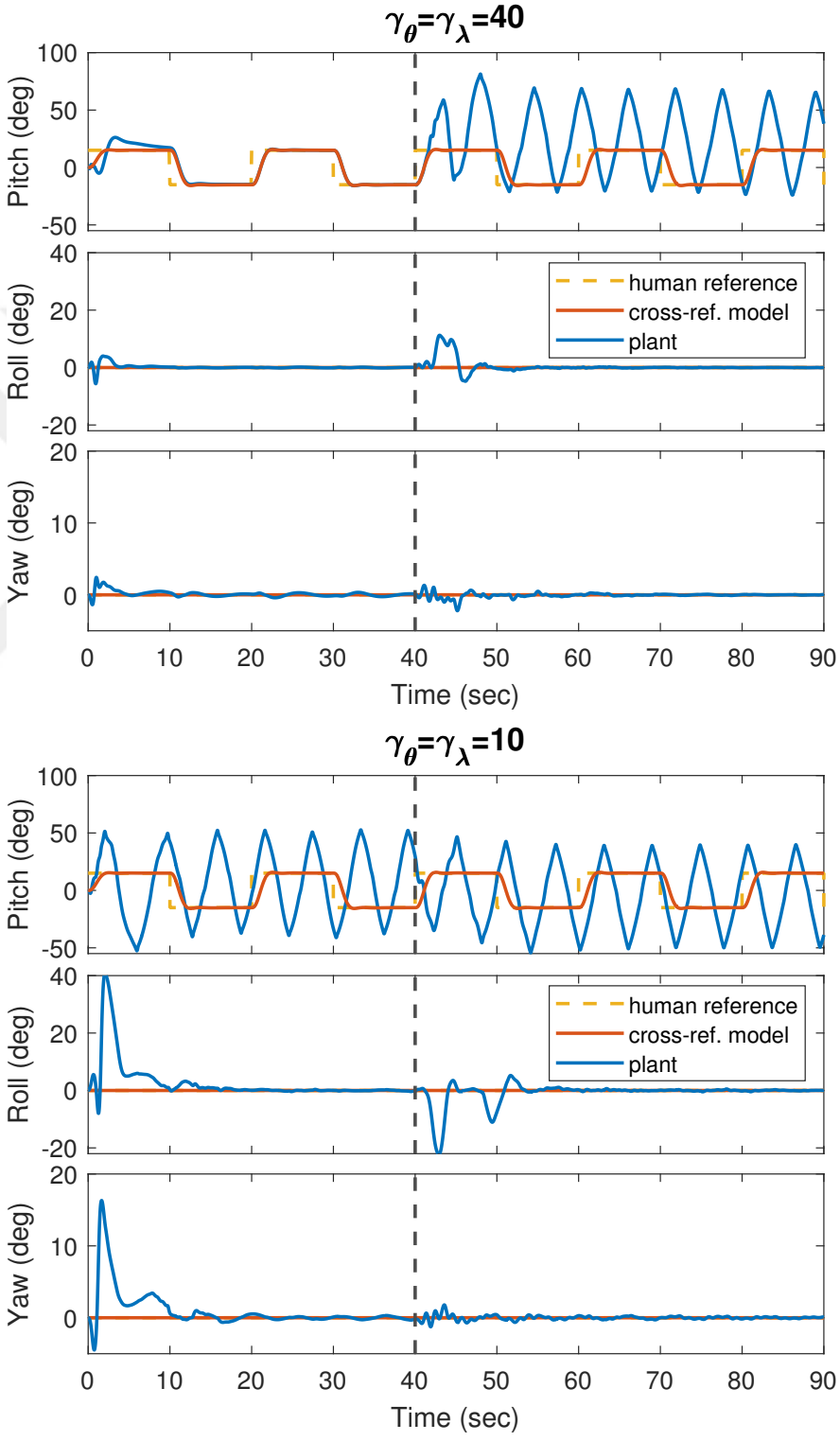

Figure 2.2: (Continued).

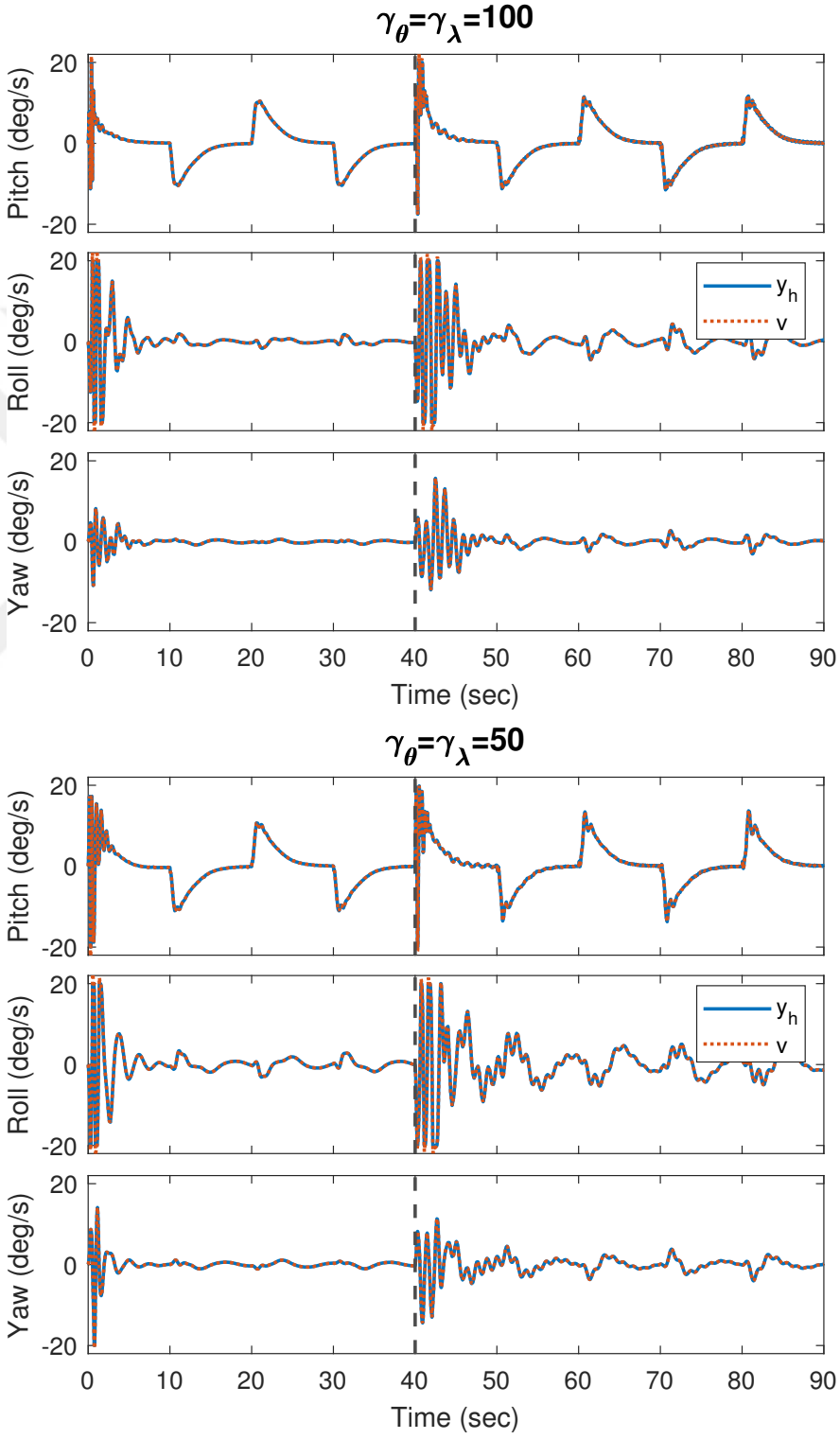

Figure 2.3: Pilot commands for different inner-loop learning rates. © 2022 IEEE.

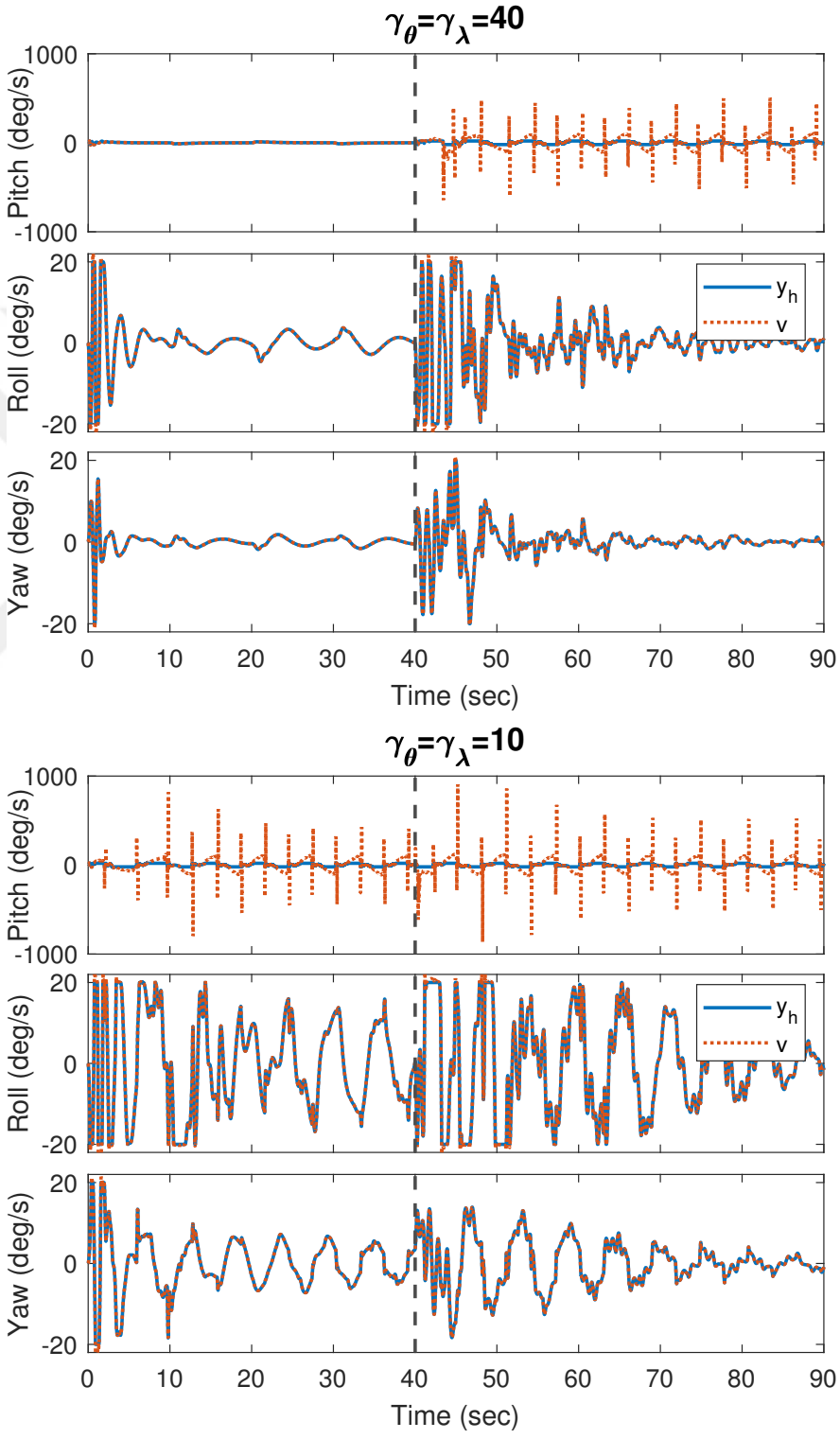

Figure 2.3: (Continued). © 2022 IEEE.

Chapter 3

An Adaptive Human Pilot Model with Reaction Time-Delay

3.1 Introduction

In Chapter 2, we introduced an adaptive human pilot model that can describe a pilot's behavior in the loop with an adaptive control system. The model is developed based on MRAC architecture, with a rigorous Lyapunov stability analysis, which can aid in the design of adaptive controllers both analytically and in the simulation environment. However, the adaptive pilot model presented in Chapter 2 does not explicitly take into account the time delay in the human pilot's response, which narrows down the class of suitable applications.

In this chapter, we build upon the work in Chapter 2, by proposing an adaptive pilot model that considers the human internal time delay while operating on an adaptive control system. The model can be used for the evaluation of adaptive controllers in piloted applications and aid in their design, especially when the delay in the pilot's response is significant. With a simpler uncertainty in the plant dynamics compared to Chapter 2, the inclusion of time delay in the human's response forms a major difficulty, which necessitates the prediction of the future

states of a time-varying uncertain adaptive control system. We propose a novel approach by resorting to the fundamental theory of linear systems, and MRAC to provide a rigorous Lyapunov-Krasovskii stability analysis. The results of this chapter were partially presented in our conference paper [23].[§]

For the sake of completeness, this chapter has been written to be self-contained. Therefore, the reader does not need to refer to Chapter 2 to grasp the contents of this chapter, as similar steps are re-explained here.

3.1.1 Notations

We use $\mathbb{R}^{p\times q}$ $[\mathbb{S}^{p\times q}]\{\mathbb{D}^{p\times q}\}$ to denote the set of real [symmetric real]{diagonal real} p by q matrices, and $\|.\|$ refers to the euclidean norm for vectors ($q = 1$), and the induced-2 norm for matrices. $\|.\|_F$ refers to the Frobenius norm for matrices, Tr{.} refers to the trace operator, and $(.)^T[(.)^{-1}]$ denotes the transpose [inverse] operator. $\text{Proj}(\hat{\theta}(t), Y)$ is the element-wise projection operator, defined in [17], used to bound each element $\hat{\theta}_{i,j}(t)$ of an adaptive parameter $\hat{\theta}(t)$ in a compact set $[\hat{\theta}_{min_{i,j}}, \hat{\theta}_{max_{i,j}}]$. Finally, we write $\lambda_{min}(A)$ for the minimum eigenvalue of the matrix A and we denote the set of positive definite real matrices by $\mathbb{R}_+^{p\times p}$.

3.2 Problem Statement

To model the human's adaptive control behavior with an adaptive controller in the loop, we start with a block diagram given in Fig. 3.1. In the figure, the block diagram is divided into inner and outer loops. The inner-loop consists of an adaptive controller controlling a plant with uncertain dynamics such that the plant states follow those of a reference model by adjusting the control parameters using an adaptive law.

The outer-loop consists of the human controlling the inner-loop such that

[§]

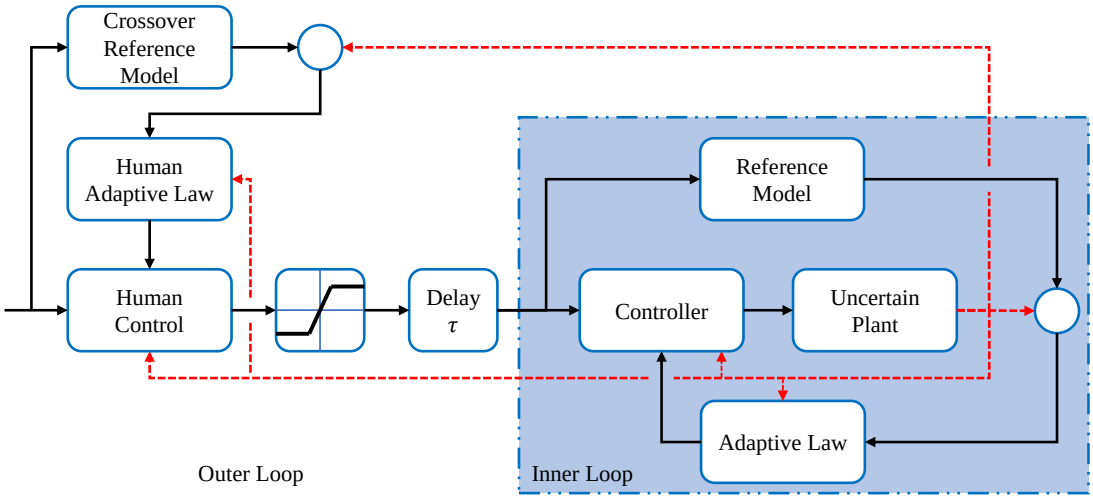

Figure 3.1: Block Diagram. © 2022 IEEE.

the plant output follows a reference input. A significant delay is present in the human's response, and physical manipulator limits impose magnitude saturation on the human control input. The human is assumed to be well trained, i.e, familiar with the nominal plant-controller dynamics. However, he/she is not aware of the uncertainties in the plant dynamics. This motivates modeling the human as an adaptive outer-loop controller, where an adaptive law is utilized to force the plant states to follow the states of the crossover-reference model.

3.3 Inner loop

Consider the following uncertain plant dynamics

$$\begin{aligned} \dot{x}_p(t) =& A_p x_p(t) + B_p \Lambda u_p(t), \\ y_1(t) =& C_1^T x_p(t), \\ y_2(t) =& C_2^T x_p(t), \end{aligned} \tag{3.1}$$

where $x_p(t) \in \mathbb{R}^{n_p}$ is the accessible state vector, $u_p(t) \in \mathbb{R}^m$ is the plant control input, $\Lambda \in \mathbb{R}_+^{m\times m} \cap \mathbb{D}^{m\times m}$ is an unknown control effectiveness matrix with the diagonal elements $\lambda_{i,i} \in (0, 1]$, $A_p \in \mathbb{R}^{n_p\times n_p}$ is an unknown system matrix, $B_p \in \mathbb{R}^{n_p\times m}$ is a known control input matrix, and $C_1 \in \mathbb{R}^{n_p\times m}$ and $C_2 \in \mathbb{R}^{n_p\times m}$ are

both known output matrices. The outputs $y_1(t) \in \mathbb{R}^m$ and $y_2(t) \in \mathbb{R}^m$ are the outputs of interest for the inner and outer loops, respectively. Furthermore, it is assumed that the pair (A_p, B_p) is controllable.

Let the nominal plant dynamics be given as

$$\dot{x}_n(t) = A_n x_n(t) + B_p u_n(t), \tag{3.2}$$

where $u_n(t) \in \mathbb{R}^m$ is a nominal controller given as

$$u_n(t) = -L_x x_n(t) + L_r y_h(t-\tau), \tag{3.3}$$

where $y_h(t-\tau) \in \mathbb{R}^m$ is the human command to the inner-loop with an internal human time delay $\tau \in \mathbb{R}^+$, and $L_x \in \mathbb{R}^{m\times n_p}$ is such that $A_r \triangleq A_n - B_p L_x$ is Hurwitz. It is noted that the human input $y_h(t)$ is bounded due to physical manipulator limits. In the design of the outer loop, given in the following section, human input saturation bounds imposed by the manipulator limits are considered in the stability analysis. Defining $B_r \triangleq B_p L_r$, the reference model is assigned as

$$\dot{x}_r(t) = A_r x_r(t) + B_r y_h(t-\tau), \quad x_r(t_0) = 0. \tag{3.4}$$

For a constant y_h, at steady state, it is obtained using (3.4) that $\dot{x}_r(\infty) = 0 = A_r x_r(\infty) + B_r y_h$, and therefore $x_r(\infty) = -A_r^{-1} B_p L_r y_h$. This means that once the reference model state tracking is achieved, i.e., $\lim_{t\to\infty} x_p(t) = x_r(t)$, the plant output $y_1(t)$, given in (3.1), takes the form $y_1(\infty) = -C_1^T A_r^{-1} B_p L_r y_h$. To achieve $\lim_{t\to\infty} y_1(t) = y_h$, we select

$$L_r = -(C_1^T A_r^{-1} B_p)^{-1}. \tag{3.5}$$

Considering (3.1), we assume that there exist $K_x^* \in \mathbb{R}^{m\times n_p}$ and $K_r^* \in \mathbb{R}^{m\times m}$ such that the matching conditions

$$A_p - B_p \Lambda K_x^* = A_r \tag{3.6a}$$

$$B_p \Lambda K_r^* = B_r \triangleq B_p L_r \tag{3.6b}$$

are satisfied, where the second matching condition implies that $K_r^* = \Lambda^{-1} L_r$. We define the plant control law as

$$u_p(t) = -\hat{K}_x(t) x_p(t) + \mathrm{diag}(\hat{\lambda}(t)) L_r y_h(t-\tau), \tag{3.7}$$

where $\hat{K}_x(t) \in \mathbb{R}^{m\times n_p}$ and $\hat{\lambda}(t) \in \mathbb{R}^m$ are adjustable adaptive parameters serving as estimates for the ideal values K_x^* and λ^*, respectively. It is noted that $\text{diag}\,(\lambda^*) = \Lambda^{-1}$ exists since Λ is diagonal positive definite.

Substituting (3.7) into (3.1), one can rewrite (3.1) as

$$\begin{aligned}\dot{x}_p(t) =& A_r x_p(t) + B_r y_h(t-\tau) + B_p \Lambda \text{diag}(\tilde{\lambda}(t)) L_r y_h(t-\tau) \\ & - B_p \Lambda \tilde{K}_x(t) x_p(t).\end{aligned} \tag{3.8}$$

where $\tilde{K}_x(t) \triangleq \hat{K}_x(t) - K_x^*$ and $\tilde{\lambda}(t) \triangleq \hat{\lambda}(t) - \lambda^*$.

By subtracting (3.4) from (3.8), and using $\Lambda \text{diag}(\tilde{\lambda}(t)) L_r y_h(t-\tau) = \text{diag}(L_r y_h(t-\tau))\Lambda\tilde{\lambda}(t)$, we obtain that

$$\dot{e}_1(t) = A_r e_1(t) + B_p \text{diag}(L_r y_h(t-\tau))\Lambda\tilde{\lambda}(t) - B_p\Lambda\tilde{K}_x(t)x_p(t), \tag{3.9}$$

where $e_1(t) \triangleq x_p(t) - x_r(t)$ is the inner-loop tracking error. We define the inner-loop adaptive laws as

$$\dot{\tilde{K}}_x^T(t) = \dot{\hat{K}}_x^T(t) = \gamma_x x_p(t) e_1(t)^T P_1 B_p, \tag{3.10a}$$

$$\dot{\tilde{\lambda}}(t) = \dot{\hat{\lambda}}(t) = \gamma_\lambda \text{Proj}\left(\hat{\lambda}(t),\ -\text{diag}(L_r y_h(t-\tau)) B_p^T P_1 e_1(t)\right), \tag{3.10b}$$

where positive bounds are set, by the projection operator, on each element $\hat{\lambda}_i(t)$, i.e., $\hat{\lambda}_{max_i} > \hat{\lambda}_{min_i} > 0$ for all $i = 1, \ldots, m$. Furthermore, $\gamma_x, \gamma_\lambda \in \mathbb{R}_+$ are learning rates, and $P_1 \in \mathbb{R}_+^{n_p\times n_p} \cap \mathbb{S}^{n_p\times n_p}$ is the solution of the Lyapunov equation $A_r^T P_1 + P_1 A_r = -Q_1$, for some $Q_1 \in \mathbb{R}_+^{n_p\times n_p} \cap \mathbb{S}^{n_p\times n_p}$. In this thesis, without loss of generality, all learning rates are taken as scalars, instead of diagonal positive definite matrices, for simplicity of notation.

Lemma 3.1. Consider the uncertain dynamical system (3.1), the reference model (3.4), and the feedback control law given by (3.7) and (3.10). The solution $(e_1(t), \tilde{K}_x(t), \tilde{\lambda}(t))$ is Lyapunov stable in the large. Furthermore, since the human command $y_h(t)$ is bounded, due to imposed saturation limits by the physical manipulators, $\lim_{t\to\infty} e_1(t) = 0$ and $\dot{\tilde{K}}_x(t)$ and $\dot{\tilde{\lambda}}(t)$ remain bounded along with all the signals in the inner-loop.

Proof. The proof of Lemma 3.1 is similar to the proof of Lemma 2.1. ■

3.4 Outer Loop

Using (3.6), and $\text{diag}(\lambda^*) = \Lambda^{-1}$, (3.8) can be rewritten as

$$\dot{x}_p(t) = A_r x_p(t) + B_p \Lambda \text{diag}(\hat{\lambda}(t)) L_r y_h(t-\tau) - B_p \Lambda \tilde{K}_x(t) x_p(t). \tag{3.11}$$

Since we assume that the human operator is familiar with the nominal dynamics (3.2) and (3.3), the only unknowns in (3.11) are Λ, $\hat{\lambda}(t)$ and $\tilde{K}_x(t)$. Furthermore, it is assumed that the internal time delay τ is known by the human pilot.

Defining the unknown time-varying parameters as

$$H^T(t) \triangleq -\Lambda \tilde{K}_x(t), \tag{3.12a}$$

$$\Lambda_2(t) \triangleq \Lambda \text{diag}(\hat{\lambda}(t)), \tag{3.12b}$$

equation (3.11) can be rewritten as

$$\dot{x}_p(t) = (A_r + B_p H^T(t)) x_p(t) + B_p \Lambda_2(t) L_r y_h(t-\tau). \tag{3.13}$$

It is noted that although (3.13) is a non-linear control system, it is viewed by the pilot as a linear-time-varying system whose state matrix is represented by $A(t) = A_r + B_p H^T(t)$. The goal of the human is to control the system such that the plant states follow that of a unity feedback reference model with an open loop crossover model transfer function. We refer to the latter as the *crossover-reference model* (Fig. 3.1). Let the crossover-reference model be given as

$$\dot{x}_m(t) = A_m x_m(t) + B_m r(t-\tau), \tag{3.14}$$

where $x_m(t) \in \mathbb{R}^{n_p}$ is the crossover-reference model state vector, $r(t) \in \mathbb{R}^m$ is a bounded reference input, $A_m \in \mathbb{R}^{n_p \times n_p}$ is Hurwitz and $B_m \triangleq B_r \theta_r \in \mathbb{R}^{n_p \times m}$. Similar to the inner-loop, and for a constant reference input r, the nominal feed-forward gain $\theta_r \in \mathbb{R}^{m \times m}$ is selected as

$$\theta_r = -(C_2^T A_m^{-1} B_r)^{-1} \tag{3.15}$$

to achieve $\lim_{t\to\infty} y_2(t) = r$ if $\lim_{t\to\infty} x_p(t) = x_m(t)$.

In an ideal case where the human input is not saturated, and both $H(t)$ and $\Lambda_2(t)$ are known, the following non-causal control law achieves the crossover-reference model dynamics

$$\begin{aligned} \mathcal{G}^*(t) &= -\theta_x x_p(t+\tau) + \theta_r r(t) - L_r^{-1} H^T(t+\tau) x_p(t+\tau), \\ y_h^*(t) &= L_r^{-1} \Lambda_2^{-1}(t+\tau) L_r \mathcal{G}^*(t), \end{aligned} \tag{3.16}$$

where we assume that there exists $\theta_x \in \mathbb{R}^{m \times n_p}$ such that $A_m = A_r - B_p L_r \theta_x$. The future state of the plant $x_p(t+\tau)$ is predicted by solving the time-varying differential equation (3.13) as

$$\begin{aligned} x_p(t+\tau) =& \Phi(t+\tau, t) x_p(t) \\ &+ \int_{-\tau}^{0} \Phi(t+\tau, t+\eta+\tau) B_p \Lambda_2(t+\eta+\tau) L_r y_h(t+\eta) \, \mathrm{d}\eta \end{aligned} \tag{3.17}$$

where $\Phi(t_2, t_1) \in \mathbb{R}^{n_p \times n_p}$ is the state transition matrix of (3.13). Motivated by (3.16) and (3.17), we define the human control input as

$$\mathcal{G}(t) = \hat{\Phi}_1(t) x_p(t) + \theta_r r(t) + \int_{-\tau}^{0} \hat{\Phi}_2(t, \eta) L_r y_h(t+\eta) \, \mathrm{d}\eta, \tag{3.18a}$$

$$v(t) = L_r^{-1} \mathrm{diag}(\hat{\lambda}_2(t)) L_r \mathcal{G}(t), \tag{3.18b}$$

$$y_{h_i}(t) = \begin{cases} v_i(t), & \text{if } |v_i(t)| \leq y_{o_i}, \\ y_{o_i} \mathrm{sgn}(v_i(t)), & \text{if } |v_i(t)| > y_{o_i}, \end{cases} \tag{3.18c}$$

where $\hat{\Phi}_1(t) \in \mathbb{R}^{m \times n_p}$, $\hat{\Phi}_2(t, \eta) \in \mathbb{R}^{m \times m}$ and $\hat{\lambda}_2(t) \in \mathbb{R}^m$ are adaptive parameters serving as estimates for the ideal values

$$\begin{aligned} \Phi_1^*(t) &= \bar{H}(t) \Phi(t+\tau, t), \\ \Phi_2^*(t, \eta) &= \bar{H}(t) \Phi(t+\tau, t+\eta+\tau) B_p \Lambda_2(t+\eta+\tau), \end{aligned} \tag{3.19}$$

and $\lambda_2^*(t)$, respectively, where $\bar{H}(t) \triangleq -(\theta_x + L_r^{-1} H^T(t+\tau))$. It is noted that $\mathrm{diag}\,(\lambda_2^*(t)) = \Lambda_2^{-1}(t+\tau)$ exists for all $t \geq 0$ since $\Lambda_2(t)$, defined in (3.12b), is diagonal positive definite at all time instants. This is guaranteed due to the positive lower bounds imposed by the projection operator in (3.10b) on the inner-loop adaptive parameter $\hat{\lambda}(t)$. Furthermore, (3.18c) is an element-wise saturation function where $y_{o_i} \in \mathbb{R}_+$ is the saturation limit of $y_{h_i}(t)$ (the i^{th} element of $y_h(t)$).

Substituting (3.18) into (3.13), and with some algebraic manipulations, we obtain that

$$\begin{aligned}\dot{x}_p(t) =& A_m x_p(t) + B_m r(t-\tau) + B_p\Lambda_2(t)L_r\Delta y(t-\tau)\\ &+ B_p\Lambda_2(t)\mathrm{diag}(\tilde{\lambda}_2(t-\tau))L_r\mathcal{G}(t-\tau)\\ &+ B_pL_r\tilde{\Phi}_1(t-\tau)x_p(t-\tau)\\ &+ B_pL_r\int_{-\tau}^{0}\tilde{\Phi}_2(t-\tau,\eta)L_r y_h(t+\eta-\tau)\mathrm{d}\eta,\end{aligned} \tag{3.20}$$

where $\tilde{\Phi}_1(t) \triangleq \hat{\Phi}_1(t) - \Phi_1^*(t)$, $\tilde{\Phi}_2(t,\eta) \triangleq \hat{\Phi}_2(t,\eta) - \Phi_2^*(t,\eta)$ and $\tilde{\lambda}_2(t) \triangleq \hat{\lambda}_2(t) - \lambda_2^*(t)$ are outer-loop adaptive parameters errors, and $\Delta y(t) \triangleq y_h(t) - v(t)$ is the control deficiency due to human input saturation.

Subtracting (3.14) from (3.20), and using $\Lambda_2\mathrm{diag}(\tilde{\lambda}_2)L_r\mathcal{G} = \mathrm{diag}(L_r\mathcal{G})\Lambda_2\tilde{\lambda}_2$ results in the outer-loop error dynamics

$$\begin{aligned}\dot{e}_2(t) =& A_m e_2(t) + B_p\Lambda_2(t)L_r\Delta y(t-\tau)\\ &+ B_p\mathrm{diag}(L_r\mathcal{G}(t-\tau))\Lambda_2(t)\tilde{\lambda}_2(t-\tau)\\ &+ B_pL_r\tilde{\Phi}_1(t-\tau)x_p(t-\tau)\\ &+ B_pL_r\int_{-\tau}^{0}\tilde{\Phi}_2(t-\tau,\eta)L_r y_h(t+\eta-\tau)\mathrm{d}\eta,\end{aligned} \tag{3.21}$$

where $e_2(t) \triangleq x_p(t) - x_m(t)$ is the outer-loop tracking error.

We generate an auxiliary signal $e_\Delta(t)$ as in [20, 21]

$$\begin{aligned}&\dot{e}_\Delta(t) = A_m e_\Delta(t) + B_p\mathrm{diag}(\hat{\lambda}_3(t))L_r\Delta y(t-\tau),\\ &e_\Delta(t_0) = 0,\end{aligned} \tag{3.22}$$

where $\hat{\lambda}_3(t) \in \mathbb{R}^m$ is an adjustable adaptive parameter serving as an estimate for the ideal value $\lambda_3^*(t)$, and $\mathrm{diag}(\lambda_3^*(t)) = \Lambda_2(t)$. Defining an augmented error signal as $e_y(t) \triangleq e_2(t) - e_\Delta(t)$, and exploiting the fact that $\mathrm{diag}(\tilde{\lambda}_3)L_r\Delta y = \mathrm{diag}(L_r\Delta y)\tilde{\lambda}_3$ yields

$$\begin{aligned}\dot{e}_y(t) =& A_m e_y(t) - B_p\mathrm{diag}(L_r\Delta y(t-\tau))\tilde{\lambda}_3(t)\\ &+ B_p\mathrm{diag}(L_r\mathcal{G}(t-\tau))\Lambda_2(t)\tilde{\lambda}_2(t-\tau)\\ &+ B_pL_r\tilde{\Phi}_1(t-\tau)x_p(t-\tau)\\ &+ B_pL_r\int_{-\tau}^{0}\tilde{\Phi}_2(t-\tau,\eta)L_r y_h(t+\eta-\tau)\mathrm{d}\eta,\end{aligned} \tag{3.23}$$

where $\tilde{\lambda}_3(t) \triangleq \hat{\lambda}_3(t) - \lambda_3^*(t)$. Equation (3.23) is in a standard error model form [7, 24]. We propose the adaptive laws

$$\dot{\hat{\lambda}}_2(t) = \gamma_2 \text{Proj}\left(\hat{\lambda}_2(t),\, -\text{diag}(L_r \mathcal{G}(t-\tau)) B_p^T P_2 e_y(t)\right), \tag{3.24a}$$

$$\dot{\hat{\lambda}}_3(t) = \gamma_3 \text{Proj}\left(\hat{\lambda}_3(t),\, \text{diag}(L_r \Delta y(t-\tau)) B_p^T P_2 e_y(t)\right), \tag{3.24b}$$

$$\dot{\hat{\Phi}}_1^T(t) = \gamma_{\phi_1} \text{Proj}\left(\hat{\Phi}_1^T(t),\, -x_p(t-\tau) e_y^T(t) P_2 B_p L_r\right), \tag{3.24c}$$

$$\dot{\hat{\Phi}}_2^T(t,\eta) = \gamma_{\phi_2} \text{Proj}\left(\hat{\Phi}_2^T(t,\eta),\, -L_r y_h(t+\eta-\tau) e_y^T(t) P_2 B_p L_r\right), \tag{3.24d}$$

where $\gamma_2, \gamma_3, \gamma_{\phi_1}, \gamma_{\phi_2} \in \mathbb{R}_+$ are learning rates, and $P_2 \in \mathbb{R}_+^{n_p \times n_p} \cap \mathbb{S}^{n_p \times n_p}$ is the solution of the Lyapunov equation $A_m^T P_2 + P_2 A_m = -Q_2$, for some $Q_2 \in \mathbb{R}_+^{n_p \times n_p} \cap \mathbb{S}^{n_p \times n_p}$.

The following Lemma establishes key bounds on the state transition matrix of (3.13) and its time derivative, which is then utilized in the remarks that follow to show that all ideal values, of the outer-loop adaptive parameters, and their time derivatives are bounded. Such bounds play a crucial role in the stability proof that follows in Theorem 3.1.

Lemma 3.2. The state transition matrix $\Phi(t+\tau, t)$ and its time derivative $\dot{\Phi}(t+\tau, t)$ are bounded, i.e., there exist $\phi \in \mathbb{R}_+$ and $\dot{\phi} \in \mathbb{R}_+$ such that $\|\Phi(t+\tau, t)\|_F \leq \phi$ and $\|\dot{\Phi}(t+\tau, t)\|_F \leq \dot{\phi}$ for all $t \geq t_0$. In addition, the same bounds apply for $\Phi(t+\tau, t+\eta+\tau)$ and its time derivative for all $t \geq t_0$, $-\tau \leq \eta \leq 0$.

Proof. It follows from Lemma 3.1 that the origin $\{e_1 = 0,\, \tilde{K}_x = 0,\, \tilde{\lambda} = 0\}$ is uniformly stable in the large. The state transition matrix $\Phi(t+\tau, t)$ defines the solution $x_p(t+\tau) = \Phi(t+\tau, t) x_p(t)$ of the homogeneous part of (3.13)

$$\dot{x}_p(t) = (A_r + B_p H^T(t)) x_p(t). \tag{3.25}$$

Since $x_p(t) = e_1(t) + x_r(t)$, and $x_r(t_0) = 0$, then the homogeneous part of (3.4)

$$\dot{x}_r(t) = A_r x_r(t),\ x_r(t_0) = 0, \tag{3.26}$$

yields the solution $x_r(t) = 0$, which implies that $x_p(t) = e_1(t)$ for all $t \geq t_0$. This shows that the origin $x_p = 0$ of (3.25) is uniformly stable in the large.

It then follows from Theorem 6.4 in [25] that there exists $\phi \in \mathbb{R}_+$ such that $\|\Phi(t_2, t_1)\|_F \leq \phi$ for all t_1, t_2, where $t_2 \geq t_1$. This in turn implies that

$$\begin{aligned} \|\Phi(t+\tau, t)\|_F \leq \phi, \text{ for all } t \geq t_0, \\ \|\Phi(t+\tau, t+\eta+\tau)\|_F \leq \phi, \text{ for all } t \geq t_0,\ -\tau \leq \eta \leq 0. \end{aligned} \tag{3.27}$$

Furthermore, the state transition matrix can be defined by the so-called fundamental matrix $X(t)$ of (3.25) as

$$\Phi(t+\tau, t) = X(t+\tau)X(t)^{-1}, \tag{3.28}$$

where $X(t)$ is non-singular for all $t \geq t_0$ [26], and satisfies $\dot{X}(t) = A(t)X(t)$. Denoting $A(t) \triangleq (A_r + B_p H^T(t))$, and differentiating (3.28) yields

$$\begin{aligned} \dot{\Phi}(t+\tau, t) =& \dot{X}(t+\tau)X(t)^{-1} + X(t+\tau)\frac{\mathrm{d}}{\mathrm{d}t}X(t)^{-1} \\ =& \dot{X}(t+\tau)X(t)^{-1} - X(t+\tau)X(t)^{-1}\dot{X}(t)X(t)^{-1} \\ =& A(t+\tau)\Phi(t+\tau, t) - \Phi(t+\tau, t)A(t). \end{aligned} \tag{3.29}$$

Since the boundedness of $H^T(t) \triangleq -\Lambda\tilde{K}_x(t)$ follows from Lemma 3.1, then $A(t)$ is also bounded. Together with (3.27), this shows that all the terms in (3.29) are bounded, which implies that there exists $\dot{\phi} \in \mathbb{R}_+$ such that

$$\begin{aligned} \|\dot{\Phi}(t+\tau, t)\|_F \leq \dot{\phi}, \text{ for all } t \geq t_0, \\ \|\dot{\Phi}(t+\tau, t+\eta+\tau)\|_F \leq \dot{\phi}, \text{ for all } t \geq t_0,\ -\tau \leq \eta \leq 0. \end{aligned} \tag{3.30}$$

■

Remark 3.1. It follows from Lemma 3.1 that $\tilde{K}(t)$, $\hat{\lambda}(t)$, $\dot{\tilde{K}}(t)$ and $\dot{\hat{\lambda}}(t)$ are bounded, which implies the boundedness of $H(t)$, $\Lambda_2(t)$, $\dot{H}(t)$ and $\dot{\Lambda}_2(t)$. Therefore, there exist $h \in \mathbb{R}_+$, $\dot{h} \in \mathbb{R}_+$, $\beta_3 \in \mathbb{R}_+$ and $\dot{\beta}_3 \in \mathbb{R}_+$ such that $\|H(t)\| \leq h$, $\|\dot{H}(t)\| \leq \dot{h}$, $\|\Lambda_2(t)\|_F \leq \beta_3$ and $\|\dot{\Lambda}_2(t)\|_F \leq \dot{\beta}_3$ for all $t \geq t_0$. The latter implies that $\|\lambda_3^*(t)\| \leq \beta_3$ and $\|\dot{\lambda}_3^*(t)\| \leq \dot{\beta}_3$. Moreover, as $\hat{\lambda}_{min_i} > 0$ for $i = 1, \ldots, m$, there exists $\beta_2 \in \mathbb{R}_+$ such that $\|\Lambda_2^{-1}(t)\|_F \leq \beta_2$. And since $\frac{\mathrm{d}\Lambda_2^{-1}}{\mathrm{d}t} = -\Lambda_2^{-1}\dot{\Lambda}_2\Lambda_2^{-1}$, then there exists $\dot{\beta}_2 \in \mathbb{R}_+$ such that $\|\frac{\mathrm{d}\Lambda_2^{-1}}{\mathrm{d}t}\|_F \leq \dot{\beta}_2$. This implies that $\|\lambda_2^*(t)\| \leq \beta_2$ and $\|\dot{\lambda}_2^*(t)\| \leq \dot{\beta}_2$ for all $t \geq t_0$.

Remark 3.2. Together with Remark 3.1, the bounds (3.27) and (3.30), established in Lemma 3.2, show that all the terms of the ideal values (3.19) and

their time derivatives are bounded. Hence, there exist $\phi_1, \dot{\phi}_1, \phi_2, \dot{\phi}_2 \in \mathbb{R}_+$ such that $\|\Phi_1^*(t)\|_F \leq \phi_1$, $\|\dot{\Phi}_1^*(t)\|_F \leq \dot{\phi}_1$ for all $t \geq t_0$, and $\|\Phi_2^*(t,\eta)\|_F \leq \phi_2$, $\|\dot{\Phi}_2^*(t,\eta)\|_F \leq \dot{\phi}_2$ for all $t \geq t_0$, $-\tau \leq \eta \leq 0$.

Theorem 3.1. Consider the uncertain dynamical system given by (3.1), the adaptive controller given by (3.4), (3.7) and (3.10), and the adaptive human pilot model given by (3.14), (3.18) and (3.24). Then, there exists $\tau^* \in \mathbb{R}_+$ such that for all $\tau \in [0,\, \tau^*]$, the solution $(e_y(t), \tilde{\lambda}_2(t), \tilde{\lambda}_3(t), \tilde{\Phi}_1(t), \tilde{\Phi}_2(t,\eta))$ remains bounded for all $t \geq t_0$ and converges to the compact set defined in (3.58). Furthermore, the closed-loop system is stable in the large, and all signals are bounded.

Proof. Consider the Lyapunov-Krasovskii functional

$$\begin{aligned} V_2 =& e_y^T(t)P_2e_y(t) + \gamma_3^{-1}\tilde{\lambda}_3^T(t)\tilde{\lambda}_3(t) \\ &+ \gamma_2^{-1}\tilde{\lambda}_2^T(t)\Lambda_2(t)\tilde{\lambda}_2(t) + \int_{-\tau}^{0}\int_{t+\nu}^{t}\dot{\tilde{\lambda}}_2^T(\xi)\dot{\tilde{\lambda}}_2(\xi)\mathrm{d}\xi\mathrm{d}\nu \\ &+ \gamma_{\phi_1}^{-1}\mathrm{Tr}\{\tilde{\Phi}_1^T(t)\tilde{\Phi}_1(t)\} + \int_{-\tau}^{0}\int_{t+\nu}^{t}\mathrm{Tr}\{\dot{\tilde{\Phi}}_1^T(\xi)\dot{\tilde{\Phi}}_1(\xi)\}\mathrm{d}\xi\mathrm{d}\nu \\ &+ \gamma_{\phi_2}^{-1}\int_{-\tau}^{0}\mathrm{Tr}\{\tilde{\Phi}_2^T(t,\eta)\tilde{\Phi}_2(t,\eta)\}\mathrm{d}\eta \\ &+ \int_{-\tau}^{0}\int_{t+\nu}^{t}\int_{-\tau}^{0}\mathrm{Tr}\{\dot{\tilde{\Phi}}_2^T(\xi,\eta)\dot{\tilde{\Phi}}_2(\xi,\eta)\}\mathrm{d}\eta\mathrm{d}\xi\mathrm{d}\nu. \end{aligned} \tag{3.31}$$

For brevity, we define

$$\begin{aligned} W(t) \triangleq& \int_{-\tau}^{0}\int_{t+\nu}^{t}\dot{\tilde{\lambda}}_2^T(\xi)\dot{\tilde{\lambda}}_2(\xi)\mathrm{d}\xi\mathrm{d}\nu \\ &+ \int_{-\tau}^{0}\int_{t+\nu}^{t}\mathrm{Tr}\{\dot{\tilde{\Phi}}_1^T(\xi)\dot{\tilde{\Phi}}_1(\xi)\}\mathrm{d}\xi\mathrm{d}\nu \\ &+ \int_{-\tau}^{0}\int_{t+\nu}^{t}\int_{-\tau}^{0}\mathrm{Tr}\{\dot{\tilde{\Phi}}_2^T(\xi,\eta)\dot{\tilde{\Phi}}_2(\xi,\eta)\}\mathrm{d}\eta\mathrm{d}\xi\mathrm{d}\nu, \end{aligned} \tag{3.32}$$

where

$$\begin{aligned}\dot{W}(t) =&\tau\dot{\tilde{\lambda}}_2^T(t)\dot{\tilde{\lambda}}_2(t) - \int_{-\tau}^{0}\dot{\tilde{\lambda}}_2^T(t+\nu)\dot{\tilde{\lambda}}_2(t+\nu)\mathrm{d}\nu \\ &+ \tau\mathrm{Tr}\{\dot{\tilde{\Phi}}_1^T(t)\dot{\tilde{\Phi}}_1(t)\} - \int_{-\tau}^{0}\mathrm{Tr}\{\dot{\tilde{\Phi}}_1^T(t+\nu)\dot{\tilde{\Phi}}_1(t+\nu)\}\mathrm{d}\nu \\ &+ \tau\int_{-\tau}^{0}\mathrm{Tr}\{\dot{\tilde{\Phi}}_2^T(t,\eta)\dot{\tilde{\Phi}}_2(t,\eta)\}\mathrm{d}\eta \\ &- \int_{-\tau}^{0}\int_{-\tau}^{0}\mathrm{Tr}\{\dot{\tilde{\Phi}}_2^T(t+\nu,\eta)\dot{\tilde{\Phi}}_2(t+\nu,\eta)\}\mathrm{d}\eta\mathrm{d}\nu.\end{aligned} \tag{3.33}$$

Differentiating (3.31) along the trajectories (3.23) and (3.24), and using (3.33), we obtain that

$$\begin{aligned}\dot{V}_2 =&\dot{e}_y^T(t)P_2e_y(t) + e_y^T(t)P_2\dot{e}_y(t) + 2\gamma_3^{-1}\tilde{\lambda}_3^T(t)\dot{\tilde{\lambda}}_3(t) \\ &+ 2\gamma_2^{-1}\tilde{\lambda}_2^T(t)\Lambda_2(t)\dot{\tilde{\lambda}}_2(t) + \gamma_2^{-1}\tilde{\lambda}_2^T(t)\dot{\Lambda}_2(t)\tilde{\lambda}_2(t) \\ &+ 2\gamma_{\phi_1}^{-1}\mathrm{Tr}\{\dot{\tilde{\Phi}}_1^T(t)\tilde{\Phi}_1(t)\} \\ &+ 2\gamma_{\phi_2}^{-1}\int_{-\tau}^{0}\mathrm{Tr}\{\dot{\tilde{\Phi}}_2^T(t,\eta)\tilde{\Phi}_2(t,\eta)\}\mathrm{d}\eta + \dot{W}(t) \\ =&- e_y^T(t)Q_2e_y(t) - 2\tilde{\lambda}_3^T(t)\mathrm{diag}(L_r\Delta y(t-\tau))B_p^TP_2e_y(t) \\ &+ 2\tilde{\lambda}_2^T(t-\tau)\Lambda_2(t)\mathrm{diag}(L_r\mathcal{G}(t-\tau))B_p^TP_2e_y(t) \\ &+ 2e_y^T(t)P_2B_pL_r\tilde{\Phi}_1(t-\tau)x_p(t-\tau) \\ &+ 2e_y^T(t)P_2B_pL_r\int_{-\tau}^{0}\tilde{\Phi}_2(t-\tau,\eta)L_ry_h(t+\eta-\tau)\mathrm{d}\eta \\ &+ 2\gamma_3^{-1}\tilde{\lambda}_3^T(t)\dot{\tilde{\lambda}}_3(t) + 2\gamma_{\phi_1}^{-1}\mathrm{Tr}\{\dot{\tilde{\Phi}}_1^T(t)\tilde{\Phi}_1(t)\} \\ &+ 2\gamma_2^{-1}\tilde{\lambda}_2^T(t)\Lambda_2(t)\dot{\tilde{\lambda}}_2(t) + \gamma_2^{-1}\tilde{\lambda}_2^T(t)\dot{\Lambda}_2(t)\tilde{\lambda}_2(t) \\ &+ 2\gamma_{\phi_2}^{-1}\int_{-\tau}^{0}\mathrm{Tr}\{\dot{\tilde{\Phi}}_2^T(t,\eta)\tilde{\Phi}_2(t,\eta)\}\mathrm{d}\eta + \dot{W}(t).\end{aligned} \tag{3.34}$$

Using the fact that $g(t-\tau) = g(t) - \int_{-\tau}^{0}\dot{g}(t+\nu)\mathrm{d}\nu$ for $\tilde{\lambda}_2^T(t-\tau)$, $\tilde{\Phi}_1(t-\tau)$ and $\tilde{\Phi}_2(t-\tau,\eta)$, and decomposing $\dot{\tilde{\lambda}}_2(t) = \dot{\hat{\lambda}}_2(t) - \dot{\lambda}_2^*(t)$, $\dot{\tilde{\lambda}}_3(t) = \dot{\hat{\lambda}}_3(t) - \dot{\lambda}_3^*(t)$,

$\dot{\tilde{\Phi}}_1(t) = \dot{\hat{\Phi}}_1(t) - \dot{\Phi}_1^*(t)$ and $\dot{\tilde{\Phi}}_2(t,\eta) = \dot{\hat{\Phi}}_2(t,\eta) - \dot{\Phi}_2^*(t,\eta)$, we get

$$\begin{aligned}
\dot{V}_2 = & - e_y^T(t)Q_2e_y(t) - 2\tilde{\lambda}_3^T(t)\mathrm{diag}(L_r\Delta y(t-\tau))B_p^TP_2e_y(t) \\
& + 2\tilde{\lambda}_2^T(t)\Lambda_2(t)\mathrm{diag}(L_r\mathcal{G}(t-\tau))B_p^TP_2e_y(t) \\
& - 2\left(\int_{-\tau}^{0}\dot{\tilde{\lambda}}_2^T(t+\nu)\mathrm{d}\nu\right)\Lambda_2(t)\mathrm{diag}(L_r\mathcal{G}(t-\tau))B_p^TP_2e_y(t) \\
& + 2e_y^T(t)P_2B_pL_r\Bigg[\tilde{\Phi}_1(t)x_p(t-\tau) \\
& - \left(\int_{-\tau}^{0}\dot{\tilde{\Phi}}_1(t+\nu)\mathrm{d}\nu\right)x_p(t-\tau) \\
& + \int_{-\tau}^{0}\tilde{\Phi}_2(t,\eta)L_ry_h(t+\eta-\tau)\mathrm{d}\eta \\
& - \int_{-\tau}^{0}\left(\int_{-\tau}^{0}\dot{\tilde{\Phi}}_2(t+\nu,\eta)\mathrm{d}\nu\right)L_ry_h(t+\eta-\tau)\mathrm{d}\eta\Bigg] \\
& + 2\gamma_3^{-1}\tilde{\lambda}_3^T(t)\dot{\tilde{\lambda}}_3(t) - 2\gamma_3^{-1}\tilde{\lambda}_3^T(t)\dot{\lambda}_3^*(t) \\
& + 2\gamma_2^{-1}\tilde{\lambda}_2^T(t)\Lambda_2(t)\dot{\tilde{\lambda}}_2(t) - 2\gamma_2^{-1}\tilde{\lambda}_2^T(t)\Lambda_2(t)\dot{\lambda}_2^*(t) \\
& + \gamma_2^{-1}\tilde{\lambda}_2^T(t)\dot{\Lambda}_2(t)\tilde{\lambda}_2(t) \\
& + 2\gamma_{\phi_1}^{-1}\mathrm{Tr}\{\dot{\tilde{\Phi}}_1^T(t)\tilde{\Phi}_1(t)\} - 2\gamma_{\phi_1}^{-1}\mathrm{Tr}\{\dot{\Phi}_1^{*T}(t)\tilde{\Phi}_1(t)\} \\
& + 2\gamma_{\phi_2}^{-1}\int_{-\tau}^{0}\mathrm{Tr}\{\dot{\tilde{\Phi}}_2^T(t,\eta)\tilde{\Phi}_2(t,\eta)\}\mathrm{d}\eta \\
& - 2\gamma_{\phi_2}^{-1}\int_{-\tau}^{0}\mathrm{Tr}\{\dot{\Phi}_2^{*T}(t,\eta)\tilde{\Phi}_2(t,\eta)\}\mathrm{d}\eta + \dot{W}(t).
\end{aligned} \tag{3.35}$$

Defining

$$\begin{aligned}
N^*(t) \triangleq & \ \gamma_2^{-1}\tilde{\lambda}_2^T(t)\dot{\Lambda}_2(t)\tilde{\lambda}_2(t) - 2\gamma_2^{-1}\tilde{\lambda}_2^T(t)\Lambda_2(t)\dot{\lambda}_2^*(t) \\
& - 2\gamma_3^{-1}\tilde{\lambda}_3^T(t)\dot{\lambda}_3^*(t) - 2\gamma_{\phi_1}^{-1}\mathrm{Tr}\{\dot{\Phi}_1^{*T}(t)\tilde{\Phi}_1(t)\} \\
& - 2\gamma_{\phi_2}^{-1}\int_{-\tau}^{0}\mathrm{Tr}\{\dot{\Phi}_2^{*T}(t,\eta)\tilde{\Phi}_2(t,\eta)\}\mathrm{d}\eta,
\end{aligned} \tag{3.36}$$

using $\mathrm{Tr}(AB) = \mathrm{Tr}(BA)$, and rearranging, we get

$$\begin{aligned}
\dot{V}_2 = & -e_y^T(t)Q_2e_y(t) + N^*(t) + \dot{W}(t) \\
& + 2\tilde{\lambda}_3^T(t)\left(-\mathrm{diag}(L_r\Delta y(t-\tau))B_p^TP_2e_y(t) + \gamma_3^{-1}\dot{\hat{\lambda}}_3(t)\right) \\
& + 2\tilde{\lambda}_2^T(t)\Lambda_2(t)\left(\mathrm{diag}(L_r\mathcal{G}(t-\tau))B_p^TP_2e_y(t) + \gamma_2^{-1}\dot{\hat{\lambda}}_2(t)\right) \\
& + 2\mathrm{Tr}\{\tilde{\Phi}_1(t)\left(x_p(t-\tau)e_y^T(t)P_2B_pL_r + \gamma_{\phi_1}^{-1}\dot{\hat{\Phi}}_1^T(t)\right)\} \\
& + 2\int_{-\tau}^{0}\mathrm{Tr}\{\tilde{\Phi}_2(t,\eta)\Big(L_ry_h(t+\eta-\tau)e_y^T(t)P_2B_pL_r + \gamma_{\phi_2}^{-1}\dot{\hat{\Phi}}_2^T(t,\eta)\Big)\}\mathrm{d}\eta \\
& - 2\int_{-\tau}^{0}\dot{\tilde{\lambda}}_2^T(t+\nu)\Lambda_2(t)\mathrm{diag}(L_r\mathcal{G}(t-\tau))B_p^TP_2e_y(t)\mathrm{d}\nu \\
& - 2\int_{-\tau}^{0}\mathrm{Tr}\{\dot{\tilde{\Phi}}_1(t+\nu)x_p(t-\tau)e_y^T(t)P_2B_pL_r\}\mathrm{d}\nu \\
& - 2\int_{-\tau}^{0}\int_{-\tau}^{0}\mathrm{Tr}\{\dot{\tilde{\Phi}}_2(t+\nu,\eta)L_ry_h(t+\eta-\tau)e_y^T(t)P_2B_pL_r\}\mathrm{d}\nu\mathrm{d}\eta
\end{aligned} \tag{3.37}$$

Substituting the adaptive laws (3.24) in (3.37) yields

$$\begin{aligned}
\dot{V}_2 = & -e_y^T(t)Q_2e_y(t) + N^*(t) + \dot{W}(t) \\
& + 2\tilde{\lambda}_3^T(t)\left(\mathrm{Proj}(\hat{\lambda}_3(t),\, Y_3(t)) - Y_3(t)\right) \\
& + 2\tilde{\lambda}_2^T(t)\Lambda_2(t)\left(\mathrm{Proj}(\hat{\lambda}_2(t),\, Y_2(t)) - Y_2(t)\right) \\
& + 2\mathrm{Tr}\{\tilde{\Phi}_1(t)\left(\mathrm{Proj}(\hat{\Phi}_1(t),\, Y_{\phi_1}(t)) - Y_{\phi_1}(t)\right)\} \\
& + 2\int_{-\tau}^{0}\mathrm{Tr}\{\tilde{\Phi}_2(t,\eta)\Big(\mathrm{Proj}(\hat{\Phi}_2(t,\eta),\, Y_{\phi_2}(t,\eta)) - Y_{\phi_2}(t,\eta)\Big)\}\mathrm{d}\eta \\
& + 2\int_{-\tau}^{0}\dot{\tilde{\lambda}}_2^T(t+\nu)\Lambda_2(t)Y_2(t)\mathrm{d}\nu \\
& + 2\int_{-\tau}^{0}\mathrm{Tr}\{\dot{\tilde{\Phi}}_1(t+\nu)Y_{\phi_1}(t)\}\mathrm{d}\nu \\
& + 2\int_{-\tau}^{0}\int_{-\tau}^{0}\mathrm{Tr}\{\dot{\tilde{\Phi}}_2(t+\nu,\eta)Y_{\phi_2}(t,\eta)\}\mathrm{d}\nu\mathrm{d}\eta,
\end{aligned} \tag{3.38}$$

where

$$\begin{aligned}
Y_2(t) &\triangleq -\mathrm{diag}(L_r\mathcal{G}(t-\tau))B_p^TP_2e_y(t), \\
Y_3(t) &\triangleq \mathrm{diag}(L_r\Delta y(t-\tau))B_p^TP_2e_y(t), \\
Y_{\phi_1}(t) &\triangleq -x_p(t-\tau)e_y^T(t)P_2B_pL_r, \\
Y_{\phi_2}(t,\eta) &\triangleq -L_ry_h(t+\eta-\tau)e_y^T(t)P_2B_pL_r.
\end{aligned} \tag{3.39}$$

Using the projection property $(\theta_{i,j} - \theta^*_{i,j})(\text{Proj}(\theta_{i,j}, Y_{i,j}) - Y_{i,j}) \leq 0$, and the fact that $\Lambda_2(t)$ is diagonal positive definite, it follows from (3.38) that

$$\begin{aligned}\dot{V}_2 \leq & -e_y^T(t)Q_2e_y(t) + N^*(t) + \dot{W}(t) \\ & + 2\int_{-\tau}^{0} \dot{\tilde{\lambda}}_2^T(t+\nu)\Lambda_2(t)Y_2(t)\mathrm{d}\nu \\ & + 2\int_{-\tau}^{0} \mathrm{Tr}\{\dot{\tilde{\Phi}}_1(t+\nu)Y_{\phi_1}(t)\}\mathrm{d}\nu \\ & + 2\int_{-\tau}^{0}\int_{-\tau}^{0} \mathrm{Tr}\{\dot{\tilde{\Phi}}_2(t+\nu,\eta)Y_{\phi_2}(t,\eta)\}\mathrm{d}\nu\mathrm{d}\eta.\end{aligned} \tag{3.40}$$

Using the algebraic inequality $\mathrm{Tr}\{2A^TB\} \leq \mathrm{Tr}\{A^TA + B^TB\}$, we obtain that

$$\begin{aligned}\dot{V}_2 \leq & -e_y^T(t)Q_2e_y(t) + N^*(t) + \dot{W}(t) \\ & + \int_{-\tau}^{0} \dot{\tilde{\lambda}}_2^T(t+\nu)\dot{\tilde{\lambda}}_2(t+\nu)\mathrm{d}\nu \\ & + \int_{-\tau}^{0} Y_2^T(t)\Lambda_2(t)\Lambda_2(t)Y_2(t)\mathrm{d}\nu \\ & + \int_{-\tau}^{0} \mathrm{Tr}\{\dot{\tilde{\Phi}}_1^T(t+\nu)\dot{\tilde{\Phi}}_1(t+\nu)\}\mathrm{d}\nu \\ & + \int_{-\tau}^{0} \mathrm{Tr}\{Y_{\phi_1}^T(t)Y_{\phi_1}(t)\}\mathrm{d}\nu \\ & + \int_{-\tau}^{0}\int_{-\tau}^{0} \mathrm{Tr}\{\dot{\tilde{\Phi}}_2^T(t+\nu,\eta)\dot{\tilde{\Phi}}_2(t+\nu,\eta)\}\mathrm{d}\nu\mathrm{d}\eta \\ & + \int_{-\tau}^{0}\int_{-\tau}^{0} \mathrm{Tr}\{Y_{\phi_2}^T(t,\eta)Y_{\phi_2}(t,\eta)\}\mathrm{d}\nu\mathrm{d}\eta.\end{aligned} \tag{3.41}$$

Substituting (3.33) in (3.41) yields

$$\begin{aligned}\dot{V}_2 \leq & -e_y^T(t)Q_2e_y(t) + N^*(t) \\ & + \tau Y_2^T(t)\Lambda_2(t)\Lambda_2(t)Y_2(t) \\ & + \tau\mathrm{Tr}\{Y_{\phi_1}^T(t)Y_{\phi_1}(t)\} \\ & + \tau\int_{-\tau}^{0} \mathrm{Tr}\{Y_{\phi_2}^T(t,\eta)Y_{\phi_2}(t,\eta)\}\mathrm{d}\eta \\ & + \tau\dot{\tilde{\lambda}}_2^T(t)\dot{\tilde{\lambda}}_2(t) + \tau\mathrm{Tr}\{\dot{\tilde{\Phi}}_1^T(t)\dot{\tilde{\Phi}}_1(t)\} \\ & + \tau\int_{-\tau}^{0} \mathrm{Tr}\{\dot{\tilde{\Phi}}_2^T(t,\eta)\dot{\tilde{\Phi}}_2(t,\eta)\}\mathrm{d}\eta.\end{aligned} \tag{3.42}$$

Using the algebraic inequality

$$\begin{aligned}\mathrm{Tr}\{\dot{\hat{\Phi}}_1^T(t)\dot{\hat{\Phi}}_1(t)\} =&\mathrm{Tr}\{\dot{\hat{\Phi}}_1^T(t)\dot{\hat{\Phi}}_1(t)\} + \mathrm{Tr}\{\dot{\Phi}_1^{*T}(t)\dot{\Phi}_1^*(t)\}\\ &- 2\mathrm{Tr}\{\dot{\hat{\Phi}}^T(t)\dot{\Phi}^*(t)\}\\ \leq&2\mathrm{Tr}\{\dot{\hat{\Phi}}_1^T(t)\dot{\hat{\Phi}}_1(t)\} + 2\mathrm{Tr}\{\dot{\Phi}_1^{*T}(t)\dot{\Phi}_1^*(t)\},\end{aligned} \tag{3.43}$$

for the last three terms in (3.42), one can write

$$\begin{aligned}\dot{V}_2 \leq& - e_y^T(t)Q_2e_y(t) + N^*(t)\\ &+ \tau Y_2^T(t)\Lambda_2(t)\Lambda_2(t)Y_2(t)\\ &+ \tau\mathrm{Tr}\{Y_{\phi_1}^T(t)Y_{\phi_1}(t)\}\\ &+ \tau\int_{-\tau}^{0}\mathrm{Tr}\{Y_{\phi_2}^T(t,\eta)Y_{\phi_2}(t,\eta)\}\mathrm{d}\eta\\ &+ 2\tau\dot{\hat{\lambda}}_2^T(t)\dot{\hat{\lambda}}_2(t) + 2\tau\dot{\lambda}_2^{*T}(t)\dot{\lambda}_2^*(t)\\ &+ 2\tau\mathrm{Tr}\{\dot{\hat{\Phi}}_1^T(t)\dot{\hat{\Phi}}_1(t)\} + 2\tau\mathrm{Tr}\{\dot{\Phi}_1^{*T}(t)\dot{\Phi}_1^*(t)\}\\ &+ 2\tau\int_{-\tau}^{0}\mathrm{Tr}\{\dot{\hat{\Phi}}_2^T(t,\eta)\dot{\hat{\Phi}}_2(t,\eta)\}\mathrm{d}\eta\\ &+ 2\tau\int_{-\tau}^{0}\mathrm{Tr}\{\dot{\Phi}_2^{*T}(t,\eta)\dot{\Phi}_2^*(t,\eta)\}\mathrm{d}\eta.\end{aligned} \tag{3.44}$$

Let $Y_2(t) = [a_1(t),\ldots,a_m(t)]^T$ and $\Lambda_2(t) = \mathrm{diag}([b_1(t),\ldots,b_m(t)])$ for some $a_i(t)\in\mathbb{R}$, $b_i(t)\in\mathbb{R}_+$, for $i = 1,\ldots,m$. Since $\Lambda_2(t)$, defined in (3.12b), is shown to be bounded in Remark 3.1, then $b_i(t)\leq\lambda_{i,i}\hat{\lambda}_{max_i}$ for all $t\geq t_0$, $i = 1,\ldots,m$, where $\lambda_{i,i}$ is the i^{th} diagonal element of Λ, and $\hat{\lambda}_{max_i}$ is the i^{th} projection upper bound of $\hat{\lambda}(t)$ in (3.10b). Then, one can write

$$\begin{aligned}Y_2^T(t)\Lambda_2(t)\Lambda_2(t)Y_2(t) =&b_1^2(t)a_1^2(t) + \cdots + b_m^2(t)a_m^2(t)\\ \leq&\mu(a_1^2(t) + \cdots + a_m^2(t)) = \mu Y_2^T(t)Y_2(t),\end{aligned} \tag{3.45}$$

where $\mu\triangleq\max_i(\lambda_{i,i}\hat{\lambda}_{max_i})^2$. Furthermore, using the property that the projection operator bounds an adaptive parameter in a compact set, then from the element-wise projection operator's definition in [17], it can be shown that

$$\mathrm{Tr}\{\dot{\hat{\Phi}}_1^T(t)\dot{\hat{\Phi}}_1(t)\}\leq\gamma_{\phi_1}^2\mathrm{Tr}\{Y_{\phi_1}^T(t)Y_{\phi_1}(t)\} \tag{3.46}$$

Using (3.45) and (3.46) in (3.44), we obtain that

$$\begin{aligned}
\dot{V}_2 \leq & -e_y^T(t)Q_2e_y(t) + N^*(t) \\
& + \tau\mu Y_2^T(t)Y_2(t) + \tau\mathrm{Tr}\{Y_{\phi_1}^T(t)Y_{\phi_1}(t)\} \\
& + \tau\int_{-\tau}^{0}\mathrm{Tr}\{Y_{\phi_2}^T(t,\eta)Y_{\phi_2}(t,\eta)\}\mathrm{d}\eta \\
& + 2\tau\gamma_2^2Y_2^T(t)Y_2(t) + 2\tau\dot{\lambda}_2^{*T}(t)\dot{\lambda}_2^*(t) \\
& + 2\tau\gamma_{\phi_1}^2\mathrm{Tr}\{Y_{\phi_1}^T(t)Y_{\phi_1}(t)\} + 2\tau\mathrm{Tr}\{\dot{\Phi}_1^{*T}(t)\dot{\Phi}_1^*(t)\} \\
& + 2\tau\gamma_{\phi_2}^2\int_{-\tau}^{0}\mathrm{Tr}\{Y_{\phi_2}^T(t,\eta)Y_{\phi_2}(t,\eta)\}\mathrm{d}\eta \\
& + 2\tau\int_{-\tau}^{0}\mathrm{Tr}\{\dot{\Phi}_2^{*T}(t,\eta)\dot{\Phi}_2^*(t,\eta)\}\mathrm{d}\eta \\
= & -e_y^T(t)Q_2e_y(t) + N^*(t) \\
& + \tau(\mu+2\gamma_2^2)Y_2^T(t)Y_2(t) + \tau(1+2\gamma_{\phi_1}^2)\mathrm{Tr}\{Y_{\phi_1}^T(t)Y_{\phi_1}(t)\} \\
& + \tau(1+2\gamma_{\phi_2}^2)\int_{-\tau}^{0}\mathrm{Tr}\{Y_{\phi_2}^T(t,\eta)Y_{\phi_2}(t,\eta)\}\mathrm{d}\eta \\
& + 2\tau\dot{\lambda}_2^{*T}(t)\dot{\lambda}_2^*(t) + 2\tau\mathrm{Tr}\{\dot{\Phi}_1^{*T}(t)\dot{\Phi}_1^*(t)\} \\
& + 2\tau\int_{-\tau}^{0}\mathrm{Tr}\{\dot{\Phi}_2^{*T}(t,\eta)\dot{\Phi}_2^*(t,\eta)\}\mathrm{d}\eta
\end{aligned} \tag{3.47}$$

Using the property $\mathrm{Tr}\{Y^TY\} = \|Y\|_F^2$ for a matrix Y, we can rewrite (3.47) as

$$\begin{aligned}
\dot{V}_2 \leq & -e_y^T(t)Q_2e_y(t) + N^*(t) \\
& + \tau(\mu+2\gamma_2^2)\|Y_2(t)\|^2 + \tau(1+2\gamma_{\phi_1}^2)\|Y_{\phi_1}(t)\|_F^2 \\
& + \tau(1+2\gamma_{\phi_2}^2)\int_{-\tau}^{0}\|Y_{\phi_2}(t,\eta)\|_F^2\mathrm{d}\eta \\
& + 2\tau\dot{\lambda}_2^{*T}(t)\dot{\lambda}_2^*(t) + 2\tau\mathrm{Tr}\{\dot{\Phi}_1^{*T}(t)\dot{\Phi}_1^*(t)\} \\
& + 2\tau\int_{-\tau}^{0}\mathrm{Tr}\{\dot{\Phi}_2^{*T}(t,\eta)\dot{\Phi}_2^*(t,\eta)\}\mathrm{d}\eta
\end{aligned} \tag{3.48}$$

Substituting (3.39) into (3.48), yields

$$\begin{aligned}
\dot{V}_2 \leq & - e_y^T(t)Q_2e_y(t) + N^*(t) \\
& + \tau(\mu + 2\gamma_2^2)\|\mathrm{diag}(L_r\mathcal{G}(t-\tau))B_p^TP_2e_y(t)\|^2 \\
& + \tau(1+2\gamma_{\phi_1}^2)\|x_p(t-\tau)e_y^T(t)P_2B_pL_r\|_F^2 \\
& + \tau(1+2\gamma_{\phi_2}^2)\int_{-\tau}^{0}\|L_ry_h(t+\eta-\tau)e_y^T(t)P_2B_pL_r\|_F^2\mathrm{d}\eta \\
& + 2\tau\dot{\lambda}_2^{*T}(t)\dot{\lambda}_2^*(t) + 2\tau\mathrm{Tr}\{\dot{\Phi}_1^{*T}(t)\dot{\Phi}_1^*(t)\} \\
& + 2\tau\int_{-\tau}^{0}\mathrm{Tr}\{\dot{\Phi}_2^{*T}(t,\eta)\dot{\Phi}_2^*(t,\eta)\}\mathrm{d}\eta \\
\leq & - \lambda_{min}(Q_2)\|e_y(t)\|^2 + N^*(t) \\
& + \tau(\mu + 2\gamma_2^2)\|\mathrm{diag}(L_r\mathcal{G}(t-\tau))\|^2\|P_2B_p\|^2\|e_y(t)\|^2 \\
& + \tau(1+2\gamma_{\phi_1}^2)\|x_p(t-\tau)\|^2\|e_y(t)\|^2\|P_2B_pL_r\|_F^2 \\
& + \tau(1+2\gamma_{\phi_2}^2)\int_{-\tau}^{0}\|L_ry_h(t+\eta-\tau)\|^2\|e_y(t)\|^2\|P_2B_pL_r\|_F^2\mathrm{d}\eta \\
& + 2\tau\dot{\lambda}_2^{*T}(t)\dot{\lambda}_2^*(t) + 2\tau\mathrm{Tr}\{\dot{\Phi}_1^{*T}(t)\dot{\Phi}_1^*(t)\} \\
& + 2\tau\int_{-\tau}^{0}\mathrm{Tr}\{\dot{\Phi}_2^{*T}(t,\eta)\dot{\Phi}_2^*(t,\eta)\}\mathrm{d}\eta.
\end{aligned} \tag{3.49}$$

Substituting (3.36) for $N^*(t)$ in (3.49), yields

$$\begin{aligned}
\dot{V}_2 \leq & - \lambda_{min}(Q_2)\|e_y(t)\|^2 \\
& + \tau(\mu + 2\gamma_2^2)\|\mathrm{diag}(L_r\mathcal{G}(t-\tau))\|^2\|P_2B_p\|^2\|e_y(t)\|^2 \\
& + \tau(1+2\gamma_{\phi_1}^2)\|x_p(t-\tau)\|^2\|e_y(t)\|^2\|P_2B_pL_r\|_F^2 \\
& + \tau(1+2\gamma_{\phi_2}^2)\int_{-\tau}^{0}\|L_ry_h(t+\eta-\tau)\|^2\|e_y(t)\|^2\|P_2B_pL_r\|_F^2\mathrm{d}\eta \\
& + 2\tau\dot{\lambda}_2^{*T}(t)\dot{\lambda}_2^*(t) + 2\tau\mathrm{Tr}\{\dot{\Phi}_1^{*T}(t)\dot{\Phi}_1^*(t)\} \\
& + 2\tau\int_{-\tau}^{0}\mathrm{Tr}\{\dot{\Phi}_2^{*T}(t,\eta)\dot{\Phi}_2^*(t,\eta)\}\mathrm{d}\eta \\
& + \gamma_2^{-1}\tilde{\lambda}_2^T(t)\dot{\Lambda}_2(t)\tilde{\lambda}_2(t) - 2\gamma_2^{-1}\tilde{\lambda}_2^T(t)\Lambda_2(t)\dot{\lambda}_2^*(t) \\
& - 2\gamma_3^{-1}\tilde{\lambda}_3^T(t)\dot{\lambda}_3^*(t) - 2\gamma_{\phi_1}^{-1}\mathrm{Tr}\{\dot{\Phi}_1^{*T}(t)\tilde{\Phi}_1(t)\} \\
& - 2\gamma_{\phi_2}^{-1}\int_{-\tau}^{0}\mathrm{Tr}\{\dot{\Phi}_2^{*T}(t,\eta)\tilde{\Phi}_2(t,\eta)\}\mathrm{d}\eta,
\end{aligned} \tag{3.50}$$

Using Remarks 3.1 and 3.2, and denoting $p \triangleq \max(\|P_2B_p\|^2, \|P_2B_pL_r\|_F^2)$, yields

$$\begin{aligned}\dot{V}_2 \leq & -\lambda_{min}(Q_2)\|e_y(t)\|^2 \\ & + \tau p(\mu + 2\gamma_2^2)\|\mathrm{diag}(L_r\mathcal{G}(t-\tau))\|^2\|e_y(t)\|^2 \\ & + \tau p(1+2\gamma_{\phi_1}^2)\|x_p(t-\tau)\|^2\|e_y(t)\|^2 \\ & + \tau p(1+2\gamma_{\phi_2}^2)\int_{-\tau}^{0}\|L_ry_h(t+\eta-\tau)\|^2\|e_y(t)\|^2\mathrm{d}\eta \\ & + 2\tau\dot{\beta}_2^2 + 2\tau\dot{\phi}_1^2 + 2\tau^2\dot{\phi}_2^2 + \gamma_2^{-1}\tilde{\beta}_2^2\dot{\beta}_3 + 2\gamma_2^{-1}\tilde{\beta}_2\beta_3\dot{\beta}_2 \\ & + 2\gamma_3^{-1}\tilde{\beta}_3\dot{\beta}_3 + 2\gamma_{\phi_1}^{-1}\dot{\phi}_1\tilde{\phi}_1 + 2\gamma_{\phi_2}^{-1}\tau\dot{\phi}_2\tilde{\phi}_2,\end{aligned} \tag{3.51}$$

where $\tilde{\beta}_2 \triangleq \|\hat{\lambda}_{2max}\| + \beta_2$, $\tilde{\beta}_3 \triangleq \|\hat{\lambda}_{3max}\| + \beta_3$, $\tilde{\phi}_1 \triangleq \|\hat{\Phi}_{1max}\| + \phi_1$, and $\tilde{\phi}_2 \triangleq \|\hat{\Phi}_{2max}\| + \phi_2$. Defining $q \triangleq \lambda_{min}(Q_2)/p$, and rearranging, one can rewrite (3.51) as

$$\begin{aligned}\dot{V}_2 \leq & p\|e_y(t)\|^2\Big(-q + \tau\Big\{(\mu+2\gamma_2^2)\|\mathrm{diag}(L_r\mathcal{G}(t-\tau))\|^2 \\ & + (1+2\gamma_{\phi_1}^2)\|x_p(t-\tau)\|^2 + (1+2\gamma_{\phi_2}^2)\int_{-\tau}^{0}\|L_ry_h(t+\eta-\tau)\|^2\mathrm{d}\eta\Big\}\Big) \\ & + 2\tau(\dot{\beta}_2^2 + \dot{\phi}_1^2 + \tau\dot{\phi}_2^2) + \gamma_2^{-1}\tilde{\beta}_2^2\dot{\beta}_3 + 2\gamma_2^{-1}\tilde{\beta}_2\beta_3\dot{\beta}_2 \\ & + 2\gamma_3^{-1}\tilde{\beta}_3\dot{\beta}_3 + 2\gamma_{\phi_1}^{-1}\dot{\phi}_1\tilde{\phi}_1 + 2\gamma_{\phi_2}^{-1}\tau\dot{\phi}_2\tilde{\phi}_2.\end{aligned} \tag{3.52}$$

It follows from Lemma 3.1 that $x_p(t)$ is bounded, which implies that there exists $\alpha_1 \in \mathbb{R}_+$ such that $\|x_p(t)\|^2 \leq \alpha_1$ for all $t \geq t_0$. Since $\|y_h(t)\| \leq \|y_o\|$ for all $t \geq t_0$ due to human input saturation, then there exists $\alpha_2 \in \mathbb{R}_+$ such that $\|L_ry_h(t)\|^2 \leq \alpha_2$ for all $t \geq t_0$. In addition, as $r(t)$ is bounded, then all the terms in (3.18a) are bounded due to the usage of the projection operator in (3.24), which implies the boundedness of $\mathcal{G}(t)$ and hence the existence of $\alpha_3 \in \mathbb{R}_+$ such that $\|\mathrm{diag}(L_r\mathcal{G}(t))\|^2 \leq \alpha_3$ for all $t \geq t_0$. Therefore, using (3.52), one can write

$$\begin{aligned}\dot{V}_2 \leq & p\|e_y(t)\|^2\Big(-q + \tau\Big\{(\mu+2\gamma_2^2)\alpha_3 + (1+2\gamma_{\phi_1}^2)\alpha_1 + (1+2\gamma_{\phi_2}^2)\tau\alpha_2\Big\}\Big) \\ & + 2\tau(\dot{\beta}_2^2 + \dot{\phi}_1^2 + \tau\dot{\phi}_2^2) + \gamma_2^{-1}\tilde{\beta}_2^2\dot{\beta}_3 + 2\gamma_2^{-1}\tilde{\beta}_2\beta_3\dot{\beta}_2 \\ & + 2\gamma_3^{-1}\tilde{\beta}_3\dot{\beta}_3 + 2\gamma_{\phi_1}^{-1}\dot{\phi}_1\tilde{\phi}_1 + 2\gamma_{\phi_2}^{-1}\tau\dot{\phi}_2\tilde{\phi}_2.\end{aligned} \tag{3.53}$$

Then, there exists a small enough $\tau^* \in \mathbb{R}_+$ such that

$$\tau^*\Big\{(\mu+2\gamma_2^2)\alpha_3 + (1+2\gamma_{\phi_1}^2)\alpha_1 + (1+2\gamma_{\phi_2}^2)\tau^*\alpha_2\Big\} < q, \tag{3.54}$$

which implies, from (3.53), that for any $\tau \in [0, \tau^*]$, $\dot{V}_2 < 0$ whenever

$$\|e_y(t)\|^2 > \frac{z_1}{z_2}, \tag{3.55}$$

where

$$\begin{aligned} z_1 \triangleq & 2\tau(\dot{\beta}_2^2 + \dot{\phi}_1^2 + \tau\dot{\phi}_2^2) + \gamma_2^{-1}\tilde{\beta}_2^2\dot{\beta}_3 + 2\gamma_2^{-1}\tilde{\beta}_2\beta_3\dot{\beta}_2 \\ & + 2\gamma_3^{-1}\tilde{\beta}_3\dot{\beta}_3 + 2\gamma_{\phi_1}^{-1}\dot{\phi}_1\tilde{\phi}_1 + 2\gamma_{\phi_2}^{-1}\tau\dot{\phi}_2\tilde{\phi}_2, \end{aligned} \tag{3.56}$$

$$z_2 \triangleq p\Big(q - \tau\Big\{(\mu + 2\gamma_2^2)\alpha_3 + (1 + 2\gamma_{\phi_1}^2)\alpha_1 + (1 + 2\gamma_{\phi_2}^2)\tau\alpha_2\Big\}\Big). \tag{3.57}$$

Hence, for any $\tau \in [0, \tau^*]$, the solution $(e_y(t), \tilde{\lambda}_2(t), \tilde{\lambda}_3(t), \tilde{\Phi}_1(t), \tilde{\Phi}_2(t, \eta))$ is bounded and converges to the compact set

$$\begin{aligned} E \triangleq \Bigg\{ & \Big(e_y(t), \tilde{\lambda}_2(t), \tilde{\lambda}_3(t), \tilde{\Phi}_1(t), \tilde{\Phi}_2(t, \eta)\Big) : \|e_y(t)\|^2 \le \frac{z_1}{z_2}, \\ & \|\tilde{\lambda}_2(t)\| \le \tilde{\beta}_2, \|\tilde{\lambda}_3(t)\| \le \tilde{\beta}_3, \|\tilde{\Phi}_1(t)\| \le \tilde{\phi}_1, \|\tilde{\Phi}_2(t, \eta)\| \le \tilde{\phi}_2 \Bigg\}. \end{aligned} \tag{3.58}$$

According to (3.14), since $r(t)$ is bounded, then so is $x_m(t)$. This with the fact that $x_p(t)$ is bounded (by Lemma 3.1) imply the boundedness of $e_2(t)$. And since $e_y(t) = e_2(t) - e_\Delta(t)$ is bounded, then $e_\Delta(t)$ is also bounded, which implies by (3.22) that $\Delta y(t)$ is bounded and completes the proof. ■

Remark 3.3. While the existence of the upper bound on the time delay τ^* is guaranteed, its value depends on the selection of the outer-loop learning rates $\gamma_{out} \triangleq \{\gamma_2, \gamma_{\phi_1}, \gamma_{\phi_2}\}$. Note from (3.54) that as larger values of γ_{out} are used, the allowable maximum time delay τ^* becomes smaller. On the other hand, in the limit where $\gamma_{out} \to 0$, which corresponds to no adaptation, τ^* approaches its ultimate value τ_{max} satisfying

$$\tau_{max}\Big(\mu\alpha_3 + \alpha_1 + \tau_{max}\alpha_2\Big) < q. \tag{3.59}$$

On the contrary, the ultimate bound $z \triangleq z_1/z_2$ on the error $e_y(t)$, which is defined by the set (3.58), (3.56) and (3.57), is inversely proportional to the values of γ_{out}. That is, to achieve a better tracking performance, which corresponds to smaller values of z, the outer-loop learning rates γ_{out} should be selected as large as possible. And in the limit where $\gamma_{out} \to \infty$, the upper bound $z \to 0$. Therefore, given any delay value $\tau < \tau_{max}$, the optimal outer-loop learning rates $\gamma_{out,opt}$ are

the ones that satisfy $\tau^* = \tau$. A further increase in $\gamma_{out} > \gamma_{out,opt}$ renders our stability analysis inapplicable due to $\tau > \tau^*$, while a decrease in $\gamma_{out} < \gamma_{out,opt}$ allows for higher delay values to be tolerated at the expense of a deteriorated tracking performance.

3.5 Simulations

Consider the longitudinal motion of the 747 airplane cruising in level flight at an altitude of 40 kft and a velocity of 774 ft/sec, the perturbation equations of which are represented in the form of (3.1). The state vector is

$$x_p(t) = \begin{bmatrix} x_{p1}(t) & x_{p2}(t) & x_{p3}(t) & x_{p4}(t) \end{bmatrix}^T, \tag{3.60}$$

where $x_{p1}(t)$ and $x_{p2}(t)$ are the components of the aircraft's velocity (in ft/s) along the x and z-axes, respectively, with respect to the reference axis, $x_{p3}(t)$ is the aircraft's pitch rate (in crad/s), and $x_{p4}(t)$ is the pitch angle of the aircraft (in crad). The control input $u_p(t)$ represents the elevator deflection (in crad). Under these conditions, nominal dynamics are available in the form of (3.2), where the nominal system and control input matrices are given as [27]

$$\begin{aligned} A_n &= \begin{bmatrix} -0.0030 & 0.0390 & 0 & -0.3220 \\ -0.0650 & -0.3190 & 7.7400 & 0 \\ 0.0200 & -0.1010 & -0.4290 & 0 \\ 0 & 0 & 1 & 0 \end{bmatrix}, \\ B_p &= \begin{bmatrix} 0.0100 & -0.1800 & -1.1600 & 0 \end{bmatrix}^T, \end{aligned} \tag{3.61}$$

with the eigenvalues at $-0.3750 \pm 0.8818i$ and $-0.0005 \pm 0.0674i$. The control objective is for a pilot to be able to track a desired trajectory. Particularly, the pilot controls the aircraft to achieve a desired pitch angle $y_2(t) = x_{p4}(t)$. This is done by feeding pitch rate commands through a joystick to the inner-loop, which consists of a control augmentation system designed to track the pilot's pitch rate commands, i.e., $y_1(t) = x_{p3}(t)$.

3.5.1 Inner Loop: Adaptive Control Augmentation System

The design of the inner-loop adaptive controller starts with the determination of the nominal control law (3.3) which is used to define the reference model. Achieving pilot command following by assigning the feed-forward gain L_r as in (3.5) is not possible since the transfer function $x_{p3}(s)/u_p(s)$ has a zero at the origin. Instead, as is common practice in the literature, we design the inner-loop nominal controller by assuming short-period approximation of the nominal dynamics, given by

$$A_{sp} = \begin{bmatrix} -0.3190 & 7.7400 \\ -0.1010 & -0.4290 \end{bmatrix}, \quad B_{sp} = \begin{bmatrix} -0.1800 \\ -1.1600 \end{bmatrix}, \tag{3.62}$$

where the eigenvalues are at $-0.3740 \pm 0.8824i$, which makes a good approximation of the fast dynamics of (3.61). Using (3.62), a feedback gain L_{sp} is designed to place the short-period eigenvalues at -1.5 and -0.5. Then, the feed-forward gain is selected as $L_r = -\left(C_{sp}^T (A_{sp} - B_{sp}L_{sp})^{-1} B_{sp}\right)^{-1}$, where $C_{sp} = [0,\, 1]^T$. The implementation of these values to the full longitudinal dynamics is applied as in (3.3), where $L_x = [0,\, L_{sp},\, 0]$, allowing for the reference model (3.4) to be defined using $A_r = A_n - B_p L_x$ and $B_r = B_p L_r$.

An adaptive controller is employed as in (3.7) and (3.10) to achieve reference model following in the presence of uncertainty, where the adaptive parameters are initialized at the nominal values $\hat{K}_x(0) = L_x$ and $\hat{\lambda}(0) = 1$. Furthermore, the Lyapunov matrix is selected as $Q_1 = 0.01 I_{4\times 4}$, and the learning rates are set to $\gamma_x = \text{diag}([0.01,\, 0.001,\, 0.01,\, 0.01])$ and $\gamma_\lambda = 0.001$.

3.5.2 Outer Loop: Adaptive Pilot Model

For the outer loop, the proposed adaptive human pilot model is employed as in (3.14), (3.18), (3.22), and (3.24), where manipulator limits of ± 10 crad/s (i.e., $y_o = 10$) are imposed on the pilot's input. Reflecting the overall nominal response,

the crossover-reference model (3.14) defines how a well-trained pilot controls the aircraft under nominal circumstances, providing satisfactory performance and adequate stability margins. While its determination is application-dependent and can require experimental analysis, to serve the purpose of this section, we define the crossover-reference model using the LQR method by calculating θ_x using $Q_{LQR} = \text{diag}([0,\ 0.01,\ 0.6,\ 10])$ and $R_{LQR} = 0.6$, with θ_r given in (3.15), and assigning $A_m = A_r - B_r\theta_x$, and $B_m = B_r\theta_r$.

The time delay τ in the pilot's response to visual stimuli can be broken down into approximate components [28, 29] constituting the latency of the visual process (≈ 0.075 s), the motor nerve conduction time (≈ 0.030 s), and the central processing time (≈ 0.030 s). While exact values may vary depending on the pilot's attention, these average values are convenient for use in this section, yielding a total delay of $\tau = 0.135$ s in the pilot response.

The finite integral term in (3.18a) and the adaptive law (3.24d) are implemented by discretizing the integral into 5 intervals as illustrated in [30]. The outer-loop adaptive parameters are initialized at the nominal values $\hat{\lambda}_2(0) = \hat{\lambda}_3(0) = 1$, $\hat{\Phi}_1(0) = -\theta_x e^{A_r\tau}$, and $\hat{\Phi}_2(0,\eta) = -\theta_x e^{-A_r\eta}B_p$. This initialization implies that the pilot initially starts with the nominal control law

$$v_n(t) = -\theta_x x_n(t+\tau) + \theta_r r(t) \tag{3.63a}$$

$$x_n(t+\tau) = e^{A_r\tau}x_n(t) + \int_{-\tau}^{0} e^{-A_r\eta}B_r y_h(t+\eta)\,\mathrm{d}\eta \tag{3.63b}$$

$$y_{hn}(t) = \begin{cases} v_n(t), & \text{if } |v_n(t)| \le y_o, \\ y_o \text{sgn}(v_n(t)), & \text{if } |v_n(t)| > y_o, \end{cases} \tag{3.63c}$$

which matches the crossover-reference model in the absence of plant uncertainty and input saturation. Finally, the Lyapunov matrix is selected as $Q_2 = 0.01I_{4\times4}$, and the outer-loop learning rates are set to $\gamma_2 = 0.5$, $\gamma_3 = 1000$, $\gamma_{\phi_1} = \text{diag}([0.01,\ 0.01,\ 0.1,\ 0.1])$, and $\gamma_{\phi_2} = 0.01$.

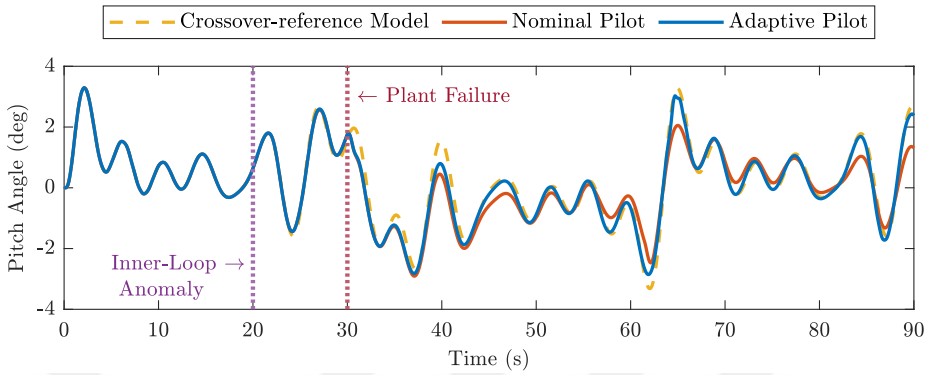

Figure 3.2: Pitch angle trajectory tracking of the proposed adaptive model, compared with a nominal non-adaptive pilot model.

3.5.3 Failure Scenario

In the simulated scenario, we start with an uncertainty in the modeled dynamics with $\Lambda = 1$, and the system matrix

$$t < 30: \; A_p = \begin{bmatrix} -0.0067 & 0.0410 & -0.0037 & -0.3223 \\ 0.0010 & -0.3558 & 7.8068 & 0.0047 \\ 0.4454 & -0.3380 & 0.0015 & 0.0302 \\ 0 & 0 & 1 & 0 \end{bmatrix}, \tag{3.64}$$

placing the eigenvalues at $-0.1800 \pm 1.6000i$ and $-0.0005 \pm 0.1400i$. An anomaly is then introduced into the inner-loop controller at $t = 20$ s, failing the adaptation in the $\hat{K}_x(t)$ channel (i.e., $\gamma_x = 0_{4\times4}$ for $t \geq 20$ s). It is noted that the other inner-loop adaptive parameter, $\hat{\lambda}(t)$, is kept actively adapting throughout the simulation. At $t = 30$ s, a failure is introduced into the plant dynamics, where the control effectiveness reduces to $\Lambda = 0.5$ for $t \geq 30$ s, and the system matrix becomes

$$t \geq 30: \; A_p = \begin{bmatrix} -0.0127 & 0.0427 & -0.0040 & -0.3227 \\ 0.1100 & -0.3859 & 7.8124 & 0.0131 \\ 1.1479 & -0.5323 & 0.0376 & 0.0847 \\ 0 & 0 & 1 & 0 \end{bmatrix}, \tag{3.65}$$

placing the eigenvalues at $-0.1800 \pm 2.0000i$ and $-0.0005 \pm 0.1750i$.

Figure 3.2 shows the pitch angle tracking trajectory for the aforementioned scenario, where the performance of the proposed adaptive pilot model is compared with a fixed (non-adaptive) pilot model utilizing the nominal control law (3.63). The effectiveness of adaptation in the proposed model is evident as it learns to compensate for the plant failure, converging back to the desired trajectory of the crossover-reference model. On the other hand, for the nominal pilot model, the plant failure causes a permanent deviation from the desired trajectory, which persists since the model is non-adaptive and is therefore a poor representation of what a well-trained pilot would do in such a situation.

The pitch angle tracking error and pilot inputs are displayed in Fig. 3.3 for both the nominal and the adaptive models. While the adaptive model achieves enhanced transients, it comes at the expense of an increase in the pilot control effort. This can be observed from Fig. 3.3, particularly in the time frame between $63 - 67$ seconds, where the control inputs of the adaptive model are more oscillatory than those of the nominal one, but leading to a 70% reduction in the pitch angle tracking error. Under the effect of a failure, such a behavior can be expected from a pilot attempting to compensate for the uncertainty, which also raises the question of how to better design the control system by taking the human pilot into consideration.

3.6 Summary

An adaptive human pilot model is proposed in this chapter to describe the pilot behavior in the loop with an adaptive controller. What distinguishes this model from the one proposed in Chapter 2, is that it takes into consideration the time delay in the human pilot response, which makes it suitable for a broader range of applications. The pilot is modeled as a model reference adaptive control architecture in the presence of time delay and input saturation. The effectiveness of the proposed adaptive model is validated through a detailed simulation study for the longitudinal motion of the 747 airplane. We show that the proposed model gives a better representation of a well-trained pilot than a fixed nominal pilot model.

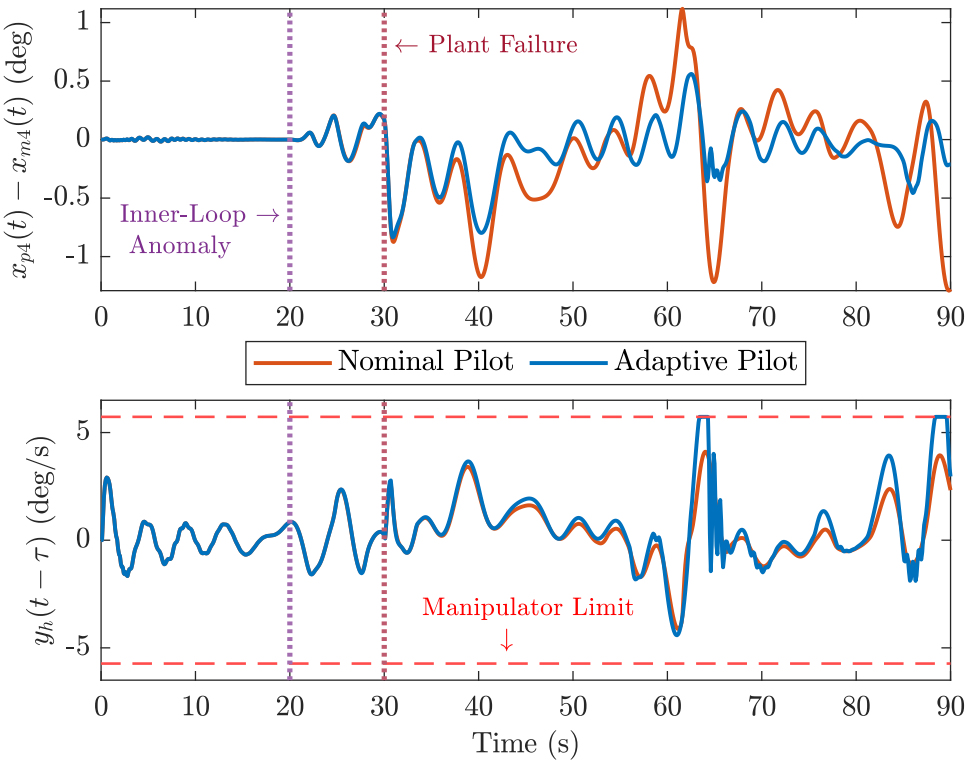

Figure 3.3: Top: Pitch angle tracking error evolution. Bottom: Pilot control inputs.

Chapter 4

Attention-Enabled Memory for Adaptive Control Systems

4.1 Introduction

Humans' episodic memory enables them to remember self-experienced events to be used later if a similar event is encountered again [8, 9]. For example, drivers having a tire blowout would react better if they have experienced it before in their life. This is because when drivers experience a tire blowout for the first time, they are not familiar with the failure, and hence, they begin exploring the situation in an attempt to recover from it. Such exploration can be lethal, but is necessary when little is known about the system. On the second encounter of a tire blowout, drivers rely on useful data from their episodic memory to recover with minimal exploration.

Many works in the literature are devoted to enhancing the transients of adaptive systems [31–34]. However, an adaptive control system exhibits similar transients even for previously experienced failures. This is due to a lack of an architecture that allows the controller to recall and use significant information about previously encountered uncertainties. Inspired by episodic memory in humans, in

this chapter, we aim to provide adaptive controllers with an analogous memory architecture. In this regard, the first issue to be addressed is memory content. What type of data about a failure would be beneficial for future use if we were to encounter a similar failure again? A well-established answer to this question is found in the literature under the name of *concurrent learning* [35].

In concurrent learning adaptive control, recorded data (termed *history stack*) and present measurements are used concurrently for adaptation. With sufficiently rich data in the history stack, this approach yields exponential stability, which has been shown to result in enhanced transients. In traditional adaptive control, exponential stability is only possible if the system is *persistently exciting* [36,37], which accounts for continuous exploration of the uncertainty. Therefore, the usage of concurrent learning minimizes the need for exploration by using stored data about a previous failure [35].

When it comes to using the history stack of concurrent learning as a memory, several issues must be considered. For the recorded data to be usable for adapting to a specific failure, the history stack must only consist of data that represent the same failure. Thus, the controller can only recall information about a single failure/uncertainty. This poses a limitation in the sense that the same failure must be experienced by the plant at all times. Any changes to the system (including unexpected failures) render the history stack inapplicable since their usage can deteriorate the adaptive control performance. This requires the history stack to be cleared and repopulated with new data once a new failure occurs [35].

In this chapter, we build upon the idea of concurrent learning to propose a memory architecture that allows the adaptive controller to recall and use significant information about the past to aid in learning. The proposed memory can store data about several uncertainties/failures without the need to know which data corresponds to which uncertainty. To use the stored data in the adaptive law, an attention-based reading mechanism is proposed which enables the controller to selectively use only the data that are relevant to the encountered uncertainty without requiring any knowledge about the uncertainty. Throughout the work, we augment the proposed memory with a modified version of the

composite model reference adaptive controller (CMRAC) [38], and show the stability of the memory-augmented adaptive controller through a rigorous Lyapunov analysis. The results of this chapter have been published in [39].[§]

In Section 4.2, we explain the adopted CMRAC architecture, concurrent learning, and formulate the problem. In Section 4.3, the proposed memory architecture is presented with a rigorous stability analysis. At last, the effectiveness of the proposed memory is elucidated through numerical simulations in Section 4.4, while a summary is provided in Section 4.5

4.1.1 Notations

We use $\mathrm{Tr}\{.\}$ to denote the trace operator, $\|.\|$ refers to the euclidean norm, and $\|.\|_F$ refers to the Frobenius norm. We denote a positive definite (positive semi-definite) matrix X as $X > 0$ ($X \geq 0$), and a negative definite (negative semi-definite) function V as $V < 0$ ($V \leq 0$). Finally, we write $\lambda_{min}(X)$ for the minimum eigenvalue of the matrix X.

4.2 Problem Statement

Consider the uncertain plant dynamics

$$\begin{aligned} \dot{x}(t) =& A_p x(t) + B_p \left(u(t) + \Theta^T f(x(t))\right), \\ y(t) =& C_p x(t), \end{aligned} \tag{4.1}$$

where $x(t) \in \mathbb{R}^n$ is the accessible state vector, $u(t) \in \mathbb{R}^m$ is the plant control input, $f(x(t)) : \mathbb{R}^n \to \mathbb{R}^s$ is a known possibly non-linear function, whose components are locally Lipschitz-continuous functions of $x(t)$, $\Theta \in \mathbb{R}^{s\times m}$ is an unknown weight matrix, $A_p \in \mathbb{R}^{n\times n}$ is an unknown state matrix, and $B_p \in \mathbb{R}^{n\times m}$ is a known full column rank input matrix. The output of interest $y(t) \in \mathbb{R}^m$ is defined by

[§]

the known output matrix $C_p \in \mathbb{R}^{m\times n}$, and the pair (A_p, B_p) is assumed to be controllable.

The adaptive control task is to achieve command following of a bounded reference input $r(t) \in \mathbb{R}^m$, through tracking the state $x_r(t) \in \mathbb{R}^n$ of a reference model

$$\dot{x}_r(t) = A_r x_r(t) + B_r r(t), \tag{4.2}$$

where $A_r \in \mathbb{R}^{n\times n}$ is Hurwitz. B_r is selected as $B_r \triangleq B_p K_r$, where $K_r \in \mathbb{R}^{m\times m}$ is the feed-forward controller gain, which is determined as

$$K_r \triangleq -(C_p A_r^{-1} B_p)^{-1}, \tag{4.3}$$

to achieve $\lim_{t\to\infty} y(t) = r$ whenever $\lim_{t\to\infty} x(t) = x_r(t)$, for a constant $r(t) = r$ [15]. It is assumed that there exist a feedback controller gain $K_x \in \mathbb{R}^{m\times n}$ that satisfies the matching condition

$$A_r = A_p - B_p K_x. \tag{4.4}$$

It is noted that the matching condition (4.4) is commonly used in the adaptive control literature, and the controllers designed based on this condition are shown to be effective in practical implementations [16, 35, 36, 38].

Using (4.4) in (4.1), one can rewrite (4.1) as

$$\dot{x}(t) = A_r x(t) + B_p \left(u(t) + K_x x(t) + \Theta^T f(x(t))\right). \tag{4.5}$$

Defining the unknown parameter $W \triangleq [K_x, \Theta^T]^T \in \mathbb{R}^{\phi\times m}$ and $\Phi(x(t)) \triangleq [x(t)^T, f(x(t))^T]^T \in \mathbb{R}^{\phi}$, with $\phi \triangleq n + s$, (4.5) can be written as

$$\dot{x}(t) = A_r x(t) + B_p \left(u(t) + W^T \Phi(x(t))\right). \tag{4.6}$$

Then, the plant control input is chosen as

$$u(t) = K_r r(t) - \hat{W}^T(t)\Phi(x(t)), \tag{4.7}$$

where $\hat{W}(t) \in \mathbb{R}^{\phi\times m}$ is an adaptive parameter serving as an estimate of the ideal value W. It is noted that W is allowed to be piece-wise-constant such

that different values occur in a sufficiently separated manner temporally, without experiencing a Zeno behavior.

In CMRAC [38], $\hat{W}(t)$ is updated based on two distinct measurable errors, a *tracking error* and an *estimation error*. The tracking error is the error between the plant and reference model states $e(t) \triangleq x(t) - x_r(t)$, the derivative of which can be found, using (4.2), (4.6) and (4.7) as

$$\dot{e}(t) = A_r e(t) - B_p \tilde{W}^T(t)\Phi(x(t)), \tag{4.8}$$

where $\tilde{W}(t) \triangleq \hat{W}(t) - W$. The estimation error is based on identifying the plant dynamics as shown in the following subsection.

4.2.1 Estimation Error : Identification

In what follows, we construct an identifier based on filtered plant dynamics [40,41] to alleviate the need for the state derivative to be known. We start by adding and subtracting $Ax(t)$ to (4.6), which yields

$$\dot{x}(t) = -Ax(t) + B_p\left(u(t) + W^T\Phi(x(t))\right) + (A + A_r)x(t), \tag{4.9}$$

where

$$A \triangleq aI_{n\times n}, \;\; a > 0. \tag{4.10}$$

Then, the solution of (4.9) can be written as

$$\begin{aligned} x(t) =& e^{-at}x(0) + B_p\int_0^t e^{-a(t-\tau)}u(\tau)\mathrm{d}\tau \\ &+ B_pW^T\int_0^t e^{-a(t-\tau)}\Phi(x(\tau))\mathrm{d}\tau \\ &+ (A + A_r)\int_0^t e^{-a(t-\tau)}x(\tau)\mathrm{d}\tau. \end{aligned} \tag{4.11}$$

By defining the filtered versions of $u(t)$, $\Phi(x(t))$, and $x(t)$ respectively as

$$\begin{aligned} u_f(t) &\triangleq \int_0^t e^{-a(t-\tau)}u(\tau)\mathrm{d}\tau, \\ \Phi_f(t) &\triangleq \int_0^t e^{-a(t-\tau)}\Phi(x(\tau))\mathrm{d}\tau, \\ x_f(t) &\triangleq \int_0^t e^{-a(t-\tau)}x(\tau)\mathrm{d}\tau, \end{aligned} \tag{4.12}$$

the plant dynamics can be represented as

$$\begin{aligned} x(t) =& B_p(u_f(t) + W^T\Phi_f(t)) + (A + A_r)x_f(t), && \text{(4.13a)}\\ \dot{u}_f(t) =& - au_f(t) + u(t), \quad u_f(0) = 0, && \text{(4.13b)}\\ \dot{\Phi}_f(t) =& - a\Phi_f(t) + \Phi(x(t)), \quad \Phi_f(0) = 0, && \text{(4.13c)}\\ \dot{x}_f(t) =& - ax_f(t) + x(t), \quad x_f(0) = 0, && \text{(4.13d)} \end{aligned}$$

where it is assumed, without loss of generality, that $x(0) = 0$.

We now define the identifier based on (4.13) by replacing the unknown parameter W with its estimate $\hat{W}(t)$ as

$$\hat{x}(t) \triangleq B_p(u_f(t) + \hat{W}^T(t)\Phi_f(t)) + (A + A_r)x_f(t), \tag{4.14}$$

where $\hat{x}(t) \in \mathbb{R}^n$ is the identifier's state. Then, an identification error is obtained as

$$e_{id}(t) \triangleq \hat{x}(t) - x(t) = B_p\tilde{W}^T(t)\Phi_f(t). \tag{4.15}$$

Furthermore, the estimation error is defined as

$$\epsilon(t) \triangleq (B_p^TB_p)^{-1}B_p^Te_{id}(t) = \tilde{W}^T(t)\Phi_f(t). \tag{4.16}$$

It is noted that $B_p^TB_p$ is invertible since B_p is full column rank.

4.2.2 CMRAC: Adaptive Law

With both tracking and estimation errors defined, the adaptive law of $\hat{W}(t)$ is then defined compositely as

$$\begin{aligned} \dot{\tilde{W}}(t) = \dot{\hat{W}}(t) \triangleq& \gamma_e\Phi(x(t))e(t)^TPB_p - \gamma_\epsilon\Phi_f(t)\epsilon(t)^T\\ =& \gamma_e\Phi(x(t))e(t)^TPB_p - \gamma_\epsilon\Phi_f(t)\Phi_f^T(t)\tilde{W}(t), \end{aligned} \tag{4.17}$$

where $P = P^T > 0$ is the solution of the Lyapunov equation

$$A_r^TP + PA_r = -Q, \tag{4.18}$$

for some $Q = Q^T > 0$, and γ_e,$\gamma_\epsilon > 0$ are scalar learning rates. Using (4.17), the derivative of the Lyapunov function

$$V = e^T P e + \gamma_e^{-1} \mathrm{Tr}\{\tilde{W}^T \tilde{W}\} \tag{4.19}$$

along the trajectories of (4.8) and (4.16) yields

$$\dot{V} = -e^T Q e - 2\gamma_r \mathrm{Tr}\{\tilde{W}^T \Phi_f \Phi_f^T \tilde{W}\}, \tag{4.20}$$

where $\gamma_r \triangleq \gamma_\epsilon / \gamma_e$. Since $\Phi_f \Phi_f^T \geq 0$, then $\dot{V} \leq 0$, which by using Barbalat's lemma shows that the system is globally stable and that $e(t) \to 0$ and $\epsilon(t) \to 0$ [38].

4.2.3 Concurrent Learning

The idea behind concurrent learning [35] is to use previously recorded data concurrently with present data to achieve exponential stability. Towards that end, a collection of p data points recorded in the past is stored in a history stack as

$$Z_u = \begin{bmatrix} u_{f_1} & \dots & u_{f_p} \end{bmatrix}, \tag{4.21a}$$

$$Z_\Phi = \begin{bmatrix} \Phi_{f_1} & \dots & \Phi_{f_p} \end{bmatrix}, \tag{4.21b}$$

$$Z_x = \begin{bmatrix} x_1 & \dots & x_p \end{bmatrix}. \tag{4.21c}$$

Then, *projected errors* are defined as

$$\epsilon_j(t) = \tilde{W}^T(t) \Phi_{f_j}, \tag{4.22}$$

which represent what the estimation error would have been for a recorded data point j, if the current value of $\hat{W}(t)$ were to be used. Since $x_j = B_p(u_{f_j} + W^T \Phi_{f_j}) + (A + A_r) x_{f_j}$ (see (4.13a)), using the structures given in (4.14), (4.15) and (4.16), together with the recorded data (4.21), the projected errors can be calculated as

$$\epsilon_j(t) = (B_p^T B_p)^{-1} B_p^T \Big(B_p(u_{f_j} + \hat{W}^T(t) \Phi_{f_j}) + (A + A_r) x_{f_j} - x_j \Big), \tag{4.23}$$

where x_{f_j} is extracted from the elements of Φ_{f_j}. These errors are then used in the adaptive law as

$$\dot{\hat{W}}(t) = \dot{\hat{W}}(t) \triangleq \gamma_e \Phi(x(t)) e(t)^T P B_p - \gamma_\epsilon \Phi_f(t) \epsilon(t)^T - \gamma_\epsilon \sum_{j=1}^{p} \Phi_{f_j} \epsilon_j(t)^T, \tag{4.24}$$

where $P = P^T > 0$ is the solution of the Lyapunov equation (4.18), and γ_e,$\gamma_\epsilon > 0$ are scalar learning rates. Using (4.24), the derivative of (4.19) along the trajectories (4.8), (4.16) and (4.22) yields

$$\dot{V} = -e^T Q e - 2\gamma_r \mathrm{Tr}\{\tilde{W}^T(\Phi_f \Phi_f^T + \sum_{j=1}^{p} \Phi_{f_j} \Phi_{f_j}^T)\tilde{W}\}. \tag{4.25}$$

Since $(\Phi_f \Phi_f^T + \sum_{j=1}^{p} \Phi_{f_j} \Phi_{f_j}^T) \geq 0$, then $\dot{V} \leq 0$ which preserves the same stability properties explained after (4.20). Additionally, if $rank(Z_\Phi) = \phi$, where Z_Φ is defined in (4.21) and ϕ is defined after (4.5), then $(\Phi_f \Phi_f^T + \sum_{j=1}^{p} \Phi_{f_j} \Phi_{f_j}^T) > 0$, which makes $\dot{V} < 0$ and hence both $e(t)$ and $\tilde{W}(t)$ converge to zero exponentially.

Remark 4.1. The advantage of concurrent learning is that one can record data online that satisfy $rank(Z_\Phi) = \phi$ by exciting the system for a finite period of time, and hence guarantee exponential convergence without the need to persistently excite the system. This can be achieved through already available real-time algorithms [35].

Remark 4.2. To use the concurrent adaptive law (4.24), it is required for data to be either pre-recorded in advance or collected online. In both cases, the recorded data must represent the same uncertainty W and hence the data should be collected when the same uncertainty is encountered. This poses a limitation in the sense that the uncertainty W must be fixed throughout the operation, or each time a new uncertainty occurs, for example due to a failure, the memory should be cleared, and new data must be recorded [42]. Otherwise, the recorded data have the potential to sacrifice the performance if an unanticipated uncertainty is faced. In the following section, we propose a solution to this problem by introducing a new memory architecture.

4.3 Memory Architecture

Suppose that we store p data points in a memory as

$$M_u = \begin{bmatrix} u_{f_1} & \dots & u_{f_p} \end{bmatrix}, \tag{4.26a}$$

$$M_\Phi = \begin{bmatrix} \Phi_{f_1} & \dots & \Phi_{f_p} \end{bmatrix}, \tag{4.26b}$$

$$M_x = \begin{bmatrix} x_1 & \dots & x_p \end{bmatrix}, \tag{4.26c}$$

where each data point in the memory $\mathcal{M} \triangleq (M_u, M_\Phi, M_x)$ can correspond to a different uncertainty.

Definition 4.1. The *encountered uncertainty* W is the uncertainty that is currently existing in the system (4.6).

Definition 4.2. An uncertainty W_i is *represented* in the memory $\mathcal{M}$, if there is at least one data point $(u_{f_j}, \Phi_{f_j}, x_j)$ in $\mathcal{M}$ such that $x_j = B_p(u_{f_j} + W_i^T \Phi_{f_j}) + (A + A_r)x_{f_j}$. Such a data point is said to *represent* W_i.

Definition 4.3. Two data points are called *mutual* if they represent the same uncertainty.

Definition 4.4. A data point (or its corresponding projected error $\epsilon_j(t)$, see (4.22)) is said to be *mutual with* $\epsilon(t)$, if it represents the encountered uncertainty W.

In the proposed architecture, we assume that the memory $\mathcal{M}$, in (4.26), is representative of d different uncertainties $(W_1, \dots, W_d)$, where d is unknown (see Definition 4.2). Moreover, it is not known which data points correspond to what uncertainty, and mutual data points cannot be told apart.

The goal here is to use the stored data in $\mathcal{M}$ to enhance the transients of the control system given by (4.2), (4.6) and (4.7) when a represented uncertainty is encountered, i.e., $W = W_{i(j)}$ for some $j \in \{1, \dots, p\}$, where

$$i(j) : \{1, \dots, p\} \to \{1, \dots, d\} \tag{4.27}$$

is an unknown map that relates each data point to the uncertainty it represents. For that, projected errors are calculated at each time instant, for each data point in $\mathcal{M}$ as shown in (4.23). By substituting $x_j = B_p(u_{f_j} + W_{i(j)}^T \Phi_{f_j}) + (A + A_r)x_{f_j}$ in (4.23), these projected errors can be written as

$$\epsilon_j(t) = (\hat{W}(t) - W_{i(j)})^T \Phi_{f_j} = \tilde{W}_{i(j)}^T(t)\Phi_{f_j}, \tag{4.28}$$

where $\tilde{W}_{i(j)}(t) \triangleq \hat{W}(t) - W_{i(j)}$ is the error between the adaptive parameter $\hat{W}(t)$ and the constant uncertainty $W_{i(j)}$ represented by the j^{th} data point $(u_{f_j},\, \Phi_{f_j},\, x_j)$. If all memory slots were to be used as in conventional concurrent learning (see (4.24)) to compensate for the encountered uncertainty W, the resulting adaptive law (4.24) would try to drive the tracking error $e(t)$, the estimation $\epsilon(t)$, and all projected errors $\epsilon_j(t)$, for $j = 1, \ldots, p$, simultaneously to zero. However, since $W_1 \neq W_2 \neq \ldots \neq W_d$, $\epsilon(t)$ and $\epsilon_j(t)$ cannot converge to zero simultaneously unless all $\epsilon_j(t)$ are mutual with $\epsilon(t)$ (see (4.16) and (4.28)). This deteriorates the performance of the system, since data points that do not represent the encountered uncertainty W are being used in learning. To alleviate this problem, a reading mechanism that determines which data points to be used is needed.

4.3.1 Memory Read

In this subsection we address the question: *Given the estimation error $\epsilon(t)$ in (4.16), and the memory projected errors $\epsilon_j(t)$ in (4.28), for $j = 1, \ldots, p$, how can we determine which projected errors are mutual with $\epsilon(t)$?*

Once we answer the above question, we can selectively use only the data points that are mutual with $\epsilon(t)$ (see Definition 4.4) in the adaptive law. Hence, we propose a mechanism that allows the controller to read only the relevant data from the memory in a continuous manner. To that end, we define scalar attention weights for each memory slot as

$$\mu_j(t) = \beta \frac{\exp(-\alpha\|\epsilon(t) - \epsilon_j(t)\|)}{\sum_{k=1}^{p} \exp(-\alpha\|\epsilon(t) - \epsilon_k(t)\|)}, \tag{4.29}$$

where the scalars $\alpha, \beta > 0$ are design constants. It is noted that whenever $\tilde{W}(t) \to 0$, both $\epsilon(t)$ and its mutual projected errors approach zero (see (4.28)

and Definition 4.4). Hence, the euclidean distances $\|\epsilon(t) - \epsilon_j(t)\|$ become smaller when $\epsilon_j(t)$ is mutual with $\epsilon(t)$. Therefore, the attention weights (4.29) attribute higher weights to projected errors that are distanced closer to $\epsilon(t)$ in such a way that $\sum_{j=1}^{p} \mu_j(t) = \beta$, and $0 < \mu_j(t) < \beta$, for $j = 1, \ldots, p$. Here, α specifies the amount by which distance is penalized, and β affects how much the recorded data influences learning (see (4.30)).

We now propose the memory-augmented adaptive law

$$\dot{\hat{W}}(t) = \dot{\hat{W}}(t) \triangleq \text{Proj}(\hat{W}(t), Y(t)), \tag{4.30a}$$

$$Y(t) \triangleq \gamma_e \Phi(x(t)) e(t)^T P B_p - \gamma_\epsilon \Phi_f(t) \epsilon(t)^T - \gamma_\epsilon \sum_{j=1}^{p} \mu_j(t) \Phi_{f_j} \epsilon_j(t)^T, \tag{4.30b}$$

where $P = P^T > 0$ is the solution of the Lyapunov equation (4.18), γ_e,$\gamma_\epsilon > 0$ are scalar learning rates, and the memory read is done through scalar attention weights (4.29) that allow the controller to eventually identify and use only data that are relevant to the encountered uncertainty W. Furthermore, Proj(.,.) is the projection operator [16], used to bound the adaptive parameter $\hat{W}(t)$ in a predefined compact set $\Omega \triangleq \{\hat{W}(t) : \|\hat{W}(t)\|_F \leq W_{max}\}$, for some scalar $W_{max} > 0$.

4.3.2 Short-Term Memory

If the uncertainty W is encountered for the first time during operation, then W is not represented in the memory, and no memory slots should be utilized in learning. This however is not the case with the proposed reading mechanism (4.29) and (4.30) since

$$\sum_{j=1}^{p} \mu_j(t) = \beta, \tag{4.31}$$

which implies that the memory is always utilized. We alleviate this issue by ensuring that our memory $\mathcal{M}$ is always representative of W. This is achieved by using a *short-term memory* which holds on to q-many delayed values of the measured signals $(u_f(t - \tau_k), \Phi_f(t - \tau_k), x(t - \tau_k))$, for $k = 1, \ldots, q$. Here q is a design parameter that determines the size of the short term memory, and $0 \leq \tau_1 \leq$

$\tau_2 \leq \cdots \leq \tau_q$ are design dependent. The short-term data points are augmented into $\mathcal{M}$, i.e., q-many slots in $\mathcal{M}$ are allocated for $(u_f(t-\tau_k),\ \Phi_f(t-\tau_k),\ x(t-\tau_k))$, $k = 1, \ldots, q$. This ensures that after τ_1 seconds, there will always exist data points that are mutual with $\epsilon(t)$ in $\mathcal{M}$, and hence the reading mechanism (4.29) and (4.30) can be applied on the data points in $\mathcal{M}$ even if W is encountered for the first time.

4.3.3 Stability

We now present the main stability result of the proposed memory-augmented architecture.

Theorem 4.1. Consider the uncertain dynamical system (4.1), the adaptive controller (4.7), the reference model (4.2), the identifier (4.14), and the memory augmented adaptive law given by (4.26), (4.29), and (4.30). Then the solution $(e(t),\ \tilde{W}(t))$ is globally *uniformly ultimately bounded* (UUB) and converges to a compact set.

Proof. Differentiating the Lyapunov function (4.19) along the trajectories (4.8) and (4.30) yields

$$\begin{aligned}\dot{V} =& - e^T Q e - 2e^T P B_p \tilde{W}^T \Phi(x) + 2\gamma_e^{-1} \mathrm{Tr}\{\tilde{W}^T \dot{\tilde{W}}\} \\ =& - e^T Q e - 2\mathrm{Tr}\{e^T P B_p \tilde{W}^T \Phi(x)\} + 2\gamma_e^{-1} \mathrm{Tr}\{\tilde{W}^T \mathrm{Proj}(\hat{W}, Y)\}.\end{aligned} \tag{4.32}$$

Using $\mathrm{Tr}\{A^T B\} = \mathrm{Tr}\{B A^T\}$ and (4.30b), (4.32) becomes

$$\begin{aligned}\dot{V} =& - e^T Q e + 2\gamma_e^{-1} \mathrm{Tr}\{\tilde{W}^T (\mathrm{Proj}(\hat{W}, Y) - Y)\} \\ & - 2\gamma_r \mathrm{Tr}\{\tilde{W}^T \Phi_f \epsilon^T\} - 2\gamma_r \mathrm{Tr}\{\tilde{W}^T \sum_{j=1}^{p} \mu_j \Phi_{f_j} \epsilon_j^T\}.\end{aligned} \tag{4.33}$$

Using the projection property $\mathrm{Tr}\{\tilde{W}^T(\mathrm{Proj}(\hat{W}, Y) - Y)\} \leq 0$, (4.16), and (4.28) in (4.33) yields

$$\begin{aligned}\dot{V} \leq& - e^T Q e - 2\gamma_r \mathrm{Tr}\{\tilde{W}^T \Phi_f \Phi_f^T \tilde{W}\} \\ & - 2\gamma_r \mathrm{Tr}\{\tilde{W}^T \sum_{j=1}^{p} \mu_j \Phi_{f_j} \Phi_{f_j}^T \tilde{W}_{i(j)}\}.\end{aligned} \tag{4.34}$$

Let $\bar{W}_{i(j)} \triangleq W - W_{i(j)}$, then $\tilde{W}_{i(j)}(t) = \tilde{W}(t) + \bar{W}_{i(j)}$. Hence (4.34) can be written as

$$\begin{aligned}\dot{V} \leq & - e^T Q e - 2\gamma_r \mathrm{Tr}\{\tilde{W}^T(\Phi_f \Phi_f^T + \sum_{j=1}^{p} \mu_j \Phi_{f_j} \Phi_{f_j}^T)\tilde{W}\} \\ & - 2\gamma_r \mathrm{Tr}\{\tilde{W}^T \sum_{j=1}^{p} \mu_j \Phi_{f_j} \Phi_{f_j}^T \bar{W}_{i(j)}\}.\end{aligned} \tag{4.35}$$

Since $\mu_j(t) > 0$ for $j = 1, \ldots, p$, then $(\Phi_f(t)\Phi_f(t)^T + \sum_{j=1}^{p} \mu_j(t)\Phi_{f_j}\Phi_{f_j}^T) \geq 0$, and (4.35) reduces to

$$\begin{aligned}\dot{V} \leq & - e^T Q e - 2\gamma_r \mathrm{Tr}\{\tilde{W}^T \sum_{j=1}^{p} \mu_j \Phi_{f_j} \Phi_{f_j}^T \bar{W}_{i(j)}\} \\ \leq & - \lambda_{min}(Q)\|e\|^2 + 2\gamma_r \|\tilde{W}\|_F \sum_{j=1}^{p} \mu_j \|\Phi_{f_j} \Phi_{f_j}^T \bar{W}_{i(j)}\|_F,\end{aligned} \tag{4.36}$$

where the second inequality follows by using $\mathrm{Tr}\{A^T B\} \leq \|A\|_F \|B\|_F$. By the usage of the projection operator in (4.30), it follows that $\|\hat{W}(t)\|_F \leq W_{max}$, and hence $\|\tilde{W}(t)\|_F \leq W_{max} + \|W\|_F$. This, with the fact that $\mu_j(t) < \beta$ for $j = 1, \ldots, p$, yields

$$\dot{V} \leq -\lambda_{min}(Q)\|e\|^2 + 2\gamma_r C_1 C_2, \tag{4.37}$$

where $C_1 \triangleq W_{max} + \|W\|_F$, and $C_2 \triangleq \beta \sum_{j=1}^{p} \|\Phi_{f_j} \Phi_{f_j}^T \bar{W}_{i(j)}\|_F$. Therefore, it follows from (4.37) that $\dot{V}(t) < 0$ whenever $\|e(t)\|^2 > 2\gamma_r C_1 C_2 / \lambda_{min}(Q)$, and thus, the solution $(e(t), \tilde{W}(t))$ is globally uniformly ultimately bounded [43] and converges to the compact set

$$E \triangleq \left\{ \left(e(t), \tilde{W}(t) \right) : \|e(t)\|^2 \leq \frac{2\gamma_r C_1 C_2}{\lambda_{min}(Q)}, \|\tilde{W}(t)\|_F \leq C_1 \right\}. \tag{4.38}$$

From (4.2) we know that if $r(t)$ is bounded, then so is $x_r(t)$. Therefore, since $e(t)$ is bounded, $x(t)$ is bounded. Since components of $\Phi(x(t))$ are locally Lipschitz-continuous functions of $x(t)$, and $x(t)$ is bounded, then $\Phi(x(t))$, and therefore all system signals are bounded. ■

It is noted that under the same assumptions used in concurrent learning [35], which state that all the data points represent the encountered uncertainty and that $rank(Z_\Phi) = \phi$, the proposed method provides exponential stability.

Remark 4.3. A less conservative analysis shows, by using (4.36), that $\dot{V} < 0$ whenever $\|e(t)\|^2 > C_e(t)$, where

$$C_e(t) \triangleq \frac{2\gamma_r C_1}{\lambda_{min}(Q)} \sum_{j=1}^{p} \mu_j(t) \|\Phi_{f_j} \Phi_{f_j}^T \bar{W}_{i(j)}\|_F. \tag{4.39}$$

Note that for data points that are mutual with $\epsilon(t)$, $W_{i(j)} = W$ and $\bar{W}_{i(j)} = 0$. Hence, the size of the bound (4.39) depends solely on the contribution of the irrelevant data points in the adaptive law (4.30), where $W_{i(j)} \neq W$. It is shown in the Simulations section that the reading mechanism decreases the magnitude of $C_e(t)$ by attributing low attention weights $\mu_j(t)$ to the irrelevant data points, which results in the convergence of $(e(t), \tilde{W}(t))$ to a small compact set.

4.4 Simulations

To show the effectiveness of the proposed method, we design a control augmentation system for the short period dynamics of a generic transport aircraft [16], the nominal model of which is given by

$$\dot{x}(t) = \underbrace{\begin{bmatrix} -0.8060 & 1.0 \\ -9.1486 & -4.59 \end{bmatrix}}_{A_n} x(t) + \underbrace{\begin{bmatrix} -0.04 \\ -4.59 \end{bmatrix}}_{B_p} u(t), \tag{4.40}$$

where $x(t) \triangleq [x_1(t), x_2(t)]^T$, $x_1(t)$ is the angle of attack (rad), $x_2(t)$ is the pitch rate (rad/s), and $u(t)$ is the elevator deflection (rad). The goal is to achieve command following of the pilot's pitch rate commands, (i.e., $y(t) = x_2(t)$), in the presence of uncertainty. To obtain uncertain plant dynamics in the form of (4.1), and to satisfy the matching condition (4.4), we define an uncertain state matrix as $A_p = A_n + B_p K_x$, and a matched uncertainty $\Theta^T f(x(t))$, where $f(x(t)) = [\sin(x_1(t)), \cos(x_2(t))]^T$. The reference model is defined as in (4.2), where $A_r = A_n$, $B_r = B_p K_r$, and K_r is selected according to (4.3). The controller is defined as in (4.7), and an identifier is implemented as in (4.13) and (4.14), where $a = 10$.

Three different architectures are compared; CMRAC using (4.17), concurrent learning using (4.21) and (4.24), and the proposed memory augmented adaptive law (4.26), (4.29) and (4.30). The learning rates are assigned as $\gamma_e = 100$ and $\gamma_\epsilon = 10000$, and the Q matrix used in the Lyapunov equation (4.18) is selected as $Q = I_{2\times 2}$. It is noted that these learning rates and the value of the Q matrix are the same for all of the compared architectures.

Three destabilizing uncertainties are considered, placing the eigenvalues of A_p at $\{1, 2\}$, $\{0.5, 2.5\}$ and $\{0.1, 3\}$. In the form of (4.6), the uncertainties can be written as

$$W_1 = \begin{bmatrix} -1.0012 \\ -1.8205 \\ 0.5 \\ 0.7 \end{bmatrix}, W_2 = \begin{bmatrix} -1.1593 \\ -1.8191 \\ 0.8 \\ -1.5 \end{bmatrix}, W_3 = \begin{bmatrix} -1.3442 \\ -1.8393 \\ -1 \\ 0.5 \end{bmatrix}. \tag{4.41}$$

In all simulations, a pitch rate pilot command of $r = 5$ deg/s is given as the reference, and all initial conditions are zero.

To collect data, a simulation is run for each uncertainty in (4.41) with the CMRAC adaptive law (4.17), where 4 data points $(u_{f_j}, \Phi_{f_j}, x_j)$ are recorded about each uncertainty (12 data points in total). The history stack (4.21) used in concurrent learning is formed using only the 4 data points that represent W_1. On the other hand, for the proposed method, our memory $\mathcal{M}$ in (4.26) is populated with all 12 data points and is then augmented with the short term memory, where $q = 2$, $\tau_1 = 0$ s and $\tau_2 = 0.1$ s. Hence, $\mathcal{M}$ has a size of $p = 14$, and is representative of W_1, W_2, W_3 and the potential encountered uncertainty W. The reading mechanism (4.29) and (4.30) is then applied to $\mathcal{M}$, where we set $\alpha = 100$ and $\beta = 20$.

The first scenario we simulate is the case where the only uncertainty in the system is W_1, i.e., the encountered uncertainty is $W = W_1$ for all $t \geq 0$, which is represented in both the memory of the proposed method (4.26) and the history stack of concurrent learning (4.21). Figure 4.1 shows the evolution of the elements of the tracking error vector $e(t) = x(t) - x_r(t)$, for CMRAC, concurrent, and memory-augmented architectures, and the evolution of the attention weights $\mu_j(t)$

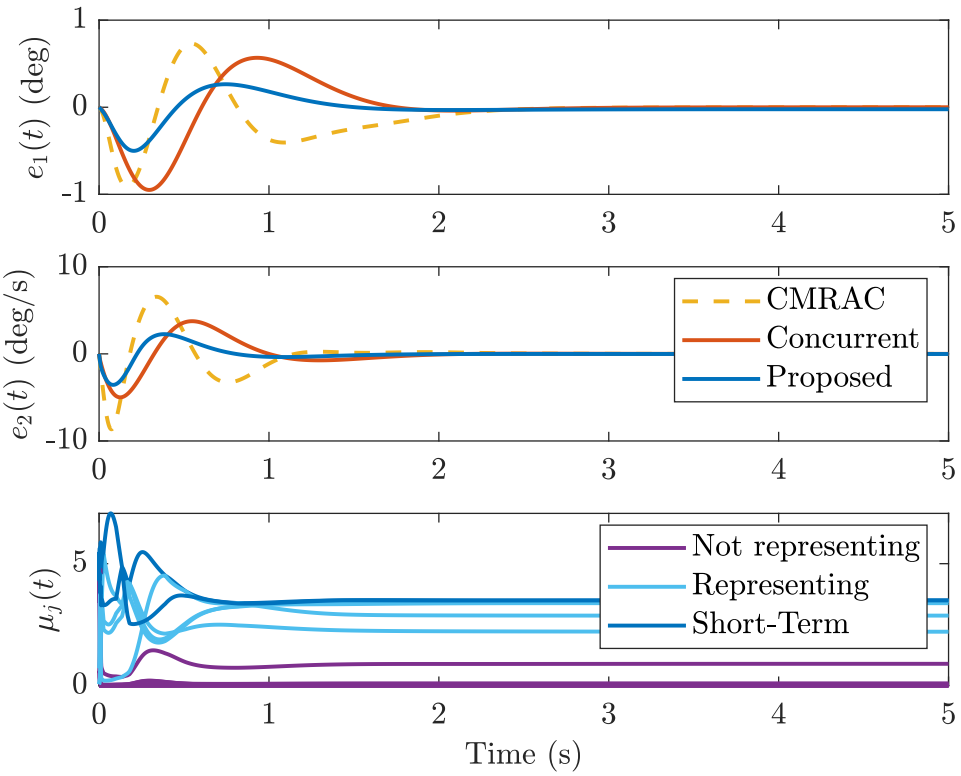

Figure 4.1: Uncertainty $W = W_1$. Top, middle: Tracking errors of CMRAC, concurrent and the proposed controller. Bottom: Attention weights of the proposed controller. "Representing" and "Not representing" denote the weights that represent and do not represent W_1.

in the memory-augmented architecture. It is noted that although the memory of the proposed method contains extra, irrelevant data, which do not represent W_1, the performance is similar to the concurrent architecture and better than the CMRAC architecture. This is achieved with the help of the reading mechanism, which attributes higher attention weights (4.29) to the data that represent W_1.

For the second scenario, we assume that the plant has a new uncertainty $W_4 = [-1.1543, -1.6013, -0.9, -0.4]^T$, which places the eigenvalues of A_p at $\{1+i, 1-i\}$. By definition, this makes the encountered uncertainty $W = W_4$. Figure 4.2 shows that since W_4 is not represented in the history stack of concurrent learning, the concurrent architecture yields an unsatisfactory performance. On the other

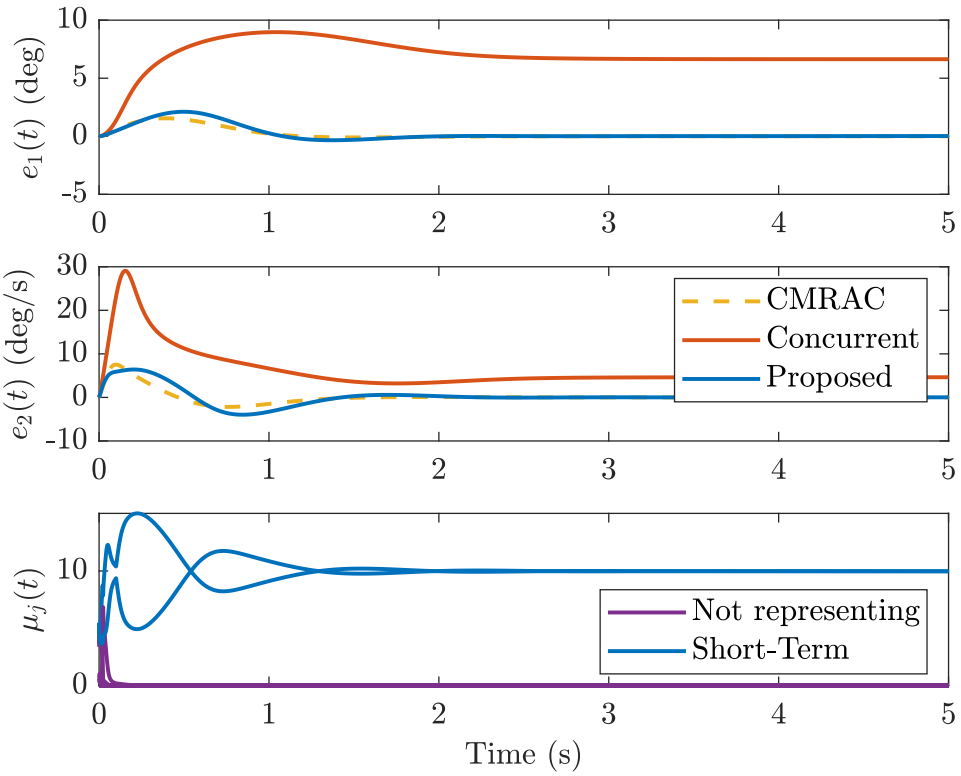

Figure 4.2: Uncertainty $W = W_4$. Top, middle: Tracking errors of CMRAC, concurrent and the proposed controller. Bottom: Attention weights of the proposed controller. "Not representing" denotes the weights that do not represent W_4.

hand, the proposed memory-augmented controller still achieves a satisfactory performance, similar to CMRAC, despite encountering W_4 for the first time. This is achieved with the help of the reading mechanism through the usage of the short-term memory: all the attention weights except the ones related to short-term memory converge to zero, which eliminates the detrimental effects of irrelevant data.

4.5 Summary

This chapter presents a novel memory architecture that enables adaptive controllers to make use of valuable data from the past to aid in learning. The proposed architecture consists of 1) a memory containing data about a variety of uncertainties, 2) a short-term memory that aids in handling new uncertainties, and 3) an attention-based reading mechanism that enables the controller to retrieve only relevant data rom the memory. The effectiveness of the architecture is validated through numerical simulations, and a rigorous Lyapunov stability analysis is provided.

Chapter 5

Conclusion

In this thesis, an adaptive human pilot model is presented, which is suited for the prediction of pilots' behavior in the loop with an adaptive control system. The model can serve as a valuable tool guiding the design of adaptive controllers as it can predict pilot-controller interactions in the simulation environment. A more sophisticated adaptive pilot model is also presented, where significant time delay in the pilot response can be taken into consideration, which expands its applicability. At last, a novel memory architecture is introduced, which provides adaptive controllers with the ability to make use of valuable data stored in the past to aid in compensating for uncertainties. The proposed architecture consists of 1) a memory containing data about a variety of uncertainties, 2) a short-term memory that aids in handling new uncertainties, and 3) an attention-based reading mechanism that enables the controller to retrieve only relevant data from the memory. The efficacy of the proposed methods is demonstrated through numerical simulations and rigorous Lyapunov stability analyses. The proposed architectures lay the foundations for promising research directions such as the development of sophisticated human pilot memory models and their employment in human-in-the-loop studies for various learning control architectures. These studies can pave the way toward more industrial implementations of reliable adaptive controllers in piloted applications.

Bibliography

[1] K. A. Wise, E. Lavretsky, and N. Hovakimyan, "Adaptive control of flight: theory, applications, and open problems," in *2006 American Control Conference*, pp. 6–pp, IEEE, 2006.

[2] D. Klyde, C.-Y. Liang, D. Alvarez, N. Richards, R. Adams, and B. Cogan, "Mitigating unfavorable pilot interactions with adaptive controllers in the presence of failures/damage," in *AIAA Atmospheric Flight Mechanics Conference*, p. 6538, 2011.

[3] M. Lone and A. Cooke, "Review of pilot models used in aircraft flight dynamics," *Aerospace Science and Technology*, vol. 34, pp. 55–74, 2014.

[4] S. Xu, W. Tan, A. V. Efremov, L. Sun, and X. Qu, "Review of control models for human pilot behavior," *Annual Reviews in Control*, vol. 44, pp. 274–291, 2017.

[5] R. A. Hess, "Modeling pilot control behavior with sudden changes in vehicle dynamics," *Journal of Aircraft*, vol. 46, no. 5, pp. 1584–1592, 2009.

[6] R. A. Hess, "Modeling human pilot adaptation to flight control anomalies and changing task demands," *Journal of Guidance, Control, and Dynamics*, vol. 39, no. 3, pp. 655–666, 2016.

[7] S. S. Tohidi and Y. Yildiz, "A control theoretical adaptive human pilot model: Theory and experimental validation," *IEEE Transactions on Control Systems Technology*, vol. 30, no. 6, pp. 2585–2597, 2022.

[8] E. Tulving, "What is episodic memory?," *Current directions in psychological science*, vol. 2, no. 3, pp. 67–70, 1993.

[9] L. R. Squire, "Memory systems of the brain: a brief history and current perspective," *Neurobiology of learning and memory*, vol. 82, no. 3, pp. 171–177, 2004.

[10] D. McRuer and D. Graham, "Pilot-vehicle control system analysis," in *Guidance and Control Conference*, p. 310, 1963.

[11] S. S. Tohidi and Y. Yildiz, "Adaptive human pilot model for uncertain systems," in *2019 18th European Control Conference (ECC)*, pp. 2938–2943, IEEE, 2019.

[12] T. Yucelen, Y. Yildiz, R. Sipahi, E. Yousefi, and N. Nguyen, "Stability limit of human-in-the-loop model reference adaptive control architectures," *International Journal of Control*, vol. 91, no. 10, pp. 2314–2331, 2018.

[13] S. Tohidi and Y. Yildiz, "Adaptive control allocation: A human-in-the-loop stability analysis," *IFAC-PapersOnLine*, vol. 53, no. 2, pp. 6321–6326, 2020.

[14] A. Habboush and Y. Yildiz, "Modeling pilot-flight control system interactions in the presence of uncertainty," in *AIAA SCITECH 2022 Forum*, p. 2030, 2022.

[15] A. Habboush and Y. Yildiz, "An adaptive human pilot model for adaptively controlled systems," *IEEE Control Systems Letters*, vol. 6, pp. 1964–1969, 2021.

[16] E. Lavretsky and K. Wise, *Robust and Adaptive Control: With Aerospace Applications*. London, UK: Springer, 2013.

[17] S. S. Tohidi, Y. Yildiz, and I. Kolmanovsky, "Adaptive control allocation for constrained systems," *Automatica*, vol. 121, p. 109161, 2020.

[18] K. J. Astrom and L. Rundqwist, "Integrator windup and how to avoid it," in *1989 American Control Conference*, pp. 1693–1698, IEEE, 1989.

[19] N. Kapoor, A. R. Teel, and P. Daoutidis, "An anti-windup design for linear systems with input saturation," *Automatica*, vol. 34, no. 5, pp. 559–574, 1998.

[20] M. Schwager and A. M. Annaswamy, "Direct adaptive control of multi-input plants with magnitude saturation constraints," in *Proceedings of the 44th IEEE Conference on Decision and Control*, pp. 783–788, IEEE, 2005.

[21] S. P. Karason and A. M. Annaswamy, "Adaptive control in the presence of input constraints," in *1993 american control conference*, pp. 1370–1374, IEEE, 1993.

[22] M. Schwager, A. M. Annaswamy, and E. Lavretsky, "Adaptation-based reconfiguration in the presence of actuator failures and saturation," in *Proceedings of the 2005, American Control Conference, 2005.*, pp. 2640–2645, IEEE, 2005.

[23] A. Habboush and Y. Yildiz, "An adaptive pilot model with reaction time-delay," in *2022 IEEE 61st Conference on Decision and Control (CDC)*, pp. 38–43, IEEE, 2022.

[24] Y. Yildiz, A. Annaswamy, I. V. Kolmanovsky, and D. Yanakiev, "Adaptive posicast controller for time-delay systems with relative degree $n^* \leq 2$," *Automatica*, vol. 46, no. 2, pp. 279–289, 2010.

[25] W. J. Rugh, *Linear System Theory (2nd Ed.)*. USA: Prentice-Hall, Inc., 1996.

[26] C.-T. Chen, *Linear System Theory and Design*. USA: Oxford University Press, Inc., 3rd ed., 1998.

[27] A. E. Bryson, *Control of spacecraft and aircraft*. Princeton university press, 1994.

[28] R. A. Hess, "Structural model of the adaptive human pilot," *Journal of guidance and control*, vol. 3, no. 5, pp. 416–423, 1980.

[29] D. T. McRuer, L. G. Hofmann, H. R. Jex, G. Moore, and A. V. Phatak, "New approaches to human-pilot/vehicle dynamic analysis," tech. rep., SYSTEMS TECHNOLOGY INC HAWTHORNE CA, 1968.

[30] Y. Yildiz, A. M. Annaswamy, D. Yanakiev, and I. Kolmanovsky, "Spark-ignition-engine idle speed control: An adaptive control approach," *IEEE Transactions on Control Systems Technology*, vol. 19, no. 5, pp. 990–1002, 2010.

[31] K. S. Narendra and J. Balakrishnan, "Improving transient response of adaptive control systems using multiple models and switching," *IEEE Transactions on automatic control*, vol. 39, no. 9, pp. 1861–1866, 1994.

[32] T. E. Gibson, A. M. Annaswamy, and E. Lavretsky, "On adaptive control with closed-loop reference models: transients, oscillations, and peaking," *IEEE Access*, vol. 1, pp. 703–717, 2013.

[33] E. Arabi, B. C. Gruenwald, T. Yucelen, and N. T. Nguyen, "A set-theoretic model reference adaptive control architecture for disturbance rejection and uncertainty suppression with strict performance guarantees," *International Journal of Control*, vol. 91, no. 5, pp. 1195–1208, 2018.

[34] D. Muthirayan and P. Khargonekar, "Memory augmented neural network adaptive controllers: Performance and stability," *IEEE Transactions on Automatic Control*, 2022.

[35] G. Chowdhary, T. Yucelen, M. Mühlegg, and E. N. Johnson, "Concurrent learning adaptive control of linear systems with exponentially convergent bounds," *International Journal of Adaptive Control and Signal Processing*, vol. 27, no. 4, pp. 280–301, 2013.

[36] K. S. Narendra and A. M. Annaswamy, *Stable adaptive systems*. Courier Corporation, 2012.

[37] S. Boyd and S. S. Sastry, "Necessary and sufficient conditions for parameter convergence in adaptive control," *Automatica*, vol. 22, no. 6, pp. 629–639, 1986.

[38] E. Lavretsky, "Combined/composite model reference adaptive control," *IEEE Transactions on Automatic Control*, vol. 54, no. 11, pp. 2692–2697, 2009.

[39] A. Habboush and Y. Yildiz, "Attention-enabled memory for concurrent learning adaptive control," *IEEE Control Systems Letters*, vol. 7, pp. 967–972, 2022.

[40] A. Vahidi-Moghaddam, M. Mazouchi, and H. Modares, "Memory-augmented system identification with finite-time convergence," *IEEE Control Systems Letters*, vol. 5, no. 2, pp. 571–576, 2020.

[41] H. Modares, F. L. Lewis, and M.-B. Naghibi-Sistani, "Adaptive optimal control of unknown constrained-input systems using policy iteration and neural networks," *IEEE Transactions on neural networks and learning systems*, vol. 24, no. 10, pp. 1513–1525, 2013.

[42] S. Kersting and M. Buss, "Removing erroneous history stack elements in concurrent learning," in *2015 54th IEEE Conference on Decision and Control (CDC)*, pp. 7604–7609, IEEE, 2015.

[43] H. K. Khalil, *Nonlinear Systems*. Upper Saddle River, NJ: Prentice Hall, 3 ed., 2002.